Wave Intensity Analysis in the Pulmonary Circulation and Pulmonary Haemodynamics in Advanced Heart Failure

by

Ivan Hoi Wing Yim FRCS(C-Th)

A thesis submitted to the University of Birmingham for the degree of

DOCTOR OF PHILOSPHY

Institute of Cardiovascular Sciences

College of Medical and Dental Sciences

The University of Birmingham

May 2024

Abstract

Wave intensity analysis (WIA) uses simultaneous changes in pressure and flow velocity to determine wave energy, type and timing of traveling waves in the circulation. It has the unique advantage over other impedance-based methods in that it analyses the pressure and velocity waveforms as successive wavefronts and not sinusoidal wavetrains. The analysis is performed in the time domain, allowing clinicians to intuitively relate the arterial waves to events in the cardiac cycle. In this thesis, I investigated WIA in patients with heart failure and durable LVAD therapy. I found that wave propagation in the pulmonary circulation in the context of heart failure was comparable with the systemic circulation; wave reflection was more likely at higher pulmonary arterial pressures and with lower pulmonary arterial compliance. There were no significant changes in wave propagation nor reflection associated with LVAD pump speed changes at +/- 300 rpm. I also investigated haemodynamic parameters associated with MCS usage following orthotopic heart transplantation and found that a lower pulmonary arterial pulsatility index (PAPI) is independently associated with MCS use for severe early graft dysfunction following heart transplantation. Using the same haemodynamic data, I also explored a stroke volume calculator derived from pulmonary haemodynamics. I found that after calibration, it was possible to track changes in stroke volume based on pulmonary pulse pressure, however, this calculator requires further validation using data from different patient cohorts. At the inception of the project, there was ambition to develop WIA into a clinical tool, however with the current technology, I conclude that this is not yet possible due to the difficulty in acquiring a clean velocity signal and the need for more data.

For Button, my light and joy.

Acknowledgements

This thesis would not have been possible without the advice and guidance of my supervisors who have both played prominent roles at different stages of this project. Without their constant encouragement and steering, I would not have finished or written up this thesis:

Dr. S Lim, Consultant Cardiologist at the Queen Elizabeth Hospital, Birmingham.

Mr. N E Drury, Associate Clinical Professor, University of Birmingham and Consultant in Paediatric Cardiac Surgery at Birmingham Children's Hospital.

I am particularly grateful to Prof. K Parker, Professor Emeritus at Imperial College London, who's input was invaluable during the planning and conduct of the project. As one of the fathers of WIA, his insights and advice throughout the whole project was indispensable and of the utmost importance in propelling the project forwards.

I am grateful to Heart Research UK who funded this study and supported my salary and university tuition fees. I would also like to thank University Hospitals Birmingham Charity who supported part of my final year's university tuition fees. Without the financial support provided by HRUK, this project would not have been possible and they have been patient and understanding throughout the project especially with the various amendments and delays to the process.

I am indebted to the enthusiasm and understanding of many colleagues within the Cardiac Surgery and Cardiology department who all facilitated the conduct of this study- *Consultant Cardiac Surgeons:* Mr. S J Rooney, Mr. M S Bhabra, Mr. A M Ranasinghe, Mr. J Mascaro, Mr. E Senanyake and Mr. A Ashoub; *Consultant Cardiologists:* Dr. C Chue, Dr. S White and Dr. A Morley-Smith, who all gave up their time during each RHC which involved the Combowire. I would also like to mention and thank all the Cath Lab staff for their patience with setting up the console and combo wire, without their understanding and support the recruitment and conduct of this study would not have been as smooth as it was. A special thank you goes to our Transplant Co-ordinators as they were instrumental in approaching the Transplant and VAD patients during the recruitment process.

In particular I would like to thank my parents Anna and K. M. Yim, for their unwavering support over the many years and without their countless sacrifices, I would not have any of my accomplishments today.

Personal Contributions

The foundation of this thesis is based on the WIA work done by Prof. Parker, the project inception was by Dr. Lim and Prof. Parker and made possible by the Heart Research UK Novel and Emerging Technology Grant. Dr Lim had been successful in the application of the NET grant and secured funding for the project including the salary for a research fellow. I was lucky enough to be chosen by Dr. Lim to be his research fellow and subsequently successfully applied for a period of 'out of programme research' from the West Midlands deanery and school of surgery. I was the Principal Investigator for the WIA study and personally responsible for all aspects of the study. I personally performed every single patient recruitment of the study, gained their written consent, acquired the haemodynamic data, acquired the pressure and velocity data for WIA, data management and offline analysis of the data on Matlab. I also personally liaised with the trust's R&D department for all aspects of the study.

Chapter 2: Systematic Review

I designed the search strategy and personally performed the search and went through all the abstracts of the initial search results. Dr. A Khan-Kheil was the second reviewer in the review. After ensuring we agreed on the articles to be included in the formal review, I synthesised the data from the full articles. I wrote the original manuscript and also subsequent edits after submission to journals. This has now been published in *Interdisciplinary Cardiovascular and Thoracic Surgery*.

Chapter 3: Methods

The study methodology was set out in the study protocol and grant application prior to my appointment as Dr. Lim's research fellow. Ethical and MRHA approval had already been obtained and UHB R&D had agreed to sponsor the study. I completed Good Clinical Practice training to comply with the NHS Research Governance framework and I was responsible for notifying the Trust R&D department of any serious adverse events and also providing the information when the study master files were audited.

Chapter 4: Results WIA in Heart Failure

After the patients were initially approached and agreed to be spoken to regarding the study, I personally recruited every single participant in this study. I was responsible for capturing the haemodynamic data and pressure/velocity data from the Combowire for WIA. I then performed the WIA analyses off line on Matlab for every single case and analysed the data including all the statistical tests. The Matlab script used for analysis was written and developed by Prof. Parker.

Chapter 5: Results WIA in LVAD Therapy

As above in Chapter 4, I personally recruited every single participant in this study. I was responsible for capturing the haemodynamic data and pressure/velocity data from the Combowire for WIA. I also was responsible for changing the LVAD pump speeds and of course returning them to their baseline speeds. I then performed the WIA analyses off line on Matlab for every single case. For this chapter only, the statistical analysis was performed by James Hodson who is a Statistician employed by University Hospitals Birmingham.

Chapter 6: Predictors of MCS Following Heart Transplantation

I processed and cleaned the haemodynamic data from both Transplant centres, Royal Papworth and Queen Elizabeth Birmingham. I performed all the data analysis including all the statistical analysis.

Chapter 7: Stroke Volume Calculator derived from Pulmonary Haemodynamics

The calculator concept was developed by Dr. Lim. I applied the haemodynamic data from Chapter 6 to the calculator and performed all the analysis of the results including the correlation analyses and Bland-Altman plots.

Publications and Abstracts

Publications in Peer-Reviewed Journals

Chapter 2: A systematic review and physiology of pulmonary artery pulsatility index in left ventricular assist device therapy.

Yim IHW, Khan-Kheil AM, Drury NE, Lim HS.

Interdiscip Cardiovasc Thorac Surg. 2023 May 4; 36(5). PMID: 37171900

Chapter 4: Pulmonary artery wave intensity analysis in pulmonary hypertension associated with heart failure and rediced left ventricular ejection fraction.

Yim IHW, Parker KH, Drury NE, Lim HS. *Pulm Circulation. 2024 Feb 12; 14(1):e12345. PMID: 38348196.*

Chapter 6: Pulmonary artery pulsatility index predicts mechanical circulatory support following heart transplantation.

Yim IHW, *Pettit SJ, Bhagra S, Berman M, Drury NE, Lim HS. JHLT Open 2023 Dec; 3:100030,* https://doi.org/10.1016/j.jhlto.2023.100030.

Chapter 7: Derivation of Stroke Volume from Pulmonary Artery Pressures.

Yim IHW, Drury NE, Lim HS. Cardiol Ther. 2024 Apr 2025. Doi: 10.1007/s40119-024-00360 PMID: 38664318.

Manuscripts in preparation

Chapter 5: Pulmonary artery wave intensity analysis in durable left ventricular assist device therapy. **Yim IHW,** Hodson J, Parker KH, Drury NE, Lim, HS.

Manuscript prepared and ready for imminent submission.

Conference Abstracts

Pulmonary artery wave intensity analysis in pulmonary hypertension due to left heart disease, **Yim I et al**. Presented at International Society for Heart and Lung Transplantation annual meeting 2022, Boston MA, USA. *Abstract published in JHLT April 2022, Vol 41, Issue 4, Supp, S139-140.*

Reservoir pressure analysis in group 2 pulmonary hypertension, **Yim et al**. Presented at International Society for Heart and Lung Transplantation annual meeting 2022, Boston MA, USA. *Abstract published in JHLT April 2022, Vol 41, Issue 4, Supp, S140.*

Table of Contents

Illustrations

Tables

Abbreviations

ACE	Angiotensin converting enzyme
ACEi	Angiotensin converting enzyme inhibitor
AHA	American Heart Association
ARB	Angiotensin receptor blocker
ARNI	Angiotensin receptor-neprilysin inhibitors
BB	Beta-blocker
C	Capacitance
CMR	Cardiac magnetic resonance
CRT	Cardiac resynchronisation therapy
CT	Computer tomography
CVP	Central venous pressure
DPAP	Diastolic pulmonary arterial pressure
DTI	Doppler tissue imaging
Ea	Arterial elastance
ECHO	Echocardiography
Ees	End systolic elastance
EF	Ejection fraction
Gd-DTPA	Gadolinium-diethylenetriamine pentaacetic acid
HF	Heart failure
LGE	Late gadolinium enhancement
LV	Left ventricle
LVAD	Left ventricular assist device
LVEDP	Left ventricular end diastolic pressure

MAP	Mean arterial pressure
MPAP	Mean pulmonary arterial pressure
MRA	Mineralocorticoid receptor antagonist
MRI	Magnetic resonance imaging
NYHA	New York Heart Association
PAC	Pulmonary arterial capacitance
PAPI	Pulmonary artery pulsatility index
PAPP	Pulmonary arterial pulse pressure
PAWP	Pulmonary arterial wedge pressure
PH	Pulmonary hypertension
Pr	Reservoir Pressure
PVR	Pulmonary vascular resistance
Px	Excess Pressure
RAAS	Renin-Angiotensin-Aldosterone- System
RIMP	Right ventricular index of myocardial performance
RV	Right Ventricle
RVAD	Right ventricular assist device
RVFAC	Right ventricular fractional area change
RVOT	Right ventricular outflow tract
RVSWi	Right ventricular stroke work index
RWA	Reservoir wave approach
SPAP	Systolic pulmonary arterial pressure
SPECT	Single photon emission computed tomography
TAPSE	Tricuspid annular plane systolic excursion

TOE	Transoesophageal Echocardiography
TPG	Trans-pulmonary gradient
TTE	Transthoracic Echocardiography
WIA	Wave intensity analysis
WRI	Wave reflection index

1. Introduction

1.1. Background

The management of advanced heart failure has evolved significantly in recent times. With the advent of left ventricular assist devices (LVAD), this provides another treatment modality for end stage heart failure for patients who are not immediately suitable for transplantation. There is evidence that LVAD improves quality of life and survival (Mehra et al., 2017). For an LVAD to be effective, it depends on blood being pumped from the right ventricle (RV), through the pulmonary circulation and into the left side of the heart to generate preload. RV failure in patients with LVAD remains a difficult problem to treat and the current modalities on assessing the RV have limitations (Vonk-Noordegraaf and Westerhof, 2013); the current techniques on assessing the RV focusses on the RV in isolation and does not take into account the pulmonary vasculature. If RV failure occurs early following LVAD implantation, and a right ventricular assist device (RVAD) is required to be implanted within 14 days then the mortality is high (Kiernan et al., 2017). Furthermore, late RV failure may impair long term survival and quality of life (Takeda et al., 2015). Therefore, there is a need to develop more effective assessment tools for the RV in order to identify RV failure earlier and to attempt to identify factors which may predict RV failure following LVAD implantation.

Wave intensity analysis (WIA) in arteries was described in 1990 (Parker and Jones, 1990a) and since then, it has been used to assess the systemic circulation. Furthermore, in chronic heart failure it has been shown that forward wave generation is impaired (Curtis et al., 2007). WIA holds promise in being a useful clinical tool to assess the RV in conjunction with the pulmonary circulation. The results from this study will determine the potential role of WIA as a clinical

tool in the assessment of patients with advanced heart failure and also tailor treatment for patients with LVADs.

1.2. Anatomy of the heart

In the 17th century, Niels Stensen, a Danish physician, anatomist and Bishop once described the heart as "simply a muscle' (Tubbs, 2016) and there is a lot of truth in this profound statement. The different morphological features of each structure of the heart have been extensively reported. Throughout the ages, there have been descriptions of the anatomy of the heart since the pre-Hippocratic era. The oldest anatomical manuscript in the world was found in the Egyptian "Ebers Papyrus" and the Egyptians recognised the heart as the centre of the vascular system (Loukas et al., 2016). Not only that but within the Ebers Papyrus, there may have been descriptions of ancient Egyptians suffering from heart failure symptoms (Saba et al., 2006). There is a wide range of well described anatomical cardiac malformations and variations, these will not be described here, and the normal cardiac anatomy of an adult will be given.

The heart consists of four main chambers, the right and left atria, and the right and left ventricles. Its main function is to receive de-oxygenated blood returning from the body via the superior and inferior vena cavae into the right atrium and then the right ventricle pumps this blood through the pulmonary circulation for it to become oxygenated; oxygenated blood then returns to the left atrium via the pulmonary veins and from there into the left ventricle for it to be pumped into the ascending aorta and the systemic circulation. There are four heart valves directing the blood flow in the sequence just described. The Mitral and Tricuspid valves are the two atrio-ventricular valves and they allow blood to enter the ventricles from the atria but on ventricular systole, they close preventing back flow of blood back into the atria. The Tricuspid

valve has three leaflets and the mitral valve has two leaflets. On the right side, from the right ventricle blood is pumped into the main pulmonary artery through the pulmonary valve. On the left, the left ventricle pumps blood through the aortic valve to egress into the systemic circulation. On ventricular diastole, both the pulmonary and aortic valves close to prevent blood from re-entering the ventricles, both valves are usually tricuspid but anatomical variations are well recognised. Separating the left and right side of the heart are the atrial septum and the ventricular septum, in normal anatomy, the atrial and ventricular septum prevents the mixing of oxygenated and deoxygenated blood. In embryology, the intact atrial septum is formed by the completed fusion of the septum primum and septum secondum, failure of this process results in a patent foramen ovale or an atrial septal defect (Anderson and Brown, 1996). The purpose of the foramen ovale in foetal life is to stream blood from the right atrium directly into the left atrium thereby bypassing the lungs as blood returning to the heart is already oxygenated from the placenta. The presence of a patent foramen ovale has been estimated at around 25% in the human population (Homma et al., 2016).

The heart's blood supply come from the coronary arteries. They originate at the aortic root with the left and right coronary ostia. The right coronary artery travels anteriorly then laterally in the atrio-ventricular groove giving off several branches including the branch to the sino-atrial node, branch to the atrio-ventricular node, posterior descending artery and terminating in the posterior lateral ventricular branch. Dominance is determined by which coronary system the posterior descending artery arises from, in 80% of the population the posterior descending artery arises from the right coronary artery, 10% arises from the left coronary artery (Koenraadt et al., 2016) and in the remaining 10% of the population there is a co-dominant system. There is also recognised variation in the blood supply of the atrio-ventricular node. It has been reported that

90% of the atrio-ventricular nodes in the population are supplied by the right coronary artery and the remaining 10% supplied by the left coronary artery (Pejković et al., 2008); this therefore explains why after an inferior acute coronary syndrome some patients develop heart block as the atrio-ventricular node may have been compromised (Aguiar Rosa et al., 2018).

The venous system of the heart is split into 3 categories, the greater cardiac venous system comprising of the coronary sinus and its tributaries, the anterior cardiac veins and finally the thebesian veins (Loukas et al., 2009). The coronary sinus and its tributaries, which include the great cardiac vein, the lateral veins, the middle cardiac vein, the oblique vein of the left atrium forms the main network of venous drainage of the heart and returns de-oxygenated blood into the right atrium (Spencer et al., 2013). The anterior cardiac veins drain the anterior aspect of the heart and opens directly into the right atrium as well. The Thebesian veins drain the intramural and subendocardial portions of the heart directly into the underlying chambers (Loukas et al., 2009).

1.3. Heart Failure and LVAD

1.3.1. Heart Failure Classification

Heart failure is recognised to be a global pandemic affecting an estimated 26 million people and it results in over one million hospital admissions in the United States of American and Europe annually (Ambrosy et al., 2014). Heart failure is defined as the inability for the heart to supply the organs with the adequate amount of oxygenated blood to meet their metabolic demands; therefore causing patients to suffer from symptoms of dyspnoea and or fatigue with clinical signs of peripheral oedema, tachycardia and in right sided failure, an elevated jugular

venous pulse (Tanai and Frantz, 2016). The New York Heart Association (NHYA) functional classification was first introduced in 1921 and is still being used in routine clinical practice over one hundred years later (White and Myers, 1921). In the NYHA class I cohort of patients, there is no limitation of physical activity and ordinary physical activity does not cause symptoms of HF. In NYHA class II, patients have slight limitation of physical activity, they are comfortable at rest but ordinary physical activity results in symptoms of HF. In NYHA class III, there is marked limitation of physical activity, patients remain comfortable at rest but less than ordinary activity causes symptoms of HF. Finally, in class IV, patients are unable to carry on any physical activity without symptoms of HF and/or they have symptoms at rest (Yancy et al., 2013).

The 2013 American Heart Association (AHA) Heart Failure Guidelines categorises heart failure into two broad categories, HF with preserved ejection fraction (HFpEF) and HF with reduced EF (HFrEF). Over time and in different trials, the threshold for reduced ejection fraction has varied; in the current AHA guidelines, HFrEF is defined as the clinical diagnosis of heart failure with a left ventricular ejection fraction of less than or equal to 40% (Yancy et al., 2013). Heart failure can also be further classified as systolic vs diastolic dysfunction, pressure overload vs volume overload failure, and low output vs high output heart failure. Pressure overload failure is caused by an increased afterload in conditions such as aortic stenosis or hypertension, whereas volume overload failure occurs when the left ventricle has too much blood during diastole and over time becomes dilated; the most common causes of volume overload are valvular heart disease, such as mitral or aortic valve regurgitation, and congenital cardiac defects, such as atrial or ventricular septal defects. Low output failure refers to any cause of heart failure which causes an inadequate amount of blood to be pumped into the systemic

circulation, whereas high output failure refers to when the cardiac output is actually normal or in some circumstances even raised but because the systemic demand has increased, for example in sepsis and the systemic metabolic rate has increased, the cardiac output is unable to match that demand even when elevated.

Heart failure with reduced ejection fraction is caused by any condition which results in a loss of myocytes. It is a progressive condition and certain risk factors result in injury to the myocardium which leads to progressive loss of cardiac function. The most common causes of heart failure in the UK are, coronary artery disease, primary cardiomyopathies, valve disease and rarer causes are other congenital abnormalities and infection (Cowie, 2017). The common risk factors for ischaemic heart disease (coronary artery disease) are hypertension, hypercholesterolaemia, diabetes, obesity, a positive family history and cardiotoxic agents such as alcohol, amphetamines, chemotherapeutic agents and radiation (Metra and Teerlink, 2017). When the loss of myocytes occurs, this eventually leads to ventricular remodelling via eccentric hypertrophy with neurohumoral stimulation and activation of the renal angiotensin aldosterone system which in turns causes fluid retention; furthermore this results in abnormal calcium cycling and changes in the proliferation of the extracellular matrix leading to accelerated apoptosis, resulting in more loss of myocytes and reduction in cardiac function (Braunwald, 2013; Metra and Teerlink, 2017)

There are, of course, genetic predispositions for heart failure and with the advances in genetic testing, over 100 different genes have been identified or associated with inherited conditions such as cardiomyopathies, but it is also important to note that cardiomyopathies are classified as familial and non-familial types. The most common of which are hypertrophic

cardiomyopathy (HCM), idiopathic dilated cardiomyopathy (DCM), arrhythmogenic right ventricular cardiomyopathy (ARVC) and non-compaction cardiomyopathy (Czepluch et al., 2018). The advent of next generation sequencing has meant that genetic testing is becoming more widely available and clinicians are sending more and more patients for screening. Rather than using traditional, individual exon by exon sequencing, which is very time consuming, next generation sequencing rapidly selects all protein exons and selectively sequences them which saves time (Punetha and Hoffman, 2013). For example, genes which have been linked to HCM include GLA, MYL2/3, MYLK2, genes which have been linked to DCM include ABCC9, CRYAB, CTF1, EMD, genes which have been linked to arrhythmogenic right ventricular cardiomyopathy include CASQ2, JUP and TMEM43; these are just a few examples and of course there are many overlaps where genes have been linked to multiple different cardiomyopathies (McNally et al., 2015). To give an example of how a genetic mutation can cause HCM, the MYH7 gene encodes myosin heavy chain which is the filament that produces force by hydrolyzing ATP, it has been shown that mutations in MYH7 causes thickening of the myosin heavy chain and that if the mutations occur in the head of the gene then the phenotypical manifestations are more severe as it exaggerated the change in hydropathy of amino acids (Walsh et al., 2010). In DCM, Titin is the filament which is affected. Titin is the largest protein within the myocyte and spans over half the sarcomere (Fürst et al., 1988). In DCM, the TTN gene has been linked as the major gene which results in DCM. If the N2B region is affected, this ultimately leads to hyper calcium sensitisation and increases length dependent activation which in turn leads to left ventricular diastolic dysfunction (Lee et al., 2010). With more evidence about the different mutations, there is great anticipation that this will lead to many different targets for gene-based therapies and bespoke treatment plans for each individual patient with a familial cardiomyopathy.

The incidence of HFpEF has been on the rise and it has been shown that up to half of the population of patients with HF have a preserved ejection fraction (Pfeffer et al., 2019). Furthermore, in epidemiological studies, it is emerging that HFpEF is the most common form of heart failure in the community (Gladden et al., 2014). Compared to patients with a reduced EF, in clinical trials such as DIG-PEF, CHARM-Preserved and I-Preserve, the cohort with HFpEF had better outcomes than the HFrEF group but still had a worse prognosis compared with patients without HF (Campbell et al., 2012). Shah et al found that the five year mortality were similar between patients with HFrEF and HFpEF (75.3% vs 75.7% respectively), however in the HFpEF cohort the patients were older, more likely to be female and had different co-morbidities; HFpEF cohort had a higher proportion of patients with chronic obstructive lung disease, hypertension, anaemia and valvulopathies (Shah et al., 2017).

The most common pathophysiological issue with HFpEF seems to be diastolic dysfunction with increased diastolic stiffness causing an increase in diastolic filling pressures (Khalid and Deswal, 2017a). Moreover, it has also been found that the diastolic filling pressures may not be affected during resting heart rates but when the heart rate rises, in HFpEF, diastolic filling pressures are increased; therefore during exercise for example, it fails to adapt and therefore causes dyspnoea (Gladden et al., 2014). It has been proposed that the increase in myocardial stiffness may be caused by an increase in extracellular collagen deposition, altered titin site specific hyperphosphorylation or hypophosphorylation, possibly altered myosin phosphorylation and thereby altering its binding potential with protein C and or other myofilament alterations (Zile et al., 2015; Khalid and Deswal, 2017a). There are ongoing work into hypotheses that HFpEF is a form of hypertensive heart disease as almost nearly all patients with HFpEF have concurrent or past history of hypertension; and secondly that HFpEF is a

form of inflammatory heart disease (Khalid and Deswal, 2017a). The later assumes that a systemic proinflammatory state causes coronary microvascular endothelial inflammation, this in turns reduces nitric oxide bioavailability, reduces cyclic guanosine monophosphate content and also reduces protein kinase G activity in adjacent myocytes. This leads to myocardial hypertrophy and promotes interstitial fibrosis, elevating the diastolic stiffness (Paulus and Tschöpe, 2013).

The diagnosis of HFpEF remains a challenge for clinicians and more research is required to further understand this entity and to formulate effective treatments. Patients who have signs and symptoms of heart failure but are found to have a preserved ejection fraction, should be investigated thoroughly with echocardiography and natriuretic peptide levels; and treatment for heart failure should be initiated. However in the past, drugs which have been shown to improve outcomes in patients with HFrEF have not been shown to be of any benefit in those with HFpEF (Khalid and Deswal, 2017b). Recently, sodium-glucose cotransporter 2 inhibitors (SGLT2i), both Empagliflozin and Dapagliflozin, have been shown to reduce the combined risk of cardiovascular death or hospitalisation in patients with HFpEF (Anker et al., 2021; Nassif et al., 2021).

1.3.2. Heart Failure Pathophysiology

There are several important concepts to discuss in order to fully understand the pathophysiology of heart failure. The preload is determined by myocardial compliance, the amount of blood filling the LV and the resting force. LVEDP is the left ventricular end diastolic pressure, LVEDR is the left ventricular end diastolic radius and ‘h’ is the left ventricular thickness (Tanai and Frantz, 2016). The afterload of the heart is determined by the resistance and capacity of the

systemic circulation, therefore it is increased in conditions such as systemic arterial hypertension and when there is a fixed obstruction in the left ventricular outflow tract such as in aortic stenosis. Therefore, the factors which determine LV function are preload, afterload, heart rate and myocardial contractility (Tanai and Frantz, 2016).

The Frank-Starling mechanism describes the interaction between preload, afterload and myocardial contractility perfectly. It states that when there is an increase in volume in the ventricle, there is also an accompanied increase strength in the myocardial contraction thereby appropriately increasing the stroke volume (Noble, 1978). In the failing LV, there is a rightward shift and reduced gradient in the Frank-Starling curve, with a higher filling pressure required to achieve the same cardiac output, and ultimately reduced myocardial contractility.

The other important factor to consider is ventricular wall stress as it is directly proportional to myocardial oxygen demand. The Young-Laplace equation defines LV wall stress:

$$LV\ wall\ stress = \frac{pr}{2h}$$

In this equation, “p” represents left ventricular pressure, “r” represents LV radius and “h” represents wall thickness (Zhang et al., 2011). From this equation, it can easily demonstrate that in heart failure, when there is LV dilatation, the radius is increased and therefore increasing the ventricular wall stress and also myocardial oxygen demand. This is the same mechanism in which valvular heart disease such as mitral valve regurgitation and cardiomyopathies cause an increase in wall stress. Similarly, in hypertension and aortic stenosis, both increase the LV pressure and also therefore increase ventricular wall stress. In ischaemic heart disease and

especially following myocardial infarction, this can lead to a reduction in LV wall thickness and thereby increasing the wall tension.

In face of chronic pressure and volume loading, there is a response from a cellular level which ultimately causes ventricular remodelling. As mentioned above and described in more detail later, as part of the heart failure syndrome, there is neurohumoral activation and the vasoactive components of the renin-angiotensin aldosterone system are released; this in turn causes vasoconstriction and increases intracellular calcium concentration in cardiomyocytes. An increase in calcium levels has positive inotropic effects (increasing myocardial contractility) but has a negative lusitropic effect (decreasing myocardial relaxation), over time this leads to a shift to myocyte apoptosis causing a diffuse loss of cardiomyocytes (Tanai and Frantz, 2016). Another important architectural change on a cellular level in heart failure is interstitial fibrosis. It has been shown that there is abnormal collagen deposition in the interstitium and over time this becomes fibrous tissue with a net loss of cardiomyocytes, therefore further reducing ventricular contractility and function (Sabbah et al., 1995).

Macrostructural changes to the left ventricle include left ventricular hypertrophy and dilatation. LV hypertrophy can be classified into concentric hypertrophy, eccentric remodelling and combined eccentric and concentric remodelling. Concentric hypertrophy is secondary to an increase in afterload and there is an increase in wall thickness with parallel organised sarcomeres; eccentric hypertrophy is caused by volume overloaded states or in dilated cardiomyopathy where there is an increase in the LV volume accompanied by wall thinning and longitudinally organised sarcomeres; finally in combined remodelling, there is dilatation in

the non-functioning myocardial segments accompanied by hypertrophy in the functioning myocardial mass and is caused by ischaemia (Tanai and Frantz, 2016).

The activation of the neurohumoral component of heart failure is important physiologically and has significant systemic sequelae. The sympathetic nervous system is activated in heart failure because the baroreceptors in the carotid sinus and aortic arch which normally inhibit the sympathetic system have decreased activity and the peripheral chemoreceptors which activate the sympathetic system have increase signalling. The activation of the sympathetic nervous system activates beta and alpha adrenergic receptors (Lefkowitz et al., 2000) which in turn causes reflex tachycardia and increase inotropy but also increases peripheral vascular tone and therefore increases afterload. Ultimately the pathological activation of the sympathetic nervous system may lead to hypertrophy, mechanical dysfunction, arrhythmias, ischaemia and activation of the renin-angiotensin-aldosterone system (RAAS) (Antoine et al., 2017).

The RAAS is intricately involved in sodium and water retention and is important in maintaining homeostasis or the "*milieu intérieur*". The sodium content in the renal tubules is regulated by the juxtaglomerular apparatus and when it senses the sodium content is low, it activates the macula densa to cause the granular cells to release renin in the afferent arteriole. Renin converts angiotensinogen in the plasma into angiotensin I which is converted to angiotensin II by angiotensin converting enzyme (ACE), mostly in the capillary network of the lungs. Angiotensin II in turn acts on the zona glomerulosa of the adrenal cortex to secrete Aldosterone. Aldosterone increases the number of sodium channels and sodium/potassium/ATPase molecules in the distal tubules which moves sodium into the blood stream whilst secreting potassium and ultimately increase the plasma volume as fluid is reabsorbed with sodium in the

distal tubules. Angiotensin II also has a secondary effect of vasoconstriction in the peripheral vasculature thereby increasing the systemic blood pressure (Higgins, 2006). In heart failure, there is inappropriate activation of the RAAS by sympathetic stimulation and therefore causing fluid retention and increase in afterload by the action of angiotensin II. Furthermore, it has been found that angiotensin II has direct independent effects on cardiomyocytes; it causes increased proliferation of medial vascular smooth muscle cells and in association with adventitial and interstitial fibroblasts of coronary arterioles eventually leading to hypertrophy, myocyte apoptosis and changes in the extracellular matrix (Tanai and Frantz, 2016; McEwan et al., 1998).

Another component of the systemic manifestation of chronic heart failure is the immune system. There has been great interest in the immunomodulation that results in patients with chronic heart failure as it could become a potential therapeutic target. Pro-inflammatory cytokines such as tumour necrosis factor alpha, interleukin 1-beta, interleukin- 6, interleukin-8 and macrophage inflammatory protein 1-alpha are all raised in the plasma and importantly, there is not a corresponding rise in the level of anti-inflammatory regulating cytokines such as interleukin-10 therefore causing a net pro-inflammatory effect (Aukrust et al., 1999). Some of the cytokines listed above have been found to have direct effects on the myocardium. Tumour necrosis factor alpha and interleukin 1-beta have negative inotropic effects by uncoupling beta-adrenergic signalling, whilst tumour necrosis factor- alpha promotes cardiomyocyte hypertrophy, ventricular dilation and fibrosis (Aukrust et al., 2005).

Finally, cardiac excitation-contraction coupling is also impaired in heart failure. In normal physiology, excitation-contraction coupling is the transition of electrical excitation to actual contraction of the heart. Calcium plays a central role during the cardiac action potential and enters the cell through depolarization activated calcium channels and promotes calcium release from the sarcoplasmic reticulum, which in turn binds to troponin C of the myofilament activating myocardial contraction (Bers, 2002). In heart failure, the mechanism for impaired excitation-contraction coupling has been proposed to be decreased cardiac L-type calcium channel activity; this causes a reduction of calcium influx and in mice, it has been shown to cause hypertrophy and heart failure (Goonasekera et al., 2012).

1.3.3. Heart Failure and Pulmonary Hypertension

Pulmonary hypertension (PH) is defined as a mean pulmonary arterial pressure (mPAP) of 25mmHg or higher at rest and measured during right heart catheterisation (Hoeper et al., 2013). Pulmonary hypertension can be broadly classified into pre-capillary, post capillary and mixed aetiology groups and the main causes of PH are chronic left heart disease, chronic pulmonary disease and pulmonary embolism (Rosenkranz et al., 2016). In chronic left heart failure and in severe mitral regurgitation, the increase in left ventricular end diastolic pressure causes a rise in the mPAP over time as the pressure backs up into the pulmonary vasculature. Given that there are important prognostic implications to the diagnosis of pulmonary hypertension in heart failure and furthermore, it is of paramount importance to distinguish between pulmonary hypertension caused by left heart disease versus pulmonary arterial hypertension as the latter has specific treatment options available, PH warrants full and proper investigating.

In HFrEF, the prevalence of PH has been reported to be up to 70% in some studies; the presence of PH signals important disease progression and patients are more likely to have worse symptoms and higher risk of death (Miller et al., 2013). In order to distinguish between pre and post- capillary PH, the pulmonary arterial wedge pressure (PAWP) is used to estimate the left ventricular end-diastolic pressure (LVEDP) and a PAWP of equal to or less than 15mmHg suggests pre-capillary PH and a pressure of over 15mmHg signals post-capillary PH. The trans-pulmonary gradient (TPG) also helps to further classify the aetiology of PH and it is routinely used in transplantation assessment. TPG is defined as mPAP – PAWP, and in chronic left HF, the gradual increase in left sided pressures, initially causes a proportionate rise in the PAP therefore maintaining a normal TPG (less than 12 mmHg) (Rosenkranz et al., 2016). However, over time, sympathetic and RAAS activation may lead to excessive vasoconstriction in the pulmonary vasculature resulting in a disproportionate rise in the pulmonary artery pressure and ultimately a raised TPG; this is classified as mixed-PH (Fang et al., 2012).

Both pre and post capillary PH can lead to right ventricular failure and this is an important marker of disease progression. In the presence of PH, the RV afterload is increased and therefore, to maintain flow, the right ventricle has to adapt by increasing its contractility. Over time, RV dilatation occurs in order to maintain the stroke volume with uncoupling and increased in wall stress as a sequela, therefore RV volumetric studies are of significance when following up patients with PH (Vonk Noordegraaf et al., 2017).

Wave intensity analysis may provide novel insights into patients with PH and help differentiate the aetiology of the disease. Su et al, in one of the few WIA articles with human data, showed that there is increased wave reflection in patients with PAH and chronic thromboembolic

pulmonary hypertension (Su et al., 2017a). WIA may be a novel method of differentiating between pre and post capillary PH.

1.3.4. Heart Failure Treatment

There is a large body of evidence and trial data regarding drug therapy in patients with heart failure and reduced ejection fraction. The mainstay of treatment which has proven to reduce mortality and morbidity includes angiotensin-converting enzyme inhibitors (ACEi), angiotensin receptor blockers (ARB), Beta-blockers (BB), mineralocorticoid receptor antagonists (MRA), sodium-glucose cotransporter 2 inhibitors (SGLT2i) and angiotensin receptor-neprilysin inhibitors (ARNI) (Burnett et al., 2017). However, there is no clear evidence that any of these pharmacotherapies improve the mortality and morbidity outcomes of patient who have heart failure with a preserved ejection fraction (Khalid and Deswal, 2017b).

As described in the previous section, the sympathetic nervous system is inappropriately activated leading to adverse sequelae to the heart. Beta blockers such as bisoprolol have been widely used in clinical practice and it has been proven to counteract the effects of sympathetic stimulation; it improves left ventricular systolic/diastolic function, reduces the heart rate, prevents potentially malignant arrythmias and lowers the afterload and therefore reduces myocardial oxygen demand (Prijic and Buchhorn, 2014). In the cohort of patients with HFpEF, there has not been clear evidence in randomised controlled trials of a reduction in mortality rates with beta blockade. However, in some observational cohort studies beta blockers have been shown to reduce mortality (Fukuta et al., 2017).

ACEi such as ramipril, enalapril, captopril and lisinopril have good evidence to show that they reduce morbidity and mortality in patients with HFrEF. In a large meta-analysis performed by Garg et al, they showed that ACEi significantly reduced mortality and hospital admission for a broad range of patients and furthermore, the patients with the lowest ejection fractions seemed to have the greatest benefit (Garg and Yusuf, 1995). Similar evidence exists for ARB and especially when they are used in combination with an ACEi, ARBs such as valsartan has been shown to significantly reduce mortality and morbidity when used in combination therapy (Cohn and Tognoni, 2001). MRAs such as spironolactone have also been proven to be beneficial to the outcomes of patients with HFrEF, moreover they are also associated with reduced fibrosis formation and promotes cardiac remodelling (Sztechman et al., 2018; Pitt et al., 1999). ANRIs are a relatively new class of drugs. Neprilysin is the enzyme which metabolises natriuretic peptides and ARNIs work in concert by inhibiting RAAS and augmenting the action of natriuretic peptides (McMurray et al., 2013). The PARADIGM-HF trial comparing sacubitril/valsartan to enalapril showed that sacubitril/valsartan was superior to enalapril in the composite outcome of cardiovascular death or hospitalisation (Smith et al., 2018).

There have been great interest in SGLT2i therapy in heart failure with promising results. As mentioned earlier in this chapter, there have been recent trails which showed the efficacy and benefits of adding SGLT2i into heart failure treatment. The Emperor trial and Nassif et al has shown Empagliflozin and Dapagliflozin are effective in reducing all cause cardiovascular death and also improves quality of life in patients with HFpEF (Anker et al., 2021; Nassif et al., 2021). Similarly, in patients with HFrEF, both Empagliflozin and Dapagliflozin have shown improvement in survival and also better renal outcomes (McMurray et al., 2019). In the Emperor-reduced trial, other than improved survival, the rate of glomerular filtration rate

decline was slower in the cohort treated with Empagliflozin (Packer et al., 2020). As such, the 2021 and the focused 2023 ESC heart failure guidelines support the use of SGLT2i in both acute and chronic heart failure (McDonagh et al., 2023).

Cardiac resynchronisation therapy (CRT) is an important non-pharmacological treatment option for selected patients with HFrEF. There are two types of devices, CRT-P which paces the right atrium and both ventricles and CRT-D which has the same functions as a CRT-P but it also incorporates an implantable cardioverter defibrillator. There are three leads, one to the right atrium, one to the right ventricle and one lead reaches the left ventricle via the coronary sinus. Currently the main selection criteria for CRT implantation are an ejection fraction of equal to or less than 35%, left bundle branch block with a QRS duration of equal to or more than 150 milliseconds and at least NYHA class II symptoms despite optimal medical therapy (Ojo et al., 2017). Many randomised controlled trials such as REVERSE, RAFT and MADIT-CRT, have confirmed the beneficial effects of CRT devices.

1.3.5. LVAD Therapy

The advent of durable left ventricular assist devices has revolutionised the treatment and outcomes of patients with advanced heart failure. Whilst the number of heart transplantations being performed has been relatively static, the implantation of LVADs continues to rise (Kirklin et al., 2013; Goldstein et al., 2019). In the UK, there were 59 durable LVADs implanted in 2022/2023 which was 31% higher than the 2021/22 period. The two main indications for LVAD therapy are bridge to transplantation and destination therapy for those patients who are not suitable for transplantation. LVAD therapy has been shown to improve prognosis in patients with advanced heart failure, in the Momentum-3 final report, 76.9% of patients with a

Heartmate 3 were alive and free of disabling stroke at two years (Mehra et al., 2019). In some studies it has enabled up to a quarter of patients to receive a heart transplant within a 3-year period in the UK (Parameshwar et al., 2019).

An LVAD provides an alternative mechanism for blood to be pumped from the left ventricle to the systemic circulation and consists of a pump, a driveline which is tunnelled subcutaneously in order to be connected to the system controller, and an external power source. The pump drains blood from the apex of the left ventricle (inflow) and pumps it to the ascending aorta via a tube graft anastomosed onto the ascending aorta (outflow). The Heartmate II system (Thoratec, Pleasanton, USA) is an axial flow pump whereas the current generation Heartmate III system is a centrifugal pump with a magnetically levitate rotor (Lim et al., 2017).

As in the normal heart, LVADs are sensitive to different pre-load and afterload conditions. However, in LVADs the pump flow can fall rapidly with reduction of preload and an increase in afterload can significantly alter cardiac output. The pressure difference between the LV pressure and the aortic pressure is called the pump head pressure and the flow produced by the LVAD is inversely correlated to the pump head pressure. Any clinical scenario which results in a raised systemic vascular resistance and therefore raised aortic pressure and/or low left ventricular pressure will alter the pump flow (Lim et al., 2017). In conditions where the preload of the LV is decreased, there is a possibility of "suction events' occurring where the LV wall is sucked into the pump and therefore completely or partially occludes the inflow of the pump causing an acute drop in flow.

During exercise, there is a limited response to increase in cardiac output in patients with an LVAD, mainly because the pump speeds are fixed. However there is a degree of compensation as during exercise, there is an increase in venous return, which increases LV preload, and heart rate. There is evidence that the mean pump flow does increase during exercise and it has been proposed that this is because of the cardiac cycle spends more time in systole where the pump flow is greater due to the increased heart rate (Akimoto et al., 1999).

An LVAD ultimately leads to unloading of the LV, reducing its dimensions almost immediately, and leading to histological changes including a reduction of wavy fibres and contraction band necrosis; both are markers of myocyte damage, however there is associated increase in fibrosis (McCarthy et al., 1995). It has also been shown that LVAD implantation promotes sarcoplasmic reticulum calcium adenosine triphosphatase 2a expression and in some studies this is back to normal expression levels at 20 days following implantation (Madigan et al., 2001).

The RV is key to LVAD functioning and for adequate cardiac output. The RV is required to pump adequate blood to the left side of the heart in order for there to be an adequate pre-load for the LV and LVAD. Implantation of a LVAD itself has significant beneficiary effects on the RV. LVADs decrease the RV afterload and over time it may reverse, what was once thought to be, fixed pulmonary hypertension, improve RV geometry and allow them to be eligible for transplantation (Zimpfer et al., 2007; Kukucka et al., 2011). However, in the immediate peri-operative period, there is an acute increase in venous return to the right side of the heart and together with intravenous fluid and blood product administration, this can lead to early RV failure, especially in patients with suboptimal RV reserve (Lim et al., 2017). Hence there is a

need to be able to assess the RV thoroughly pre-operatively and WIA may have the potential of providing important information to improve patient selection for LVAD therapy.

1.4. Wave Intensity Analysis

1.4.1. Principles of Wave Intensity Analysis

The concept of Wave Intensity Analysis (WIA) was first introduced by Parker and Jones in 1990 (Parker and Jones, 1990b). Its foundations are based on the development of gas dynamics in the Second World War when advances in aviation and aerodynamics such as jet engines and rockets required a new approach (Parker, 2009). WIA marks a departure from traditional Fourier analysis where waves are viewed as sinusoidal wavetrains, instead, it views waves as a sequence of small wavelets/wavefronts which combine to produce the observed wave(Parker, 2009). Therefore the results of WIA are produced in the time domain and not in the frequency domain, allowing clinicians and investigators to easily relate arterial waves to the precise events in the cardiac cycle (Su et al., 2017a).

Wave intensity is defined as the product of the change in pressure (P) times the change in velocity (U) during a given interval, it is positive for forward waves and negative for backward waves(Parker, 2009). WIA has the dimensions of power/unit area with the units of W/m^2. This allows the observer to assess whether waves are forward or backward waves by the net wave intensity at any time point during the cardiac cycle.

A wave originating from a proximal part of an artery can be either a forward compression wave (FCW) which increases the pressure and flow within the artery or a forward decompression wave (FDW) which decreases the pressure and flow. Conversely waves arising from the distal

portion of any artery can either be a backward compression wave (BCW) which increases the pressure whilst decreasing flow or a backward decompression wave (BDW) which decreases the pressure but increases the flow in the artery.

Table 1. Definition of forward vs backward going waves in P, U and dI

	d*P*	d*U*	d*I*
Forward	>0 compression	>0 acceleration	>0 positive
	<0 decompression	<0 deceleration	
Backward	>0 compression	<0 deceleration	<0 negative
	<0 decompression	>0 acceleration	

dP is the change in pressure, dU is the change in velocity and dI is the net wave intensity. The relationship between forward and backward waves are shown in this table. dI >0 and positive indicates a net forward wave and dI of <0 and therefore negative indicates a backward wave.

Determining the local wave speed can be difficult and there are two methods, the Pressure-Velocity (PU) loop method and the sum of squares method. The PU-loop method relies on linearity of the PU-loop where pressure is plotted against velocity and that the slope of the curve should equal local wave speed (*c*); however, this is only true if there are only forward waves present. Clinically, we would expect in early systole a period where only forward compression waves are present arising from ventricular contraction and before any backward reflections have had time to return (Parker, 2009; Davies et al., 2006b). However, there could be practical problems with this method namely temporal delays in pressure and velocity measurements and in some circumstances, this is not possible for example in the coronary circulation. In early animal work, the PU-loop method has been successfully employed in the pulmonary circulation assuming there are no reflected waves in early systole (Hollander et al., 2001). The sum of

squares method was developed as an alternative and local wave speed is calculated with the following equation (Parker, 2009; Su et al., 2017a; Davies et al., 2006b):

$$c = \frac{1}{\rho}.\sqrt{\frac{\Sigma dP^2}{\Sigma dU^2}}$$

In this equation, c is local wave speed, ρ represents blood density and it is assumed to be 1040 kg/m^3 and the sum of dP and dU squared is taken over 1 cardiac cycle.

The full mathematical proof of WIA has been published by Parker and colleagues (Parker, 2009). In brief , based on the 'water hammer' equations, Parker and Jones have shown that the forward and backward components can be found and the wave intensity for separated waves can be calculated with the following equations (Parker, 2009):

$$dP_{\pm} = \frac{1}{2}(dP \pm \rho c dU)$$

$$dU_{\pm} = \frac{1}{2}\left(dU \pm \frac{dP}{\rho c}\right)$$

$$dI_{\pm} \equiv dP_{\pm}.dU_{\pm} = \frac{\pm 1}{4\rho c}(dP \pm \rho c dU)^2$$

The pressure and velocity waveforms can then be calculated by adding up the wavefronts(Parker, 2009). P_0 and U_0 are pressure and velocity at t=0:

$$P_{\pm}(t) = \sum_{0}^{t} \mathrm{d}P_{\pm}(t) + P_0$$

$$U_{\pm}(t) = \sum_{0}^{t} \mathrm{d}U_{\pm}(t) + U_0$$

Armed with these mathematical principles, it is then possible to process and separate the *P* and *U* waves into their forward and backward components and generate d*I* as illustrated below.

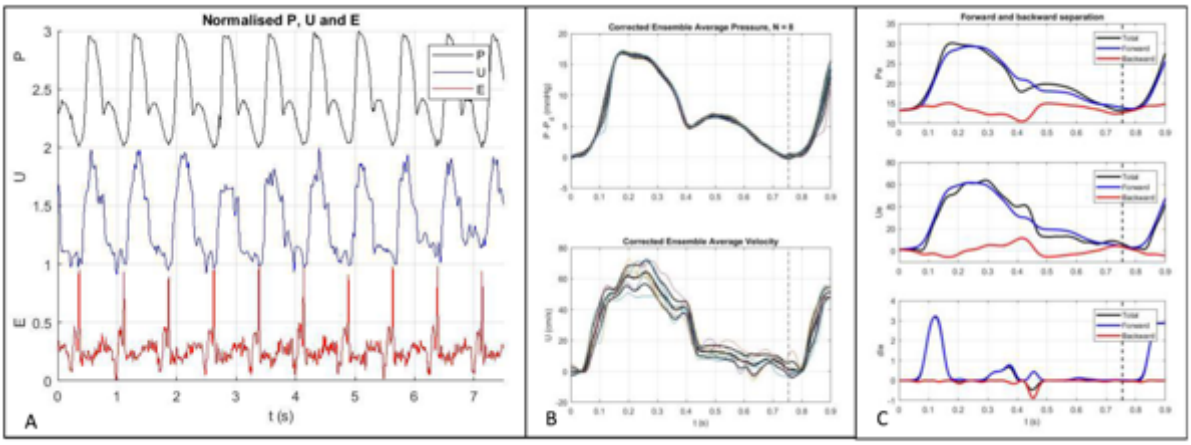

Figure 1. Shows a sample data set of pressure and velocity and an ECG trace. Fig1B., Shows the ensemble average of each beat of P and U. Fig 1C., shows the forward and backward separation of P and U and the wave intensity dI calculated and displayed.

Figures 1A, 1B and 1C display a sample data set from a patient with heart failure collected as pilot data in our unit. Figure 1A shows the individual pressure and velocity data acquired with an ECG trace displayed as well. Figure 1B shows the ensemble average of each beat of *P* and *U*, with the R wave of the ECG defining the start of each beat. Figure 1C shows clear separation of *P* and *U* in their forward and backward components and the wave intensity calculated for the forward and backward components. Looking at the d*I* graph, a FCW can be identified in early systole with two subsequent FDW and a single BDW resulting from a wave being reflected in the pulmonary vascular tree. From the backward reflected waves, the wave reflection index

(WRI) can be calculated and is defined as the ratio of energy of the backward wave to the energy of the incident FCW in mid systole (Su et al., 2017a). In the human aorta, it has been shown that in early systole there is consistently an incident FCW followed by a small reflected BCW, then in late systole, just before the closure of the aortic valve, an FDW can be observed (Hughes et al., 2013).

1.4.2. Reservoir-Wave Approach

The reservoir wave approach (RWA) separates the pressure in arteries into two distinct components, one being the reservoir pressure produced by the kinetic energy stored in the elastic arterial walls during expansion and contraction (the Windkessel effect) and secondly, the pressure that drives the waves (Parker, 2009; Hughes et al., 2013). RWA was first introduced in 2003 by Wang and colleagues (Wang et al., 2003), and it was developed to further improve on WIA. It is based on the theory that pressure in an arterial system does not only change due to the transition of waves but also due to the change in volume of the elastic tubes or the change in the ventricles' compliance or elasticity during systole and diastole (Tyberg et al., 2014). Thus, to accurately quantify and assess the effects of the forward and backward waves, the reservoir pressure must be excluded first before WIA is performed; therefore total arterial pressure is equal to the sum of the reservoir pressure $P_{reservoir}$ and the wave-related pressure P_{wave} also known as the excess pressure P_e (Wang et al., 2003; Tyberg et al., 2009).

The mathematical theory of the reservoir pressure has been published by Wang and colleagues in 2003 (Wang et al., 2003) and they make use of the Windkessel theory which states the variation of $P_{reservoir}$ ($P_{\mathrm{Windkessel(Wk)}}$) is determined by the differences between inflow and outflow and the changes in volume (Sagawa et al., 1990). To determine $P_{reservoir}$, the rate of

change ($dP_{reservoir}/dt$) must be proportional to the rate of change of the volume within a structure through the proportionality constant dP/dV, which is the reciprocal of compliance (C) and since the rate of volume is the immediate difference of inflow (Q_{in}) and outflow (Q_{out}) (Tyberg et al., 2009):

$$\frac{dP_{reservoir}}{dt} = \frac{1}{C}\,(Q_{\text{in}} - Q_{\text{out}})$$

Where outflow (Q_{out}) is assumed to be driven by the gradient between $P_{reservoir}$ and the arterial asymptotic pressure P_{∞}:

$$\mathrm{Q}_{out} = \frac{P_{reservoir} - P_{\infty}}{R_{reservoir}}$$

Therefore substituting Q_{out} with this equation:

$$\frac{dP_{reservoir}}{dt} = \frac{Q_{\text{in}}}{C} - \frac{P_{reservoir} - P_{\infty}}{\mathrm{RC}}$$

In the above equations R denotes the resistance of the systemic vascular resistance and as demonstrated by Wang and Tyberg the solution to this equation is (Wang et al., 2003; Tyberg et al., 2009):

$$P_{\text{reservoir}}(t - t_0) = P_{\infty} + (P_0 - P_{\infty})e^{\frac{-1}{RC}} + e^{\frac{-1}{RC}}\int_{t_0}^{t}\frac{Q_{in}(t')}{C}e^{\frac{t'}{RC}}dt'$$

The reservoir-wave approach has been successfully demonstrated to be useful in analysing haemodynamics and arterial wave forms(Wang et al., 2011). In humans, using the RWA, Davies et al demonstrated that the aortic pressure waveform is made up with three components: waves arising from the left ventricular contraction, Windkessel (reservoir), and reflected waves. Furthermore, during diastole, waves do not affect the pressure and flow but rather diastolic pressure is the result of capacitative discharge of pressure from the reservoir (Davies et al., 2007).

The reservoir-wave approach to haemodynamics in the arterial system has been further developed by Parker et al in 2012. In this work, they make an important distinction between reservoir pressure and Windkessel pressure. Reservoir pressure is delayed by wave travel and it is dependent on the nature of flow in the vascular system, whereas Windkessel pressure is assumed to be instantaneously uniform throughout the vascular tree; this is only possible if the wave speed is infinite. Their main conclusion was that the reservoir pressure is the minimum hydraulic work performed by the ventricles and the excess pressure is additional work done by the ventricles in addition to this minimum work (Parker et al., 2012).

In the systemic circulation, the reservoir-wave approach has been widely studied and clinical outcomes of cardiovascular events have been correlated with reservoir pressure indices. From a sub study of the Anglo-Scandinavian Cardiac Outcomes Trial (ASCOT), the excess pressure integral (XSPI) was developed and it was shown to be effective in predicting cardiovascular dysfunction and cardiovascular events (Davies et al., 2014). In 2014, Hametner et al showed that both reservoir and excess pressures were both clinical predictors of cardiovascular events using data from 674 patients (Hametner et al., 2014). In the clinical setting, flow velocity data

is not routinely available and requires invasive monitoring, therefore there has been interest in developing algorithms which would allow reservoir pressure and excess pressure to be derived using pressure data only (Aguado-Sierra et al., 2008).

In contrast to the systemic circulation, there is relatively limited reservoir-wave approach data in the pulmonary circulation. Bouwmeester published preliminary data from anaesthetised dogs (Bouwmeester et al., 2013, 2014) and there is limited data from humans (Ghimire et al., 2016; Su et al., 2017b). However, pertinent to this study, Su et al showed that the reservoir pressure and excess pressure increased in patients with pulmonary arterial hypertension (Su et al., 2017b).

1.4.3. Wave Intensity Analysis in the Systemic Circulation

Since its original description, WIA has been investigated by different groups mainly in the systemic circulation. Various studies have been performed in the aorta, carotids, venous circulation and the chambers of the heart. There are limited data of WIA in the pulmonary circulation.

In one of the first human studies performed in the ascending aorta in 1990, Parker and Jones showed that WIA can be applied to the human systemic circulation and that forward going waves dominates both the acceleration and deceleration phases of blood flow, i.e. in both systole and diastole of the cardiac cycle (Parker and Jones, 1990a). This study was carried out using linearized analysis and performed in the time domain unlike impedance analyses. Other groups have applied WIA to the ascending aorta and looked at wave reflection in the systemic circulation and the magnitude of the forward expansion waves in relation to ventricular

contractility and systemic vasoconstriction. Koh et al measured pressure and velocity in the ascending aorta in patients undergoing cardiac surgery and looked at the timing and magnitude of reflected waves. They found that the reflected waves could be accurately assessed and that the magnitude of the reflected waves directly correlated to a secondary increase in aortic pressure (Koh et al., 1998). As expected forward compression waves have been shown to increase when the force of the left ventricular contraction is increased by inotropic support and decreased under negative inotropic conditions such as beta blockade (Jones et al., 2002). Expansion wave intensity was also shown to be reduced when vasodilatation was induced using intravenous nitroglycerin. This work suggests that WIA could be a useful tool in assessing ventriculo-arterial coupling.

The concept of WIA and its unique benefit of performing analyses in the time domain led investigators to study left ventricular filling dynamics using this relatively new technique. MacCrae and colleagues applied WIA in the left ventricle in dogs. They described '5 peaks' which were observed during a single cardiac cycle. The first peak was a large negative peak caused by backward travelling expansion waves that accelerate blood from the left atrium into the left ventricle as the pressure in the LV was low during diastole. Peak 2 was a positive compression wave related to the rise in left ventricular pressure. Peak 3 was related to the continued rise in left ventricular pressure whilst the velocity decreased. Peak 4 was another forward going wave associated with further LV pressure rise by the left atrial kick. Finally, peak 5 was a backward going wave caused by further increase in pressure and decreased in velocity as end diastole is reached (MacRae et al., 1997b). This study suggested that WIA could be a useful tool to assess left ventricular filling status but unfortunately this has not translated

into human studies. A follow up study was performed in 2007 which applied reservoir pressure with WIA again in LV filling dynamics using dogs (Flewitt et al., 2007a).

The concept of 'diastolic suction' has been investigated with WIA in both the left and right ventricles. Diastolic suction has been defined as the amount of energy remaining following mitral or tricuspid valve opening and therefore the force that pulls blood into the left or right ventricles in early diastole. These studies have found that the energy of the backward going waves generated by left or right ventricular relaxation is proportional to the rate at which ventricular elastance decreases and also completeness of ejection (Wang et al., 2005a; Sun et al., 2006).

Non-invasive techniques of WIA have been developed and investigated at the Carotid arteries. Using pulsed-wave Doppler techniques with ultrasound, investigators have been able to perform WIA by estimating flow velocities and recreating PU-loops to calculate local wave speed. Significant differences in wave patterns, speed and characteristics have been shown in different peripheral arteries when comparing the carotid, brachial and radial arteries (Zambanini et al., 2005). The reproducibility of this technique had also been verified in a subsequent study (Niki et al., 2002). Using similar non-invasive techniques, Ohte et al performed WIA utilising the carotid arteries to look at left ventricular performance during early and end systole. They concluded that wave intensity may be a useful clinical tool to assess LV performance as the early forward compression waves corresponded to early LV contraction and the second forward decompression wave corresponded to late systole/early diastole during isovolumetric relaxation; the forward compression wave intensity directly correlated with rate of LV pressure

rise and the forward decompression wave corresponded with the rate of LV relaxation (Ohte et al., 2003).

Interestingly, Niki's group, using the carotid artery, compared wave intensity of patients with mitral valve regurgitation before and after mitral valve surgery. Patients with significant mitral valve regurgitation had reduced wave intensity in the forward decompression wave in late systole when compared to control subjects without mitral regurgitation. Following surgery with either mitral valve repair or replacement, they observed that the 'second peak' or the forward decompression wave intensity significantly increased suggesting that the resolution of mitral regurgitation had improved the LV's performance in late systole presumably due to an increase in forward flow through the left ventricular outflow tact (Niki et al., 1999).

Finally, WIA in patients with chronic heart failure has also been studied in the systemic circulation, again utilising non-invasive measurements of the carotid artery. Curtis et al found that patients with heart failure had significantly reduced forward compression wave intensity with the incidence of the forward compression wave also delayed. There was markedly increased wave reflection in the heart failure group of patients. They concluded that, in heart failure, the ability of the left ventricle to generate a forward compression wave is reduced and that the increased wave reflection could be a compensatory mechanism to maintain systemic blood pressure as a compensatory mechanism (Curtis et al., 2007).

1.4.4. Wave Intensity Analysis in the Coronary Circulation

The coronary circulation differs from the systemic circulation in that the majority of the coronary flow occurs during diastole when the heart is relaxed. Furthermore, whilst the pressure

waveform in the coronary arteries mimics that of the aorta, the velocity waveforms are markedly different (Hughes et al., 2008). P-U loops formed from the coronary circulation are therefore also markedly different form the systemic circulation and it is not possible to determine a linear portion during the cardiac cycling; this suggests that determining local wave speed may be inaccurate using the P-U loop method in the coronary circulation.

Sun and colleagues showed that it is possible to determine the contribution of proximal aorta flow through the coronary ostia versus the distal 'downstream' effects of the microvasculature on coronary pressure and velocity (Sun et al., 2000). Following from this, WIA has been used to provide a mechanism for coronary diastolic filling. A diastolic 'suction' wave was described by Davies et al. This group characterised WIA in the coronary circulation and found six waves are present which drive coronary circulation. The most dominant was a backward travelling 'suction' wave in diastole which is generated by microvascular decompression, this also coincided with a significant rise in coronary velocity (Davies et al., 2006a; Broyd et al., 2017).

As the different wave forms in the coronary circulation have been characterised , WIA has been used to investigate coronary artery disease. WIA is the basis of a widely used clinical tool in diagnostic cardiology called instantaneous wave-free ratio (iFR). The iFR calculated during the wave free period, where resistance is minimised and constant, provides an index for coronary stenosis severity comparable to fractional flow reserve with the additional benefit of not requiring the administration of any drugs such as adenosine to achieve hyperaemia (Sen et al., 2012). Since its original description, iFR has entered into clinical practice internationally and it has been validated by two large randomised controlled trials showing it non-inferiority over fractional flow reserve (Götberg et al., 2017; Davies et al., 2017).

WIA has also been used to investigate myocardial viability. There are several different techniques to assess myocardial viability following an infarct with cardiac magnetic resonance imaging (CMR) with gadolinium enhancement being the most commonly used. Although useful and yielding an array of data, CMR is time consuming and resource intensive. Ryan et al performed WIA in patients with ischaemic cardiomyopathy and analysed the backward compression wave energy in viable and non-viable coronary territories. They found that the backward compression wave energy was significantly higher in viable myocardial territories compared to nonviable segments and that this performed similarly to CMR late-gadolinium uptake in predicting viability (Ryan et al., 2022). This holds promise to be further developed as a clinical tool in the management of patients with ischaemic cardiomyopathy.

1.4.5. Wave Intensity Analysis in the Pulmonary Circulation

Unlike in the systemic circulation, there is limited WIA data in the pulmonary circulation and all human data is almost exclusively in the setting of pulmonary arterial hypertension and in the cohort of patients with chronic pulmonary thromboembolism. The most widely used haemodynamic parameter to determine severity of pulmonary hypertension and used as a prognostic marker is pulmonary vascular resistance (PVR). However, as PVR is defined as the ratio between the transpulmonary gradient and cardiac output, it only accounts of the non-oscillatory components of RV work and does not take into consideration the compliance of the pulmonary arterial circulation and its contribution to wave propagation (Su et al., 2016).

Su and colleagues compared WIA in patients with pulmonary arterial hypertension (PAH), chronic thromboembolic pulmonary hypertension (CTPH) and normal controls. They found

that wave speed was significantly higher in the PAH and CTPH groups compared to controls, suggesting that arterial stiffness was greater in patients with pulmonary hypertension and reduced pulmonary arterial compliance. Furthermore, wave reflection was also greater in the diseased populations indicating distal vascular impedance mismatch (Su et al., 2017a). Su's group also investigated the reservoir and excess pressure in these groups of patients. They found that in PAH and CTPH patients, the asymptotic pressure (the theoretical pressure at which flow ceases in the microvascular circulation), the reservoir pressure related to arterial compliance and the excess pressure which is caused by forward and backward going waves were all increased (Su et al., 2017b). In a follow up study in the CTPH group, they investigated the changes in wave propagation following pulmonary endarterectomy, finding that although mean pulmonary artery pressure, PVR, and wave speed all reduced, these patients continued to produce significant wave reflection with insignificant reduction in the wave reflection index at three months post-surgery (Su et al., 2019). This implies that despite an improvement or resolution in pulmonary hypertension, there still remains vascular impedance mismatch. Finally, Su's group investigated wave reflection and arterial stiffness using the augmentation index based on pulse wave analysis and they found that this technique was inaccurate and highly variable and therefore should not be pursued (Su et al., 2021).

Investigators have also looked into the effects of wave reflection and right ventricular function following lung resection and in acute pulmonary embolism in dogs (Glass et al., 2023; Yoshida et al., 2021). However, to date, there is no available data in the literature on WIA in the pulmonary circulation in the heart failure population and the data generated from this project will add to the growing body of evidence in WIA in the pulmonary circulation.

1.5. The Right Ventricle and Current Techniques of Assessment

For many decades, the RV had been neglected as it was thought to be of little physiological importance. A study performed in dogs in 1943, Starr et al showed that after electrocautery ablation of the RV free wall, not only did the dogs survive, but there was little change in the pulmonary venous pressure. Their conclusion was that the RV was merely a passive conduit (Starr et al., 1943) and therefore little work was done on the RV following this. However, this is no longer the case and there has been a paradigm shift with the RV being regarded as a structure of critical importance.

It has been proposed that it is desirable to measure right heart function independent of its loading conditions. This is important because the preload and afterload is different between patients and most treatments that alter pulmonary arterial pressure will affect the afterload. To give a clinical example, the RV loading conditions of patients before lung transplantation is very different to post transplantation and therefore during the patient's assessment, measuring the RV function independent of its loading conditions is of paramount importance (Vonk-Noordegraaf and Westerhof, 2013).

The interaction between the ventricles and the arterial system is known as "ventricular-arterial coupling" and it is a key factor for overall cardiovascular performance. Ventricular-arterial coupling is defined as the ratio between arterial elastance (Ea) and end-systolic elastance (Ees) of the ventricle (Antonini-Canterin et al., 2013). In 1988, Dell'Italia and colleagues found that right ventricular systolic performance can be estimated by a time varying elastance model (Dell'Italia and Walsh, 1988). The pressure-volume relationship and the pressure-volume loop

analysis of the right ventricle can be used to calculate end-systolic elastance. Systolic elastance is generally accepted as a load- independent characterisation of the ventricles (Vonk-Noordegraaf and Westerhof, 2013). Therefore over time, clinicians have developed methods of measuring end-systolic elastance in the clinical setting using invasive right heart catheterisation and cardiac-MRI (Trip et al., 2013). Furthermore, ventricular-arterial coupling and its parameters has also been calculated using echocardiography with relative accuracy (Antonini-Canterin et al., 2013).

In a study performed by Guihaire et al, where a porcine model of pulmonary hypertension was used, they found that the usual indicators of RV function were actually associated with ventriculo-arterial coupling rather than, what is often thought to be, ventricular contractility (Guihaire et al., 2013). This implies that the usual echocardiographic indices of RV function such as fractional area change in tricuspid annular plan systolic excursion (TAPSE) are more associated with ventricular-arterial coupling rather than contractility (Amsallem et al., 2018). Albeit these results were obtained in a model of chronic pressure overload and may not be the case in right ventricles under normal pulmonary artery pressures. There is also evidence to suggest that altered ventricular-arterial coupling occurs before actual pump dysfunction in heart failure and therefore it could be used as an early indicator for heart failure (Prabhu, 2007).

Measuring Ees, Ea and using pressure volume curves have mainly been used in animal models as they require pressure and volume data simultaneously and data obtained in human subjects are not prevalent in the literature; however, advances in 3D echocardiography may allow for simultaneous measurement of RV pressure and volumes during right heart catheterisation (Vonk-Noordegraaf and Westerhof, 2013).

The use of a conductance catheter to measure ventricular volumes, stroke volumes and cardiac output was developed in the 1980s (BAAN et al., 1981). This technique utilises the electrical conductance of blood within the ventricles and relies on multiple electrodes being deployed within the ventricle and allows clinicians to measure pressure-volume loops in real time (STEENDIJK, 2004). The end systolic pressure-volume relation and end-systolic elastance have been investigated as a load-independent marker of ventricular systolic function (Kass et al., 1987). The conductance catheter has also been validated in the assessment of the right ventricle (Danton et al., 2003; Bishop et al., 1997). Using this technique, the ratio between right ventricular ends-systolic elastance and pulmonary arterial elastance have been used to assess ventricular-arterial uncoupling (Brener et al., 2020).

1.5.1. Echocardiography

One of the most accessible and commonly used first-line imaging modalities to assess cardiac function is echocardiography, and it is heavily relied upon in most hospitals around the world. Historically, echocardiographic assessment of the RV has been, in the most part, qualitative rather than quantitative. Over recent years, clinicians have accepted that RV function is an important prognostic indicator in a wide range of cardiac disease, especially in chronic heart failure (Ghio et al., 2001). Therefore, there has been revived interest in developing more accurate quantitative measurements of the RV on echocardiography.

The RV's structural geometry is much more complex than that of the left ventricle (LV) and therefore this makes it harder to accurately image and assess on echocardiography (Jones et al., 2019). The LV is cylindrical in shape with a conical apex whilst the RV is often described as crescent shaped and wraps around the LV, therefore parts of the RV are difficult to visualise on

echo (Muresian, 2016). Moreover, the appearances of the RV can be significantly different depending on the echo plane used.

The way that the RV contracts is also significantly different compared with the LV. In normal subjects, the RV pumps against the pressures of the pulmonary artery which is much lower than that of the aorta. Therefore, it is designed to deal with change in volume rather than pumping against high pressures. The RV muscle fibres are arranged longitudinally and when contracting, they contract along the longitudinal axis and therefore has similar mechanics to a piston pump. However, there are also muscle fibres arranged circumferentially and together with the action of the septal contractions, the RV free wall and septum act like bellows (Jones et al., 2019).

Right ventricular fractional area change (RVFAC) has been found to be useful parameters of RV function. RVFAC is defined as *"(end diastolic area - end systolic area) / end diastolic area x 100"* (Jones et al., 2019). The American Society of Echocardiography guidelines have stated that RVFAC correlates well with RV ejection fraction on cardiac MRI and that a lower reference value of 35% should be considered normal (Rudski et al., 2010). A meta-analysis performed by Lee et al compared TAPSE to RVFAC and found that fractional area change provides a more accurate assessment of RV systolic function and suggested that RVFAC should be included in the routine echo assessment RV function (Lee et al., 2018). However the main limitation of using right ventricular fractional area change is that it requires good endocardial border delineation which can be difficult to achieve depending on the quality of the scan and also in highly trabeculated RVs (Jurcut et al., 2010).

In the left ventricle, the ejection fraction acquired two dimensionally is routinely used as a marker of LV function in clinical practice. In contrast in the RV, two-dimension (2D) estimation of the ejection fraction is difficult and often inaccurate due to the aforementioned geometry of the RV. The 2D estimation of RV EF can be divided into area-length methods or disk summation methods, however both are not recommended as reliable techniques for assessing RV function (Jones et al., 2019). Given this, and with the advent of three dimensional (3D) capable ultrasound systems, 3D volume measurement and estimation of ejection fraction has been developed.

Again, the technical difficulty with 3D volume assessment of the RV is the geometry of the right ventricle and accurately estimating the volume from the tricuspid valve, including the entire right ventricular outflow tract (RVOT) to the pulmonary valve. It has been found that a modified apical view is the best method with the echo transducer placed lateral to the true apex (Jones et al., 2019).

It is has been shown that using 3D echocardiography is more accurate in estimating the RV's volume and therefore its ejection fraction. Leibundgut et al used real time 3D echo to measure RV volumes and ejection fraction in humans and compared the results with MRI, which showed that the measurements obtained with 3D echo correlated well with MRI (Leibundgut et al., 2010). This therefore maybe a good alternative to cardiac MRI as it is less time consuming.

Tricuspid annular plane systolic excursion (TAPSE) is one of the most widely used echocardiographic measurements for the estimation of RV function. It has several clear advantages but also significant limitations. TAPSE was first validated in 1984 by Kaul et al

with radionuclide angiography and it is the excursion of the tricuspid valve plane from end diastole to end-systole in the four chamber view (Kaul et al., 1984). This was found to be a good reflection of RV function given that most of the RV muscle fibres are arranged longitudinally. This means that the TAPSE only assesses RV function in longitudinal contraction, but as described above, there is a radial component to RV contraction which may become important if the RV becomes dilated (Jones et al., 2019). The obvious advantage of TAPSE is its simplicity and it can be reproduced reliably by different operators. However, once again, the most important limitation is that it assumes the movement of one structure within the RV to represent the function of the entire chamber (Aloia et al., 2016).

Similar to TAPSE, Doppler tissue imaging (DTI) or tissue velocity at the tricuspid annulus, measures tissue displacement of the RV basal free wall during the cardiac cycle. Like TAPSE, it measures only a small segment of the RV and therefore cannot be used if there are regional wall-motion abnormalities present (Dutta and Aronow, 2017). Continuing on Doppler velocities, right ventricular index of myocardial performance (RIMP) is a calculation based on tissue Doppler velocities and it is defined as (*Tricuspid valve closure time – Ejection time)/RV ejection time* (Jones et al., 2019). The limitations of RIMP are that it is not reliable in patients with irregular heart rates, such as atrial fibrillation and in any condition which results in an elevated right atrial pressure as this will alter the isovolumic relaxation time and therefore tricuspid valve closure time (Dutta and Aronow, 2017). Although there have been studies which have shown that RIMP is a prognostic factor in patients with precapillary pulmonary hypertension and may hold some clinical value as a stand-alone measurement and in serial monitoring (Grapsa et al., 2015).

Right ventricular strain and the strain rate is a measure of ventricular muscle deformation. It is the percentage change in length of a segment of myocardium and the strain rate represents strain change over time (Jones et al., 2019). The most commonly used techniques to measure RV strain are 2D and 3D speckle-tracking echocardiographic strain. 2D speckle tracking strain is a relatively new technique in assessing RV function and it was originally developed for the analysis of LV function. This technique essentially tracks the 'speckles' in the myocardium generated by interference of the ultrasound waves and it has been shown to be a more sensitive and accurate measurement in patients with pulmonary hypertension, pulmonary embolism, myocardial infarction, cardiomyopathies and heart failure compared to the conventional measurements described above (Longobardo et al., 2017). There are a few limitations of 2D speckle-tracking strain echo. Firstly, the software used to calculate RV 2D strain was originally designed for the LV and augmented for the use in the RV. The software therefore has to be 'tricked' to calculate strain as the images are inverted. Secondly, RV speckle-tracking is only obtained in the apical four chamber view whereas in the LV, it is obtained by three different views (Longobardo et al., 2017).

3D speckle-tracking is still a relatively novel technique for assessing RV function. It holds promise to be more accurate than 2D speckle tracking as it theoretically overcomes the issue of the RV's geometry. In Japan, Ishizu and colleagues have developed a new 3D speckle-tracking software which they validated against cardiac MRI data and were found to be comparable (Ishizu et al., 2017). With further development and research, it may become a reliable and reproducible technique in assessing RV function in routine clinical practice.

1.5.2. Cardiac Magnetic Resonance Imaging

Cardiac magnetic resonance imaging (CMR) has been revolutionary in the diagnosis of a broad spectrum of cardiac conditions as well as the functional assessment of the heart. Over time, the application of CMR has been evolving and it is increasingly being used in clinical practice, for the purposes of this study the focus will be placed on the application of CMR in heart failure.

The main advantage of CMR is that it produces relatively high-resolution images without exposing the patient to any radiation. CMR works by creating a powerful magnetic field, roughly 30,000 times that of the earth's magnetic field depending on the magnet in the scanner, this in turn align the nuclear magnetization of the hydrogen atoms in the human body. These hydrogen atoms are then excited by specific radiofrequency waves and the signal generated are detected in the receiver coils of the scanner (Karamitsos et al., 2009). In broad terms, the images produced are displayed in two sequences based on the decay of the longitudinal and transverse components of the hydrogen atoms. T1 is the longitudinal relaxation and T2 is the transverse relaxation phase. In heart failure, the imaging sequence normally starts with T1 weighted for anatomy and chamber volumes are acquired in three long-axis and three short axis cine sequences (Peterzan et al., 2016). T1 weighted images normally show myocardium as dark and adipose tissue is bright, in T2 weighted images, water is bright and therefore any oedema in the myocardium will light up (Abdel-Aty et al., 2007).

The use of gadolinium in CMR to assess reperfusion in the myocardium was first described in the 1980s. Schaefer et al found that with the administration of gadolinium-diethylenetriamine pentaacetic acid (Gd-DTPA) together with CMR, several important things can be identified. Firstly, myocardium at risk could be identified following coronary occlusion and reperfusion;

secondly, in the T1 weighted sequence Gd-DTPA showed reperfused myocardium; thirdly, the reason for contrast enhancement of Gd-DTPA in reperfused myocardium is secondary to shortening of the T1 relaxation time (Schaefer et al., 1988). Following on from that work, late gadolinium enhancement (LGE) has been routinely used with CMR in the detection of scarring and fibrosis in the myocardium. It has been shown that the physiological basis of LGE in injured myocardium is due to prolonged washout of gadolinium because of decreased functional capillary density following irreversible injury (Rehwald et al., 2002; Karamitsos et al., 2009). Therefore, on CMR, in areas of myocardial damage, fibrosis or scarring, with gadolinium administration, those affected areas will appear to be bright on the T1 weighted sequences. The development of this technique has given clinicians valuable information on the viability of the myocardium following an ischaemic insult and thus guide revascularisation strategies.

The other main advantage of CMR is that it does not need to make any assumptions of the RV's geometry, as discussed previously that is the main limitation of echocardiography. Furthermore, CMR can image in all planes and the ventricular volumes acquired are very accurate. There is also no inter-variability between operators with different probe positions that can cause inconsistencies in echocardiography and therefore CMR is much more reproducible and consistent on serial imaging. Therefore, it has also become an invaluable tool in serial imaging over time in chronic conditions such as heart failure due to its consistency and also without exposing patients to radiation unlike computer tomography (CT).

In the context of heart failure, for any imaging modality, there are several pertinent questions that need to be answered: how impaired is LV and RV function, is it global or regional, what are the ventricular volumes and is there any dilatation, can the underlying aetiology of heart

failure be identified and are there any potentially modifiable components of the pathophysiology for which treatment can be targeted (Karamitsos et al., 2009).

In ischaemic cardiomyopathy, with the enhancement of gadolinium as discussed above, has become the gold standard to investigate the transmural extent of the damage and also myocardial viability; it has been shown that CMR with LGE can distinguish between reversible and irreversible ischaemic injury independent of when the infarct occurred (Kim et al., 1999). Furthermore, when CMR is compared with lower resolution scans such as single photon emission computed tomography (SPECT), whilst the rate of detecting transmural myocardial infarcts were similar, CMR was found to be superior at identifying smaller subendocardial infarcts which were often missed on SPECT (Wagner et al., 2003). In a landmark article by Kim et al demonstrated that CMR could be used to target revascularisation and showed an inverse relationship between the degree of transmurality of the infarct with improvement of the myocardium after surgical or percutaneous revascularisation (Kim et al., 2000).

Differentiating between dilated cardiomyopathy and other non-ischaemic causes of heart failure from ischaemic cardiomyopathy can sometimes be challenging. It is a clinical diagnosis and defined by the presence of left ventricular dilatation and left ventricular systolic dysfunction in the absence of abnormal loading conditions or coronary artery disease sufficient to cause global systolic impairment (Elliott et al., 2008). Once again LGE is helpful in the diagnosis of dilated cardiomyopathy or to identify a concurrent ischaemic component. Typically, if LGE were to be present in patients with dilated cardiomyopathy, it is found at the longitudinal striae of the mid-wall and this pattern is clearly distinct from LGE found in patients with coronary artery disease;

up to 28% of patients with dilated cardiomyopathy have been shown to display this on CMR (McCrohon et al., 2003).

Evidence is emerging that CMR may hold important prognostic information in patients with heart failure. Gulati et al performed CMR on patients with new onset heart failure symptoms and also with reduced left ventricular ejection fraction and found that patients with myocardial fibrosis had a higher rate of adverse events compared to those without any evidence of fibrosis on CMR (Gulati et al., 2018). Thus, there may be a role for performing CMR early after diagnosis to gain useful prognostic information. LGE in non-ischaemic cardiomyopathy patients has also been shown to be an independent predictor for hospitalisation and death; it was suggested that the presence of LGE may be a marker of end-organ damage from sustained adrenergic activation leading to adverse left ventricular remodelling (Wu et al., 2008).

Finally, novel CMR techniques which are being developed such as CMR-feature tracking and CMR-tagging. Similar to echocardiography, ventricular deformation strain can be obtained by these two techniques. However, currently there lacks substantial validation studies and also standardisation between the different softwares available (Almutairi et al., 2017).

1.5.3. Right Heart Catheterisation and Cardiac Output Studies

Right heart catheterisation is a procedure widely used to assess cardiopulmonary haemodynamics and it is gives clinicians important information to make the correct diagnosis and guide treatment strategy. In heart and lung transplantation, it is routinely performed as part of the candidate's work up to assess their suitability for transplantation and LVAD therapy.

During right heart catheterisation, a pulmonary vascular resistance of more than 5 Woods units and a transpulmonary gradient of over 15 mmHg are considered to be a contraindication to heart transplantation (Callan and Clark, 2016).

In the late 18th century, there were two hypotheses regarding the production of heat in living animals; the subsequent research and experimentation performed to elucidate these hypotheses resulted in the first reported right heart catheterisation in 1844 (Nossaman et al., 2010). The hypotheses were the pulmonary combustion hypothesis and the tissue combustion hypothesis (Welch, 1991). The French physician and physiologist Claude Bernard endeavoured to investigate these hypotheses and he thought if the pulmonary combustion model was to be true, blood returning to the left side of the heart would be warmer compared to the right side. In the 19th century, it was common to experiment on animals with their chest open, however with the chest open, this would lead to inaccuracies of the temperature of blood. This led Bernard to insert glass tubes into a horse's jugular vein and the carotid artery in order to gain access to the right and left side of the heart respectively; then using a mercury thermometer he was able to measure the temperatures on both sides of the heart and subsequently validate the tissue combustion hypothesis (Nossaman et al., 2010).

The first right heart catheter performed in a human was performed in 1929 by Werner Forssmann on himself. After trialling his technique on a cadaver, via left ante-cubital vein puncture, he inserted a urethral catheter into his right ventricle and confirmed the position on chest radiograph (Meyer, 1990). This technique was then further developed by Cournand and colleagues which allowed clinicians and physiologists to measure haemodynamics (Cournand et al., 1944; Cournand, 1975).

The developments of right heart catheterisation allowed the direct use of the Fick principle which states that:

$$F = \frac{VO_2}{(A - V)}$$

Where F is the flow of blood in litres per minute, VO2 is oxygen consumption and (A – V) is the difference in oxygen content between arterial and mixed venous blood (Hamilton and Riley, 1948). The successful catheterisation of the pulmonary artery allows for mixed venous blood to be collected and the direct Fick principle to be applied (Nossaman et al., 2010). However, the application of the Fick principle requires a couple of assumptions, firstly that no significant amount of oxygen uptake disappears metabolically from the circulation and secondly that the sample of mixed venous blood is fully mixed from the venous return to the right side of the heart (Hamilton and Riley, 1948). This method of estimating cardiac output has fallen out of routine clinical use because it requires constant and stable gas diffusion throughout the transit of blood through the lungs which often requires a high fractional inspired oxygen with ventilatory settings which may cause haemodynamic instability in critically ill patients (Mathews and Singh, 2008).

In 1970, a flow directed pulmonary artery catheter was developed by Swan and Ganz. This allowed for a pulmonary artery catheter to be placed without the need for fluoroscopic guidance (Swan et al., 1970). This is now commonly used in some cardiac intensive care units for pulmonary artery pressure monitoring and also for the routine use of cardiac output monitoring by using the thermodilution method. With an updated pulmonary artery catheter, Forrester et al

were able to perform thermodilution at the bedside with the indicator temperature measured extracorporeally and the distal thermistor located at the tip of the catheter in the PA (Forrester et al., 1972). In current clinical practice, the standard pulmonary artery catheter has 4 lumens, one for balloon inflation, one for indicator injection, one for solution/drug administration and pressure monitoring and the final lumen for thermistor connections to the computer (Argueta and Paniagua, 2019). The thermodilution method is based upon thermodilution curves and indicator dilution methods. The actual formula used to calculate cardiac output (L/min) is the modified Stewart-Hamilton equation (Edwards, 2005). Although convenient, there are a few limitations to the thermodilution method for calculating cardiac output. Firstly, when the cardiac output is low, the area under the thermodilution curve is smaller and therefore could potentially overestimate cardiac output; similarly right sided valvular pathology, such as tricuspid or pulmonary valve regurgitation, reduces the accuracy of the thermodilution technique (Argueta and Paniagua, 2019).

In the modern era, right heart catheterisation is routinely performed with either internal jugular, brachial or femoral vein access (Krishnan et al., 2019). Once the position of the catheter has been confirmed by pressure trace monitoring and on fluoroscopy, several haemodynamic parameters can be recorded. Pulmonary artery pressure, pulmonary capillary wedge pressure, RV pressure, CVP, and cardiac output studies can be performed using a Swan-Ganz catheter as described above. From these directly measured parameters, indirectly derived parameters can also be estimated, such as the pulmonary vascular resistance and systemic vascular resistance (Callan and Clark, 2016; Krishnan et al., 2019). Therefore right heart catheterisation is an invaluable tool for the assessment of patients with heart failure and pulmonary arterial hypertension.

1.5.4. Right Ventricular Power and Work

It has been well described that the heart converts chemical energy into mechanical energy, whilst a portion of the chemical energy is dissipated as heat, the remainder is converted into hydraulic energy achieving blood flow (Milnor, 1982; Chemla et al., 2013). RV hydraulic power can be separated into 2 components, the steady or non-pulsatile component and the oscillatory or pulsatile component. Therefore the sum of the steady and oscillatory power is the total external hydraulic power generated by the ventricle (Saouti et al., 2010; Milnor et al., 1966). It has been suggested that the oscillatory power represents surplus energy which is wasted to accelerate blood in a pulsatile fashion (Grignola et al., 2007; Chemla et al., 2013; Milnor, 1982).

RV power and energy can also be defined as the power generated by the RV to deliver a stroke volume into the PA (volume per unit of cross-sectional area of the PA) and the RV stroke work (RVSW) is calculated with the following conventionally used formulae (Su et al., 2017a; Chemla et al., 2013) representing steady flow:

$$RVSW = (mPAP - RAP) \times RVSV$$

Here, mPAP is the mean PA pressure, RAP is the right atrial pressure and RVSV is the right ventricular stroke volume. Furthermore, the RV energy density can be obtained by normalising RVSW to the cross-sectional area (CSA) of the main PA:

$$RV\ energy\ density = \frac{RVSW}{CSA} = \frac{(mPAP - RAP)\ \times\ RVSV}{RVSV\ \times \frac{HR}{U_{mean}}} = \frac{(mPAP - RAP)}{\frac{HR}{U_{mean}}}$$

Here U_{mean} is the mean velocity or flow and HR is the heart rate. Therefore, the RV hydraulic power is the pressure energy that enters the pulmonary vasculature per time unit and RVSW is the ability of the RV to generate pressure and stroke volume (Chemla et al., 2013).

In a previous study, Su et al have used the principles laid out above and employed WIA in conjunction with RVSW to assess RV performance in relation to the pulmonary vasculature. They employed FCW to RV power and Energy density ratios as a measure of RV performance and found that patients with pulmonary arterial hypertension and chronic thromboembolic pulmonary hypertension had significantly lower FCW/RV power and energy ratios (Su et al., 2017a). This could be either due to a reduction of the magnitude of the FCW as the RV fails or an increase in the RV power and energy as a mechanism to adapt to the increase afterload.

1.5.5. Pulmonary artery pulsatility index (PAPi)

Outcomes of LVAD therapy have improved with the introduction of the magnetically levitated centrifugal continuous flow device (Pagani et al., 2021), but early right heart failure (RHF) remains a major cause of morbidity and mortality following LVAD implant (Mehra et al., 2017). Therefore, preoperative assessment of the risk of RHF is central to the selection of patients for LVAD therapy.

A number of haemodynamic parameters derived from pulmonary artery catheterisation have been used to assess the risk of RHF. Of these, pulmonary artery pulsatility index (PAPi) has

been shown to be an independent predictor of mortality due to RHF in acute myocardial infarction, pulmonary arterial hypertension, heart failure, heart transplantation and cardiogenic shock (Lim et al., 2021; Kochav et al., 2018; Hochman et al., 1999; Rong et al., 2020; Aslam et al., 2021). In general, lower PAPi is associated with higher the risk of RHF. Pulmonary artery pulsatility index is defined as the ratio of pulmonary artery pulse pressure to right atrial (or central venous) pressure. Pulmonary artery pulse pressure is a function of stroke volume (SV) and pulmonary artery compliance (PAC), and the latter has a hyperbolic relationship with pulmonary vascular resistance (PVR) (Reuben, 1971).

In this chapter I have given an overview of the pathophysiology of heart failure and summarised the basic concepts of wave intensity analysis from its origins to the clinical applications to which it has been applied. I have discussed the current techniques of assessing the right ventricle and explored the different haemodynamic parameters which are commonly used in modern day clinical practice in the assessment of cardiac function and pulmonary hypertension.

There has been great interest in PAPi as a haemodynamic parameter which can potentially identify patients who would develop right ventricular failure following cardiac surgery or transplantation, however, the role of PAPi in the assessment of patients with a LVAD remains to be determined. Therefore, we conducted a systematic review to assess the current available evidence in the literature.

As discussed above, each of the techniques in current clinical use have its merits and also limitations. There is no consensus as to the current ‘gold standard’ in right ventricular assessment and clinicians will have to choose the technique most appropriate to the clinical scenario. Wave intensity analysis may add to the clinical armamentarium in the future.

In this thesis, I hypothesise that 1. in patients with heart failure and pulmonary hypertension due to left heart disease (group 2 pulmonary hypertension), a higher pulmonary vascular resistance is associated with increased wave reflection, 2. with administration of dobutamine wave reflection will be reduced and it will increase the forward compression wave on WIA in the pulmonary artery and 3. in patients with heart failure supported with a durable LVAD, WIA can be used to identify an optimal LVAD pump speed based on optimal forward compression and decompression waves with minimal wave reflection.

2. Systematic Review of Pulmonary Artery Pulsatility Index in Durable Left Ventricular Assist Device Therapy

2.1. Introduction

In the last chapter, I have discussed some of the different haemodynamic parameters currently used in the assessment of the right ventricle and also reviewed the different imaging modalities and right heart catheterisation in the assessment of patients with advanced heart failure. However, the role of PAPi in the assessment of patients with a LVAD remains to be determined.

Durable left ventricular assist devices (LVAD) have become an established therapy in patients with end-stage heart failure. Outcomes of LVAD therapy have improved with the introduction of the magnetically levitated centrifugal continuous flow device (Pagani et al., 2021), but early right heart failure (RHF) remains a major cause of morbidity and mortality following LVAD implant (Mehra et al., 2017). Therefore, preoperative assessment of the risk of RHF is central to the selection of patients for LVAD therapy.

A number of haemodynamic parameters derived from pulmonary artery catheterisation have been used to assess the risk of RHF. Of these, PAPi has been shown to be an independent predictor of mortality due to RHF in acute myocardial infarction, pulmonary arterial hypertension, heart failure, heart transplantation and cardiogenic shock (Lim et al., 2021; Kochav et al., 2018; Hochman et al., 1999; Rong et al., 2020; Aslam et al., 2021). In general, lower PAPi is associated with higher risk of RHF. Pulmonary artery pulsatility index is defined as the ratio of pulmonary artery pulse pressure to right atrial (or central venous) pressure.

Pulmonary artery pulse pressure is a function of stroke volume (SV) and pulmonary artery compliance (PAC), and the latter has a hyperbolic relationship with pulmonary vascular resistance (PVR) (Reuben, 1971). On this basis, we hypothesized that the PAPI cut-off associated with RHF would be dependent on the PVR (increase with PVR). PAPi is defined as the ratio of the pulmonary arterial pulse pressure and right atrial pressure. This may be a useful parameter as it takes into account the RV contractile function with the systolic PA pressure as a surrogate marker and the right atrial pressure as a sign of a failing RV. Furthermore, the pulmonary artery pulse pressure is an indication of the pulsatile load of the RV and the RAP is used as a sign of congestion (Kapur et al., 2017). Pulmonary arterial pulse pressure is also intricately linked to pulmonary arterial compliance and this relationship will be further explored in the discussion section of this chapter.

I therefore undertook a systematic review 1. to assessed the relationship between PAPi, RHF and death following LVAD implantation, and 2. to evaluated the relationship between the reported PAPi cut-off and PVR.

2.2. Methods

2.2.1. Eligibility

All eligibility criteria and search strategy were pre-specified and the review was prospectively registered on PROSPERO (CRD42021259009). The search results are reported in accordance with the PRISMA statement (Liberati et al., 2009).

All studies reporting measurement of PAPi in adult patients with a durable LVAD, defined as an intra- or extra-corporeal device implanted in the left ventricle for the treatment of advanced heart failure, irrespective of treatment intention (destination therapy or bridge to transplantation), and published in the English literature were included. Studies were excluded if PAPi was not reported, or data on mortality or RHF were not reported. Studies reported only as a conference abstract were excluded due to insufficient data for analysis.

2.2.2. Search Strategy

International primary research databases (PubMed, EMBASE and CENTRAL) were searched from inception to 18th August 2022 and reference lists of relevant articles to identify all eligible studies. The following search strategy was used for all three databases:

1. 'Pulmonary artery pulsatility index' OR 'PAPI'

2. 'Heart failure' OR 'ventricular failure' OR 'right ventricular failure' OR 'right heart failure' OR 'left ventricular failure' OR 'ventricular assist device' OR 'VAD' OR 'LVAD' OR 'Heartmate' OR 'Heartware'

3. 1 AND 2

2.2.3. Study selection and data extraction

Abstracts and then full text articles of all identified were screened independently by two reviewers (myself and Dr. Ayisha Khan-Kheil). All studies in patients with a durable LVAD which contained PAPi data analysed against RHF or death were included. RHF was author

defined, including the INTERMACS definition of RHF (Stewart et al., 2016). Data were extracted independently by the same two reviewers from the full text publication and any disagreements were resolved by consensus. For all studies included, the Newcastle-Ottawa Scale (Wells et al., n.d.) (NOS) for assessing quality of nonrandomised studies was employed and based on the number of stars each study gained in each domain, this was then converted to the Agency for Healthcare Research and Quality (AHRQ) standards of good, fair and poor.

2.2.4. Statistical Analysis

Statistical analysis was performed using IBM SPSS Statistics, Version 27.0 (Armonk, NY). All continuous data are expressed as medians with interquartile ranges (IQR) and all categorical data are expressed as counts and percentages where applicable.

2.3. Results

The search produced 308unique records and we identified 16 studies reporting haemodynamic assessment in 20,634 adult patients with an implanted durable LVAD (Figure 2). All full text articles were sourced online or via national libraries. Characteristics of the included studies are shown in Table 2. All studies were retrospective cohort studies originating from four countries, with nine (56%) from the USA, three (19%) from Italy, and one (6%) each from Japan, Germany, the Netherlands and Turkey. Articles were published in specialist heart failure, cardiothoracic surgery, transplantation, or anaesthetic journals.

The study periods ranged from 2004-2021. The median number of patients in each study was 95 (IQR 78.8-226.5). The types of LVAD implanted were primarily intracorporeal continuous-

flow devices, HeartMate (HM; Abbott Laboratories, USA) II or 3 and HeartWare (HVAD; Medtronic, USA), with one study evaluating the NIPRO-VAD (Nipro, Osaka, Japan) extracorporeal pulsatile pump (Kimura et al., 2012). Only six (38%) out of the 16 studies stated the goal of LVAD therapy (bridge to transplantation/candidacy or destination therapy).

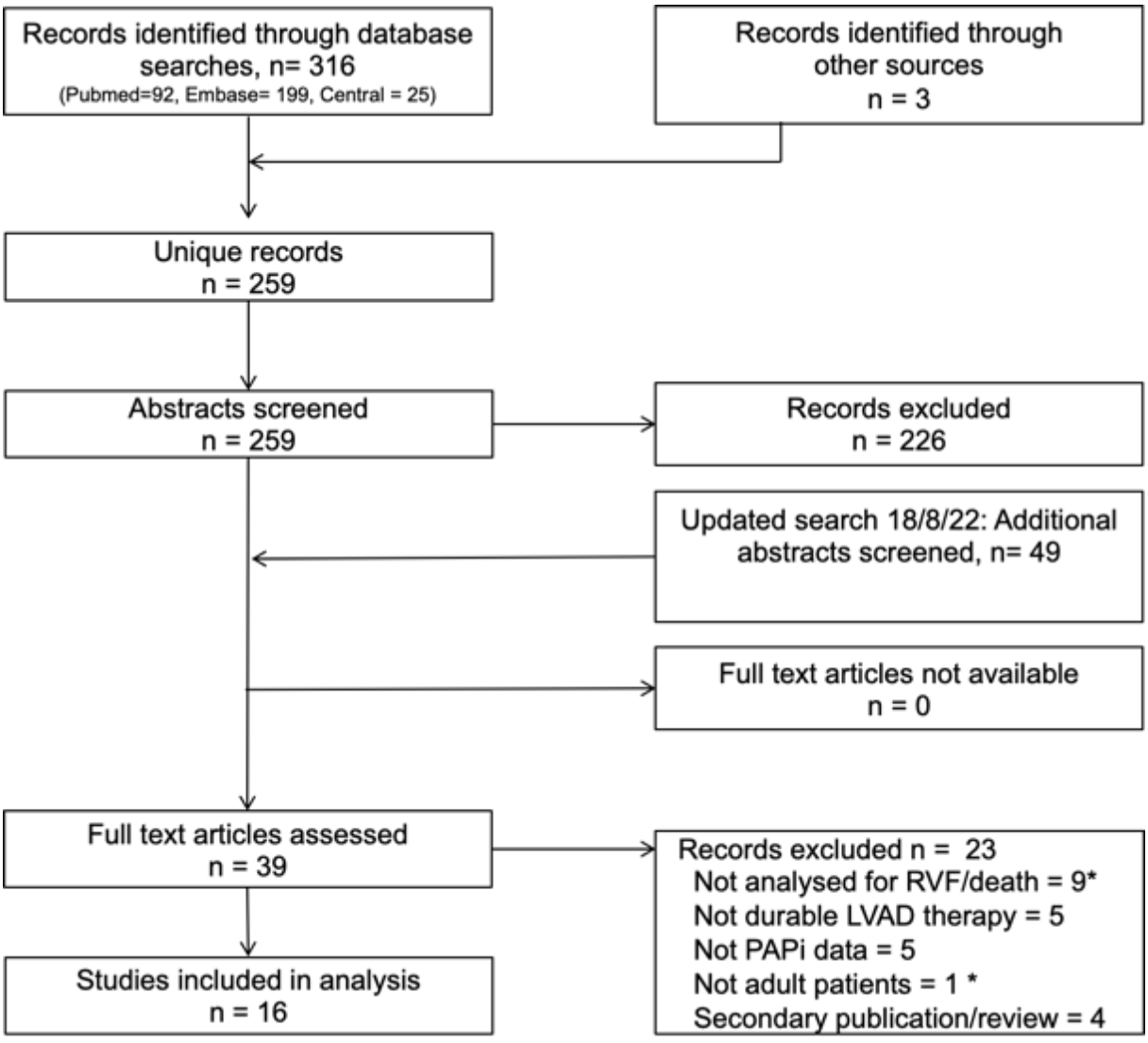

Figure 2. PRISMA flow diagram of study selection. *indicates multiple counting.

Of the 16 studies, the primary outcome was (i) RHF or the event of right ventricular assist device (RVAD) implantation in 15 (94%) and (ii) mortality associated with right atrial pressure (RAP) in 1 (6%). All 16 studies reported on the timing of PAPI measurement in relation to LVAD implant. Fourteen (88%) studies performed right heart catheterisation prior to LVAD implantation to record routine haemodynamic parameters including PAPI (although only six (38%) studies gave the exact timing in hours, days, or months of RHC from LVAD implantation) and two (13%) studies measured PAPI intraoperatively at the time of LVAD implantation. Twelve studies did not specify medical therapy at the time of hemodynamic assessment (e.g. use of inotropes or intra-aortic balloon pump).

Guglin et al analysed the INTERMACS database including 18,733 patients (Guglin and Omar, 2021) and found that RAP was a haemodynamic predictor of death with an ROC curve AUC of 0.55 (CI 0.539-0.562, $p<0.0001$) and a RAP of 13mmHg or higher had the highest combined sensitivity and specificity in predicting mortality. PAPI and other haemodynamic parameters were also analysed and compared against RAP. Survivors were found to have a significantly higher PAPI (3 ± 3.1 vs 2.6 ± 2.7; $p<0.001$) but when compared to RAP, it was found to have a lower ROC curve AUC with a difference in areas of 0.0105, $p=0.005$ and therefore RAP was found to be superior at predicting death.

Table 2. Summary of the 16 studies included in analysis.

Authors	N	LVAD	PAPi associated with RHF?	PAPi Cut-Off for RHF or Death	Summary
Grandin et al 2016	151	Not reported	No	Not reported	Single centre study. Low PAC combined with a high CVP:PCWP ratio was the strongest predictor for death at 6 months (HR 8.68, p<0.001) and RHF (OR 4.74, p=0.02). PAPI was not significantly associated with RHF (p=0.10)
Morine et al 2016	132	HM2, HVAD	Yes	<1.85 (RHF)	A lower PAPi was significantly associated with RHF p<0.01. A PAPi<1.85 provided 94% sensitivity and 81% specificity for predicting RHF and was superior to RAP:PCWP ratio, RVSWI and RAP alone.
Kang et al 2016	83	HM2, HVAD	Yes	<2 (RHF)	PAPi was an independent predictor of RHF and RVAD implantation following LVAD therapy. A higher PAPi was associated with reduced risk for RVAD placement (OR 0.31, p<0.0001). PAPi was more predictive of RVAD placement if inotropes were present at the time of catheterisation (OR 0.21 vs OR 0.49). ROC analysis showed optimal sensitivity and specificity achieved using a PAPi threshold of 2.

Nitta et al 2018	70	Nipro-VAD	Yes	<0.88 (RHF)	This study aimed to devise a scoring system for predicting RVAD placement following implantation of the Nipro-VAD paracoporeal device. Patients who required RVAD implantation post-operatively had a significantly lower PAPi (p=0.001). The authors proposed a combination score using PVR>4.5WU and RAP:PCWP > 0.8 as a scoring system for predicting RVAD requirement following paracoporeal LVAD therapy.
Loforte et al 2018	258	HM2, HM3, HVAD, Jarvik 2000, Berlin Heart	Yes	<2 (RHF)	This study aimed to devise the ALMA risk score for predicting RHF following LVAD implantation. Within the haemodynamic data of this study, a PAPi of less than 2 was found to be associated with unplanned RVAD support (p=0.001) and on multivariable logistic regression analysis PAPi<2 had an OR of 3.3 (CI 1.7-6.1, p=0.001). The ALMA score employs the following five variables: destination therapy intention, PAPI<2, RVSWi <300 mmHg/ml/m^2, RV:LV ratio>0.75 and MELD-XI score >17. The authors proposed a score of 0-1 implies low risk for RVAD requirement and a score above 4 implies very high risk for requiring RVAD following LVAD implantation.

Raymer et al 2019	216	HM2, HVAD	Yes	Not reported	This study reported the combination of TAPSE and HeartMate risk score (HMRS) as a scoring system to predict RHF following LVAD implantation. The RHF group had a lower PAPi (p=0.001). ROC analysis showed PAPi had an AUC of 0.63 (p<0.001). When the haemodynamic parameters were analysed combination of TAPSE with the HMRS was the best for predicting RHF compared to HMRS+PAPi and HMRS + sRVCPI.
Gudejko et al 2019	85	HM2, HVAD	Yes	Not reported	The data used in this study was intraoperative haemodynamic parameters and also echocardiographic data. Higher CVP, lower pre CPB and post chest closure PAPi, post CPB larger right atrial diameter, larger RVES area, lower FAC and lower TAPSE were all associated with severe RHF.
Muslem et al 2019	375	HM2, HM3,HVAD	Yes	Not Reported	PAE was found to be the most robust haemodynamic parameter to predict RHF. PAPi was significantly lower in the Severe RHF group compared to no RHF (1.8 vs 2.2, p= 0.017).

Alfirevic et al 2020	86	HM2, HM3, HVAD	No	Not reported	Intraoperative TAPSE measurement was the variable of interest in this study. As a secondary comparison, PAPi and the Michigan risk score were not significantly associated with severe RHF. Intraoperative TAPSE, Michigan risk score and PAPi were poor discriminators of RHF following LVAD therapy.
Sert et al 2020	71	HM2, HM3, HVAD	No	Not reported	This study compared TAPSE, CVP:PCWP ratio, RVSWI, PAPi, Pennsylvania Score, Michigan score, CRITT score, ALMA score and the EUROMACS score. PAPi was not significantly lower in the group with post op RHF (p=0.304). They concluded that only the EUROMACS and CRITT score had a ROC AUC above 0.7 and that the combination of TAPSE and the Pennsylvania score was found to be the most sensitive (85%) whereas TAPSE +Michigan score + CVP:PCWP ratio was the most specific (97%).
Benjamin et al	104	HM2, HVAD	No	Not reported	Primary end point was duration of inotropic support and the association with RVF. They found patients who were on long term milrinone had a significant ly increased risk of developing RVF post LVAD insertion. PAPi was not significantly different between the RVF and the group without RVF post LVAD implant (4+/-3.9 vs 3.2+/-2.3 p=0.255).

Ruiz-Cano et al	80	HM3, HVAD	No	Not reported	PAPi was not significantly different between the early RVF group vs no early RVF (2.5 vs 3, p= 0.283). This study found that blood urea nitrogen >44.5mg/dL and CVP/PCWP>0.55 were the parameters with the strongest association with early RHF.
Guglin et al 2021	18608	Not reported	No data	Not reported	This was a retrospective cohort study looking at data from the INTERMACS database and primarily assessing RAP and its ability to predict death. RAP was the main predictor of mortality in LVAD recipients. PAPi was lower in non-survivors (p<0.001), but RAP had superior discriminatory value with a difference in AUC of 0.0105 (p=0.0052).
Gonzalez et al 2021	315	HM2, HVAD	Yes	Optimal PAPi <3.3 (RHF); Delta PAPi <2.08 (Death at 6 months)	This study assessed the change in PAPi during pre-operative haemodynamic optimisation prior to LVAD implantation. The mean optimal PAPi was lower (p<0.001) in the group that developed early RHF. A delta PAPI of <2.08 during optimization was associated with higher mortality at 180 days (p=0.003).

Cacioli et al2022	75	HM2, HM3	Yes	Not reported	A lower PAPi was strongly associated with RVF following LVAD implant. This study also demonstrated in those who did not develop RHF post LVAD had a significantly higher PAPi following vasodilator challenge at pre op RHC (5.3 +/-3.9 vs 2.7+/-1.3, p=0.003). Furthermore, PAPi when combined with established risk scores provided incremental risk stratificationfor post LVAD RHF.
Stricagnoli et al 2022	38	HM3, Jarvik 2000	Yes	Not reported	PAPi was the most robust haemodynamic parameter which predicted post LVAD RHF, (1.52+/-0.26 vs 3.95+/-3.39, p=0.003) with a ROC AUC of 0.85.

Gonzalez et al (Gonzalez et al., 2021) studied PAPI at serial time points before LVAD implantation and during the period of medical optimisation, hypothesizing that the magnitude of change of PAPI and other invasive haemodynamic measurements would provide an incremental risk stratification for RHF following LVAD therapy with a secondary end point of death at 180 days. After optimising their patients with a combination of diuretic, intravenous sodium nitroprusside, inotropes and non-durable mechanical circulatory support where appropriate, they found that an optimised preoperative PAPi of >3.33 was associated with a significant reduction in early RHF ($p<0.001$). In patients with a change in PAPi (delta PAPi) of > 2.08 during the optimisation period (time period not specified), there was a significant reduction in 6 month mortality following LVAD implantation presumably from reduced early RHF. In a recently published study, Cacioli et al (Cacioli et al., 2022) showed that PAPi following vasodilator challenge with sodium nitroprusside provided incremental risk stratification when combined with established risk scores (EUROMACS-RHF and CRITT). In this study PAPi alone was significantly lower in patients who developed RHF post LVAD implantation compared with those who did not have RVF (2.2+/-1.3 vs 3.3 +/-1.5, $p=0.008$). This was even more striking following vasodilator therapy (5.3+/-3.9 vs 2.7 +/-3, $p= 0.003$) suggesting a higher PAPi following vasodilator therapy indicates more right ventricular reserve. Similarly to the findings of Gonzalez et al, this study reported a post-vasodilator challenge PAPi cut-off of 3.2 (with a sensitivity 66% and specificity 68%) for right ventricular failure. Furthermore, the authors combined RV fractional area change and systolic pulmonary artery pressure with post vasodilator challenge PAPi and found that it had an AUC of 0.949.

The majority of studies used the Interagency Registry of Mechanically Assisted Circulatory Support (INTERMACS) definition to describe the endpoint of RHF [Table 3.2]. Fifteen studies

reported RHF data relating to PAPi: in ten(Kang et al., 2016; Nitta et al., 2018; Raymer et al., n.d.; Loforte et al., n.d.; Gonzalez et al., 2021; Gudejko et al., 2019; Morine et al., 2016; Cacioli et al., 2022; Stricagnoli et al., 2022; Muslem et al., 2019), a lower PAPi was associated with RHF, but in the other five studies (Alfirevic et al., 2020; Sert et al., 2020; Grandin et al., 2017; Benjamin et al., 2020; Ruiz-Cano et al., 2020), there was no significant association between PAPi and RHF. Six (38%) studies performed ROC analyses to determine the optimal PAPi cut-off for RHF following durable LVAD implantation, ranging from 0.88 to 3.3, with a mean of 2.2 and the ROC AUC values ranged from 0.70 to 0.94 with a mean of 0.80.

All six studies provided data on PVR in patients with and without severe RHF. There was a direct relationship between the PAPi cut-offs and PVR for patients with/without severe RHF ($r=0.6613$, $p=0.019$) (Figure 3.). In assessing the quality of the included studies using the Newcastle-Ottawa Scale, all achieved an AHRQ grading of good, with at least one star in each domain.

Table 3. Definition of right heart failure used in each study.

Authors	RHF Definition
Kang et al	INTERMACS definition
Nitta et al	RVAD implantation within 2 weeks of LVAD implantation
Raymer et al	Post-implant inotropic support>14 days, RVAD implantation or death within 14 days due to RHF
Loforte et al	Short or long term right sided MCS despite maximal dosage of continuous inotropic support and NO ventilation within 30 days of LVAD implantation.
Gonzalez et al	INTERMACS definition
Gudejko et al	INTERMACS definition
Alfirevic et al	INTERMACS definition
Morine et al	INTERMACS definition
Sert et al	INTERMACS definition
Grandin et al	RVAD or inotropic support >14 days or death from RHF within 14 days of LVAD implantation.
Benjamin et al	RVAD or inotropic support >14 days within 30 days of LVAD implantation.
Muslem et al	INTERMACS definition
Ruiz-Cano et al	INTERMACS definition
Cacioli et al	INTERMACS definition
Stricagnoli et al	INTERMACS definition

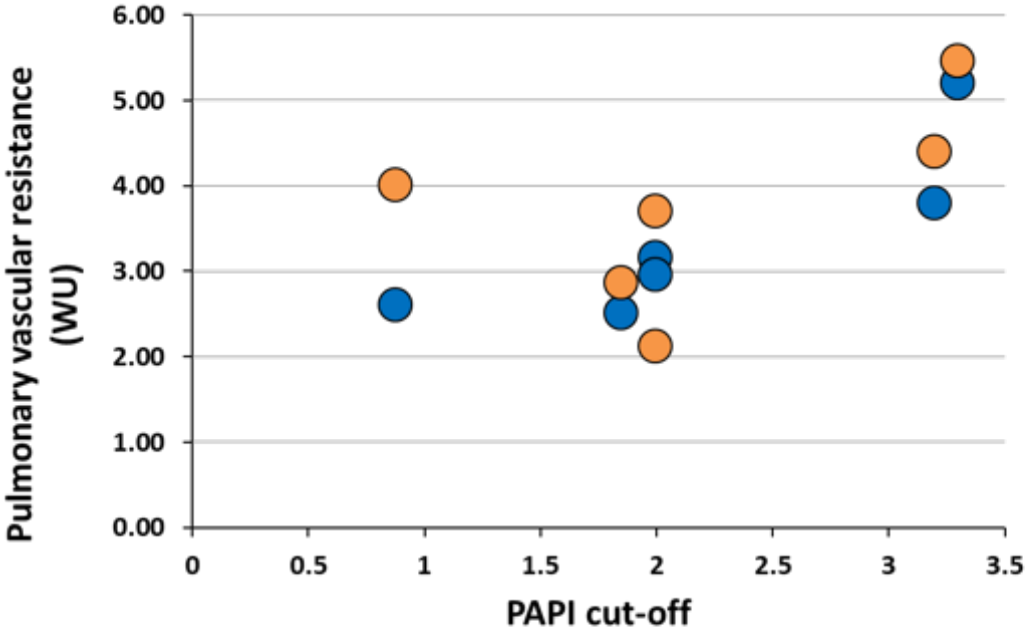

Study	N	PAPi cut-off	PVR (no RVAD)	PVR (RVAD)
Nitta et al	70	0.88	2.60	4.00
Morine et al	132	1.85	2.50	2.86
Kang et al	83	2	3.15	3.70
Loforte et al	258	2	2.95	2.11
Cacioli et al	75	3.2	3.79	4.39
Gonzalez et al	315	3.3	5.20	5.45

Figure 3. The relationship between PAPi cut-offs and PVR in the studies that reported on PAPi cut-offs. There is a direct correlation between PAPi and PVR (r=0.6613, p=0.019). At each PAPi cut-off point, Orange data point corresponds to the PVR in pateints who required RVAD and blue data point corresponds to patients who did not require RVAD.

2.4. Discussion

Pulmonary artery pulsatility index has been evaluated as a parameter to predict the risk of RHF and death following LVAD implantation. Notable findings from this systematic review were: (i) lower PAPi measurements before LVAD implantation were associated with higher risk of RHF and/or death; (ii) the reported PAPi cut-offs for discriminating patients at risk of RHF and/or death varied by more than threefold from 0.80 to 3.3; and (iii) the reported PAPi cut-offs were directly related to PVR.

Pulmonary artery pulsatility index is the ratio of PP over RAP: (Equation 1: PAPi = PP/RAP). Analogous to the charging of capacitors, a significant proportion of the right ventricular SV 'charges' the reservoir volume and increases pressure in the compliant pulmonary arteries in systole, which discharges during diastole. Pulmonary arterial compliance defines this relationship between increase in blood volume (ΔV) and increase in pressure in the pulmonary arterial system. In practice, PAC is difficult to measure because direct measurement of ΔV is not possible due to the continuous outflow from the arterial system. Therefore, in clinical practice, the ratio of SV/PP is used to determine PAC, accepting that this equation would overestimate the true PAC. Rearranging this equation, it can be appreciated that PAC and SV are the main determinants of PP (Equation 2: PP = SV/PAC).

Pulmonary arterial compliance is determined by the prevailing distending pressure (ie: mean pulmonary artery pressure, MPAP) and by the elastic properties of the pulmonary arterial wall. The latter is mainly determined by the composition of elastin and collagen in the wall. Pulmonary arterial compliance decreases when MPAP increases in non-linear relationship

(Reuben, 1971) due to the nature of the stress–strain relationship; and MPAP itself is a function of PVR and left atrial pressure (or pulmonary artery wedge pressure, PAWP), PVR, heart rate (HR) and SV (Equation 3: MPAP = (PVR x (HR x SV)) + PAWP).

Thus, PAC decreases as a result of: (i) an increasing distending pressure (MPAP) from a combination of increasing PVR, HR and SV; (ii) intrinsic changes in pulmonary arterial wall stiffness (vascular remodelling); and (iii) increase in left atrial pressure (or PAWP). Indeed, the hyperbolic relationship between PAC and PVR (Chemla et al., 2015) and inverse relationship with PAWP are well characterized (Tedford et al., 2012). By extension, the pulmonary artery PP would be similarly dependent on SV, PAWP and PVR Figure 4.). This would explain the observed relationship between the PAPi cut-off and PVR levels. I was unable to evaluate the relationship between HR, SV and PAPi, as the data were not reported in the studies.

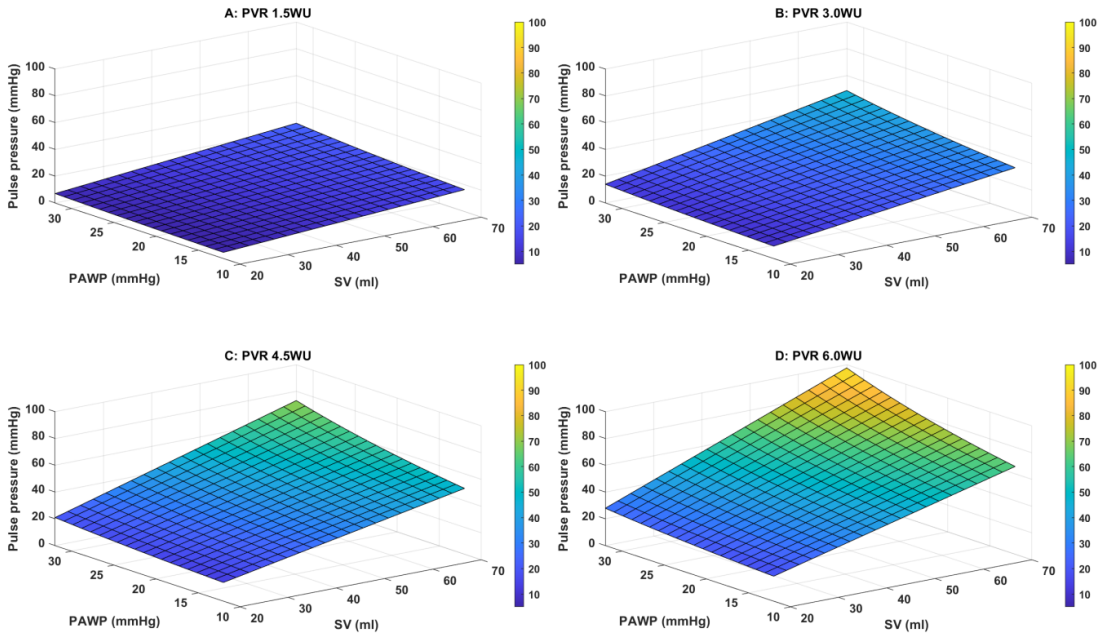

Figure 4. Pulmonary artery pulse pressure modelled over a range of pulmonary arterial wedge pressures, stroke volumes and pulmonary vascular resistances. Graphs A-D were modelled on a PVR of 1.5WU, 3WU, 4.5WU and 6WU respectively, indicating increasing pulse pressure with increasing PVR.

The implications of these physiological considerations are threefold. Firstly, in the face of increasing PVR, the right ventricle mal-adapts to maintain relatively low RAP and normal SV; the latter results in disproportionately elevated PP, and by extension an increase in PAPi (Vonk Noordegraaf et al., 2017). The increase in PAPi is a result of progressive adverse remodelling and should not be misconstrued as an improvement in right heart function. Secondly, a significant drop in PAPi would only occur when the right ventricle uncouples from the pulmonary arterial system, with resultant drop in SV and rise in RAP. Thirdly, because of the higher PVR and lower PAC, the PAPi level would remain higher in the setting of RHF related to pulmonary vascular disease compared to RHF due to primary right ventricular cardiomyopathy with low PVR and high PAC. In this context, Essandoh et al's recent description of a mean weighted PAPi of 2.17 as a cut-off to predict RHF post-LVAD implantation (Essandoh et al., 2022) should be interpreted and applied with caution, and

extrapolation to patients with other pulmonary hemodynamic profiles should be resisted.

Pulmonary artery pulse pressure is inversely related to pulmonary artery compliance (PAC), which is inextricably related to PVR. An increase in PVR increases pulmonary artery pulse pressure at any given stroke volume. In this regard, PVR is a determinant of pulmonary artery pulse pressure and PAPi, and cannot be avoided in interpreting PAPi. The interpretation of PAPi must take into consideration the underlying disease pathophysiology.

In primary right ventricular dysfunction such as right ventricular infarction with low PVR, the compliant pulmonary arterial system would result in low pulmonary artery pulse pressure for a given stroke volume and right atrial pressure (RAP). In contrast, PAPi must be higher at the same stroke volume and RAP in high conditions, such as primary arterial hypertension.
As an illustration, I describe two clinical scenarios:

Patient A, assuming a RAP of 10mmHg, has a normal PVR and normal PAC of 5ml/mmHg. Even with supranormal stroke volume of 100ml (pulse pressure=20mmHg), PAPi would only be 2. Conversely, patient B has a high RAP of 20mmHg and a low PAC of 1ml/mmHg due to pulmonary vascular disease. Even with a RAP that is two times higher and half the stroke volume (50ml, pulse pressure=50mmHg), patient B has a higher PAPi of 2.5. Despite the lower PAPi, it is physiologically implausible to suggest that patient A has more severe right heart failure compared to patient B.

These two clinical scenarios highlight the key message in this systematic review – the same PAPi cut off cannot be applied in different clinical conditions, and a single cut-off averaged

from a number of heterogenous studies is likely to be misleading. Interpretation of PAPi therefore requires an appreciation of the underlying disease and pathophysiology.

It should be noted that other factors may also contribute to the variable cut-offs and discriminatory value in patients undergoing LVAD implantation. Firstly, there are multiple causes of RHF following LVAD implantation, including technical/surgical factors. Secondly, the definition of severe RHF is related to the post-operative management strategy. The clinical threshold for the use of RVAD may explain the variable incidence of severe RHF reported in the literature (Argiriou et al., 2014). Thirdly, the timing of assessment relative to LVAD implantation was not uniformly described in the studies. PAPi would change depending on the effects of medical therapy, including diuretics, vasodilators and inotropes, as reported by Gonzalez et al (Gonzalez et al., 2021). The assessment of PAPi closer to the time of LVAD implantation may have greater discriminatory value (Lim and Gustafsson, 2020).

2.5. Limitations

With only two publications reporting on death in relation to PAPi this precludes meta-analysis and hence the descriptive nature of this systematic review. However, the above description of the relationship between PAPi and PVR (and therefore a single PAPi cutoff value cannot be defined for heterogenous conditions) is not widely appreciated, yet highly relevant to clinicians, especially with greater adoption of PAPi into clinical practice.

2.6. Conclusions

In conclusion, lower PAPi is associated with a higher risk of RHF and mortality in patients with durable LVAD therapy. However, PAPi is inherently related to PVR and the different PVR

levels may have resulted in the variable PAPi cut-offs described in the studies. The PVR level must therefore be taken into consideration in the interpretation of PAPi.

In this chapter I have reported the findings of a systematic review and discussed the physiological interpretation of PAPi in the context of heart failure and patients with a durable LVAD. I have described the physiological foundations of this thesis which now leads on to Wave Intensity Analysis, a method which I discuss in detail in the next chapter and utilise for the assessment of patients in chapters four and five.

3. Methods

In the previous chapters I have laid the foundations for this study and discussed right ventricular failure in durable LVAD therapy in a systematic review in Chapter 2. In this chapter, the methods and study protocol of this study will be laid out.

3.1. Study Aims and Hypothesis

In this study, I aim to 1. Characterise wave generation in the pulmonary artery in patients with advanced heart failure using wave intensity analysis and ii. assess the acute effects of inotropes and varying left ventricular unloading with left ventricular assist devices on right ventricular wave generation and wave reflection in the pulmonary circulation using WIA in patients with advanced heart failure.

I hypothesise that 1. in patients with heart failure and pulmonary hypertension due to left heart disease (group 2 pulmonary hypertension), a higher pulmonary vascular resistance is associated with increased wave reflection, 2. with administration of dobutamine wave reflection will be reduced and it will increase the forward compression wave on WIA in the pulmonary artery and 3. in patients with heart failure supported with a durable LVAD, WIA can be used to identify an optimal LVAD pump speed based on optimal forward compression and decompression waves with minimal wave reflection.

3.2. Study Design and Setting

This is a single centre, prospective observational study based at the Queen Elizabeth Hospital, Birmingham. The study was divided into 2 parts, the first studied 20 patients with advanced heart failure with suspected pulmonary hypertension and the second part studied 20 patients with a durable LVAD implanted at least 6 months prior to the study date.

This study had been peer reviewed and was funded by a Heart Research UK Novel and Emerging Technologies (NET) grant (RG2677/19/21). Ethical approval was obtained from the Welsh NHS Research Ethics Committee (Health and Care Research Wales) (reference 20/WM/0022) and Health Research Authority (HRA) approval (IRAS reference 268644) granted on 19th March 2020 . This study was sponsored by University Hospitals Birmingham NHS Foundation Trust and authorisation was received on 12th March 2021 (reference RRK6728).

3.2.1. Inclusion Criteria

All participants were over the age of 18 and able to give informed consent. Left sided heart disease undergoing RHC for assessment for 1. heart transplantation or 2. durable LVAD therapy, with suspected pulmonary hypertension on echocardiography or previously confirmed pulmonary hypertension on right heart catheterisation. For the LVAD group, the only inclusion criteria was a minimum of 6 months from LVAD implantation at date of RHC.

3.2.2. Exclusion Criteria

Pulmonary hypertension due to other causes such as secondary to respiratory pathology. Pregnancy, mechanical ventilation, temporary mechanical circulatory support and critical cardiogenic shock (INTERMACS 1 or 2).

3.3. Study Method

Patients were recruited either during their clinic appointments at the heart and lung transplantation clinic or on admission for their right heart catheterisation. Potential participants were approached by a healthcare professional who was not directly involved in this research study before being counselled by the myself. All participants were given a patient information leaflet to keep and also signed written consent was gained from every participant. The patient information leaflet and consent forms are available in Appendix 1. The patients were informed that they could withdraw from the study at any time and that their data will not be used.

3.3.1. Heart Failure Group

As part of their routine heart transplantation assessment, right heart catheterisation was performed on all participants. The procedure was performed via the right internal jugular vein under fluoroscopic guidance. A 7.5Fr pulmonary artery balloon flotation catheter was used in all cases and routine baseline haemodynamic measurements were taken. Following this, a combined dual-tipped pressure and doppler flow sensor wire (Combowire; Philips Volcano) was inserted through the PA catheter and advanced circa 1.5cm beyond the tip of the catheter; this was also done under fluoroscopic guidance. At the beginning of the study, measurements were taken and compared between the main PA vs the right PA and it was found that the velocity signal was much more consistent and traces cleaner in the main PA, therefore the main

PA became the standard position for data acquisition in all cases. Data was captured at a sampling rate of 200Hz. Velocity and pressure data was then used for wave intensity analysis performed off line. The criteria for an acceptable velocity signal were continuous clean velocity wave forms for at least 30 seconds but ideally throughout the entire study period, during off line analysis there needed to be at least 5-10 clean beats in order for the analysis to be performed. The manoeuvres for achieving a good quality signal revolved around prepositionaing the Swan ganz catheter and or the Combowire itself (in terms of how far the guide wire is protruding out of the swan ganz catheter). Unfortunately we did not find other manoeuvres such as breath holding made any real difference to the quality of the pressure or velocity data.

The validation of the velocity data of the Combowire has been previously published. The majority of the studies were performed in the coronary artery circulation. The original concept of a Doppler velocity wire was investigated and validated by Doucette et al in 1992, and the doppler wire was validated against electromagnetic flow probes in model tubes (Doucette et al., 1992). Further validation studies in vitro and in vivo have also been carried out (Everaars et al., 2018; Porenta et al., 1999).

In suitable and selected patients who had low cardiac output on thermodilution, they were given dobutamine which was up-titrated to 20micrograms/kg/min or until there was a heart rate response. For patients who had significant pulmonary hypertension and reversibility was required to be assessed, sodium nitroprusside (SNP) was given. SNP was started at 0.5micrograms/Kg.min and uptitrated at 2 minute intervals to either achieve a pulmonary arterial wedge pressure of less than 18mmHg or until the systemic arterial blood pressure

dropped to below 90mmHg. Wave intensity analysis was performed during each of these interventions and the effects of Dobutamine or SNP were assessed. SNP was chosen the agent to test reversibility of pulmonary hypertension as this is the agent used in our department routinely during transplantation assessment. It has been used widely in the Transplant community for this purpose and has been shown to be safe (Bixler et al., 1981; Lim and Zaphiriou, 2016).

3.3.2. LVAD Group

RHC was performed in the same manner as in the heart failure group and a Combowire was inserted and placed in the same position as described above. Following baseline haemodynamic measurements and baseline velocity data acquisition, the LVAD pump speed was reduced by 300rpm and velocity and pressure data were acquired for 2 minutes, this was followed by returning the pump speed to baseline and then increased by 300rpm and pressure and velocity data were captured once more for Heartmate 3 devices. This procedure was performed identically in patients with Heartmate 2 devices except the pump speed was altered by 400rpm instead of 300rpm. Velocity and pressure data were acquired for 2 minutes at each pump speed change. WIA was performed offline in the same manner as the heart failure group.

3.3.3. Pressure and Flow Data Analysis for WIA

Pressure and velocity data were processed offline using customized Matlab software (MathWorks) developed by Prof. K Parker (Imperial College London). The full matlab script is available in Appendix 2. Signals were ensemble- averaged with timing gated to the R wave of ECG and smoothed using a Savitzky–Golay differentiating filter (second order polynomial fit, window size 11). Within the Matlab programme, an automatic procedure for eliminating

particular noisy velocity waveforms from the ensemble is applied. This was done by calculating and ranking the cross-correlation of each beat with the global ensemble average and beats with the lowest correlation coefficient were taken out until the integral of the standard error of the ensemble average velocity waveform over the cardiac period is minimized. The ensemble averaged pressure waveform was then calculated for the same beats. Hardware-related delay between pressure and velocity signals were corrected by shifting the velocity data until the beginning of the upslope of the velocity and pressure waveforms are aligned (Su et al., 2017a). This method has been previously described and published by Su and colleagues in 2017 and developed by Parker et al.

The local wave speed, c is calculated using the PU-loop method as previously described by Parker et al. In chapter 1., section 1.4.1. the method of calculating local wave speed using the PU-loop has been described. We chose to employ the PU-loop method over the sums of squares method as the PU-loop method is thought to be the more accurate technique if the PU loop demonstrates linearity. With the knowledge of the local wave speed, waves can be separated into their forward (shown as dI+) and backward (shown as dI-) components:

$$\pm dI = \pm [(dP \pm \rho c dU)/(4\rho c)^2]$$

In this equation, as described in chapter 1, I represents wave intensity, P is pressure, ρ is the density of blood and c represents local wave speed. Separated waves can be quantified by the peak intensity of the individual waves (W/m^2) and the magnitude of wave reflection, denoted as the wave reflection index (WRI), was calculated as the ratio of the energy of the backward traveling wave in mid-systole to the energy of the incident wave related to ventricular ejection. The peak FCW intensity and any net backward deflected waves in systole (backward

compression waves) are analysed and compared against other haemodynamic parameters.

3.4. Statistical Analysis

Data were analysed using the programme Statistical Package for the Social Sciences (SPSS), (IBM® SPSS® for Mac, Version 29.0. Armonk, NY, USA). The Shapiro-Wilk test was applied to all datasets to test for normality, a *p* value of less than 0.05 was used as the threshold for rejecting the null hypothesis and data were assumed to be non-parametric. All parametric data are displayed with means +/- standard deviations and non-parametric data displayed with medians and interquartile ranges (IQR). For normally distributed data, paired or unpaired student t-test was used, for non-parametric data the Wilcoxon Signed rank/Mann-Whitney U/Kruskal Wallis tests were used and for Nominal categorical data the Chi-squared test was used.

3.4.1. Sample size calculation

There are no published studies of WIA in the pulmonary artery in patients with heart failure, nor the effects of inotropy or pulmonary vasodilatation and durable LVAD therapy. Parker's group were able to demonstrate significant differences in FCW, FDW and wave reflection index in a study of WIA in patients with pulmonary arterial hypertension (n=11) and chronic thromboembolic pulmonary hypertension (n=10) compared to normal controls (n=10) (Su et al., 2017a). Uriel and colleagues demonstrated significant changes in cardiac output and filling pressures in 14 patients with HeartWare centrifugal flow LVAD devices (Uriel et al., 2016) (comparable to the Heartmate 3 LVAD in this study) with changes in pump speed. Taken together, 20 patients would have at least 80% power at a level of significance of 5% (2-sided)

for detecting a mean change in FCW of $2W/m^2$ and wave reflection index of 15% in response to SNP and dobutamine and changes in pump speed.

3.5. Data Management

No patient identifiable information was retained as the participant's identifying information was replaced by a study-specific code at the time of data collection. The original recorded data from the Combowire in ".sdy" format (Combomap; Philips Volcano) was be kept and labelled with the same patient code, which may be used to reconstruct the study. The ".sdy" data format is proprietary and could not be modified by the investigators. The ".sdy" file was analysed using Philips Volcano software to generate text files for Matlab analysis. All data files were stored in a password-protected folder on a secure area of the NHS Trust network.

All investigators complied with the requirements of the Data Protection Act 1998 with regards to the collection, storage, processing and disclosure of personal information. Other personal information that is not relevant to the study (such as the patient's address) was not collected. All patient data was securely stored within a secure, password-protected folders on a NHS Trust network, which is maintained and regularly backed-up. Access to the data was limited to myself and the Chief Investigator (Dr. Sern Lim) for quality control, audit, and analysis. The Chief Investigator was the data custodian. The data will be stored for 10 years after completion of the study.

In this chapter, I have laid out the study protocol and methods of this study. In chapters four and five, I will report the results from this study in detail.

4. Results: WIA in Advanced Heart Failure

In the previous chapter I have laid out the methods employed in this study and in this chapter and in the next I will report the results. This chapter will focus on the results of the heart failure group of patients and in chapter 5 the results of the LVAD group will be reported.

4.1. Introduction

Pulmonary hypertension due to left sided heart disease (PHLHD) is sub-divided into isolated post-capillary pulmonary hypertension (IPC-PH) and combined pre- and post–capillary pulmonary hypertension (CPC-PH). Previously, a PVR cut off of 3WU was used to distinguish CPC-PH from IPC-PH – defined as a mean pulmonary artery pressure (mPAP) of >20mmHg, pulmonary vascular resistance (PVR) ≤ or >3 WU and pulmonary arterial wedge pressure (PAWP) >15mmHg) (Simonneau et al., 2009; Naeije and D'Alto, n.d.; Simonneau et al., 2019a). The revised European Society of Cardiology and European Respiratory society guidelines have lowered the upper limit of normal PVR to 2WU, on the basis that this is the lowest prognostically relevant threshold (Humbert et al., 2022). Identifying patients with CPC-PH is relevant for heart transplantation or left ventricular assist device therapy (Ibe et al., 2021) as patients with fixed pre-capillary pulmonary hypertension may not be candidates for heart transplantation. We sought to study the physiology of PHLHD in patients with heart failure using wave intensity analysis (WIA).

WIA was first introduced by Parker and Jones in 1990 (Parker and Jones, 1990b) to assess the changes in arterial pressure and velocity simultaneous in order to ascertain the origin, energy, type and timing of travelling waves in the circulation. It has the unique advantage over other

impedance-based methods in that it analyses the pressure and velocity waveforms as successive wavefronts and not sinusoidal wavetrains (Parker, 2009). The analysis is performed in the time domain, allowing clinicians to intuitively relate the arterial waves to events in the cardiac cycle. There have been previous studies which have suggested that wave reflection in the pulmonary circulation is an important factor to be taken into account when assessing pulmonary haemodynamics (Kussmaul et al., 1992; Laskey et al., 1993; Huez et al., 2004). WIA has been previously applied to the systemic circulation (Davies et al., 2012), as a measure of left ventricular (LV) performance (Ohte et al., 2003) and also in the coronary circulation (Hadjiloizou et al., 2008). Su et al have studied WIA in patients with primary pulmonary arterial hypertension (PAH) and chronic thromboembolic pulmonary hypertension (Su et al., 2021, 2019, 2017a, 2017b). There are no studies of WIA in the pulmonary artery in heart failure and PHLHD.

The objective of this study was to characterize wave propagation with WIA in the pulmonary artery in patients with PHLHD. We hypothesized that wave reflection is related to pulmonary arterial pressures, pulmonary vascular resistance (PVR) and pulmonary arterial capacitance (PAC).

4.2. Patient Characteristics

A total of 20 patients with left sided heart disease undergoing RHC for heart transplantation assessment were studied and data acquisition was complete in all patients. The most common diagnosis was ischaemic cardiomyopathy followed by idiopathic dilated cardiomyopathy. The mean age was 50.5+/-11.4 years, 15 (75% were) males and the median left ventricular ejection fraction was 20.5% (10.8-25%). The baseline patient characteristics are displayed in table 4.

4.3. Characterisation of Wave Propagation in Heart Failure

All patients displayed a dominant forward compression wave (FCW) which was related to right ventricular contraction. Immediately following the FCW, 14 (70%) patients displayed an early backward compression wave (BCW) suggesting wave reflection during right ventricular systole immediately following the FCW. All patients displayed a forward decompression wave (FDW) during diastole and 11 (55%) patients had a backward decompression wave (BDW) in early diastole related to the dicrotic notch. Analysis of the haemodynamic data was performed with the patients separated into 2 groups, those who had a BCW (14, 70%) and those who did not (6, 30%). Figure 5A shows a representative example of a trace from a patient who did not have a BCW and Figure 5B shows an example of a trace from a patient who had an early BCW.

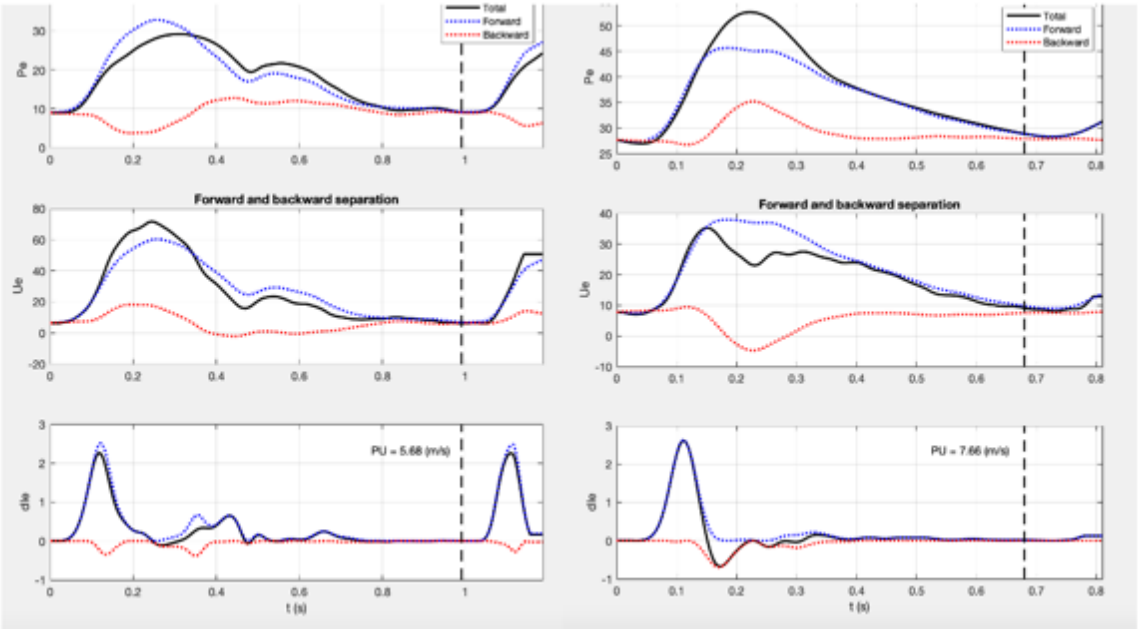

Figure 5A

Figure 5b

Figure 5. Representative WIA traces with and without early BCW: The top panels display ensemble averaged pressure data (P, mmHg), the middle panel display ensembled average velocity data (U, cm/s) and the bottom panel display wave intensity (dI, $10^4 W/m^2$). Black line represents the net P, U and dI, blue line denotes the forward component and red line represents the backward component. It is the net P, U and Wave Intensity that is used for data analysis. Fig 5 A. shows a forward compression wave (FCW) in early systole followed by a forward decompression wave in diastole related to the dicrotic notch. Whereas in 5 B. there is the addition of a backward compression wave in early systole immediately following the FCW.

Table 4. Patient Characteristics

Variables	All Patients (N=20)	No BCW (N=6)	BCW Present (N=14)	P
Male %	75%	83%	71.40%	0.025*
Age, y	50.5+/- 11.4	49.3 +/-11.4	50.9+/-11.8	0.792
BSA, m^2	1.96+/-0.26	1.93+/-0.16	1.97+/-0.30	0.685
BMI, kg/m^2	28.1+/- 4.55	25.5+/-2.46	29.3+/-4.83	0.087
Hb, g/L	134+/-14.4	147+/-8.29	128+/-12.4	0.002*
Cl, mmol/L	96.8+/-3.29	99.1+/-2.29	95.9+/-3.22	0.038*
Na, mmol/L	137+/-3.73	139+/-2.79	137+/-4	0.223
Creatinine, μmol/L	107 (55.3)	102(309)	110(61.8)	0.779
Albumin, g/L	37.7+/-5.55	40+/-4.64	36.6+/-5.75	0.224
Billirubin, μmol/L	17.5 (30)	24.5(43)	17.5(27.3)	1
NTproBNP, pg/ml	6764+/-4113	7387+/-5182	6497+/-3760	0.67
LVEF, %	20.5(14.3)	22(18.5)	17.5(17.8)	0.312
TAPSE, mm	1.4 (8.48)	6.85(14.4)	1.35(1.05)	0.239
MR	Severe=1	Severe= 0	Severe= 1	
	Moderate= 6	Moderate= 1	Moderate= 5	
	Mild= 10	Mild= 5	Mild= 5	
	None= 3	None= 0	None= 3	
TR	Severe= 3	Severe= 2	Severe= 1	
	Moderate= 6	Moderate= 1	Moderate= 5	
	Mild= 7	Mild= 3	Mild= 4	
	None= 4	None= 0	None= 4	

Table 4. Patients separated in to two groups those with a backward compression wave (BCW) and those without. *denotes statistically significant results.

4.4. Haemodynamic Data Assessment

Haemodynamic data for the entire cohort of patients and for the two separated groups with and without BCWs is shown in table 5. Patients with wave reflection had significantly higher systolic, diastolic and mean PA pressures. They also had significantly lower pulmonary arterial capacitance (PAC). Interestingly pulmonary vascular resistance (PVR), indexed PVR and wave speed were not significantly different between the two groups. The PCWP was higher in the group with wave reflection but this did not reach statistical significance.

Correlation analyses between wave intensity indices and conventionally used haemodynamic parameters (MPAP, PVR, indexed PVR, indexed RVSW and PAC) were performed. The magnitude of the FCW, magnitude of the BCW, the wave reflection index (this is the ratio of the peak BCW in relation to the peak FCW) and their association with the conventional haemodynamic parameters were investigated. The magnitude of the FCW had significant positive correlation with MPAP (ρ= 0.485, p= 0.030) and RVSWi (ρ= 0.512, p=0.021) but was not significantly correlated with PVR, indexed PVR and PAC. A scatter plot of the correlation between the FCW intensity and RVSWi is displayed in Figure 6. The magnitude of the BCW had no significant correlation with any haemodynamic parameter. The wave reflection index however, was significantly negatively correlated to PVR (ρ= -0.576, p=0.031) and positively correlated to PAC (ρ=0.733, p=0.003).

Table 5. Haemodynamic parameters for the entire cohort

Variables	All Patients (N=20)	No BCW (N=6)	BCW Present (N=14)	P
RAP, mmHg	14.7+/-5.21	15+/-4.81	14.5+/-5.54	0.85
SPAP, mmHg	50.6+/-13.9	38.7+/-8.26	55.6+/-12.7	0.008*
DPAP, mmHg	25.2+/-5.15	20.2+/-5.04	27.3+/-3.56	0.002*
PPP, mmHg	25.4+/-10.6	18.5+/-4.59	28.4+/-11.2	0.54
MPAP, mmHg	35.7+/-7.80	28.7+/-6.12	38.6+/-6.50	0.005*
PCWP, mmHg	23.9+/-5.56	20.3+/-5.92	25.4+/-4.85	0.062
TPG, mmHg	11.8+/-5.34	8.33+/-2.94	13.3+/-5.51	0.054
DGP, mmHg	0 (2)	0 (1.25)	0.5 (3.25)	0.397
PVR, WU	3.14+/-1.45	2.28+/-1.08	3.5+/-1.46	0.081
Indexed PVR, WU/m^2	5.55+/-2.27	4.27+/-1.71	6.10+/-2.31	0.098
PAC, ml/mmHg	2.28(1.39)	2.88(1.75)	1.73 (1.16)	0.02*
PAPI	1.58(1.46)	1.35 (0.92)	2.04 (1.74)	0.207
Stroke Volume, ml	52.5+/-20.6	58.8+/-20.2	49.8+/-20.9	0.384
Heart Rate, bpm	78.1+/-14.5	68.7+/-10.6	82.1+/-14.3	0.054
CO, L/min	3.89(1.42)	3.87 (2.3)	3.88 (1.27)	0.779
CI, L/min/m^2	1.92 (0.78)	2(0.9)	1.91 (0.72)	0.718
Indexed RVSW, mmHg.ml/m^2	6.77 (4.78)	5.49 (4.67)	8.04 (5.50)	0.274
FCW intensity, 10^4 W/m^2	2.85 (1.79)	2.38 (1.71)	3.11 (3.85)	0.274
Wave Speed, cm/s	3.33 (4.67)	3.28 (2.55)	3.33 (5.42)	0.904

Table 5. Cases have been split into those with a BCW and those without a BCW. *denotes statistical significance with a $p<0.05$.

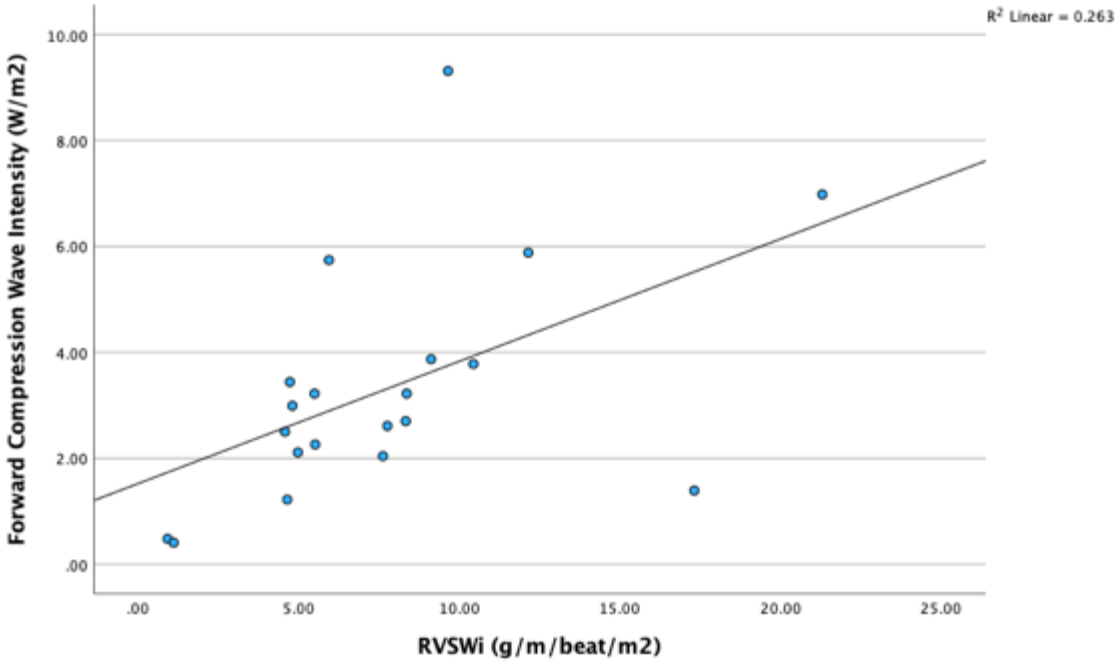

Figure 6. Correlation of right ventricular stroke work index (RVSWi) with FCW intensity R^2=0.263, ρ= 0.512, p=0.02.

Receiver operator characteristics for MPAP and PAC's ability to detect a BCW is displayed in figure 7. MPAP has an AUC of 0.881 and PAC has an AUC of 0.833. A MPAP of 34.5mmHg or greater (sensitivity = 71.4%, specificity= 16.7%) and a PAC of 2.29 ml/mmHg or lower (sensitivity= 71.4% and specificity = 16.7%) were determined to be the optimal cut-offs for early wave reflection during right ventricular systole.

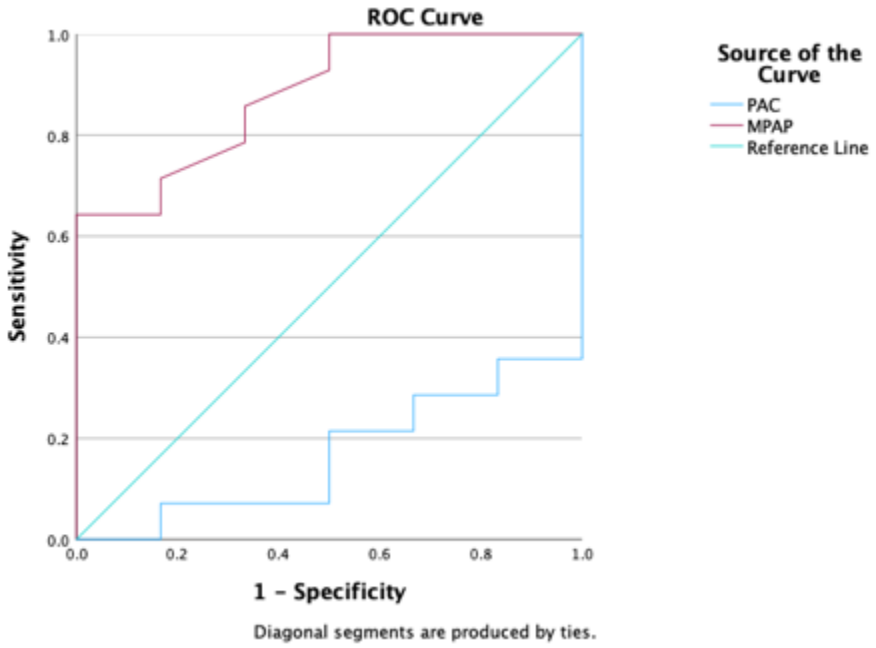

Figure 7. Receiver operator characteristics for mean pulmonary arterial pressure (MPAP) and pulmonary arterial capacitance (PAC). MPAP has an AUC of 0.881 and PAC has an AUC of 0.833.

4.5. Dobutamine and Sodium Nitroprusside Challenge

Following acquisition of baseline haemodynamic, pressure and velocity data, selected patients received a dobutamine challenge or sodium nitroprusside (SNP) challenge. In patients with a low cardiac output, dobutamine was up-titrated to 20micrograms/kg/min or until there was a heart rate response. In patients with very severe pulmonary hypertension and undergoing assessment of reversibility, SNP was started at 0.5micrograms/Kg.min and uptitrated at 2 minute intervals to either achieve a pulmonary arterial wedge pressure of less than 18mmHg or until the systemic arterial blood pressure dropped to below 90mmHg. The detailed protocol is described in Chapter 3.

4.5.1. Dobutamine

Eleven (55%) patients received Dobutamine challenge, Table 6 shows the haemodynamic and WIA parameters before and after Dobutamine. Following Dobutamine, stroke volume, cardiac output, cardiac index, indexed right ventricular stroke-work and forward compression wave intensity significantly increased. The box plots in Figure 8 display the changes following Dobutamine challenge. There were no significant changes in backward compression wave intensity, wave reflection index nor wave-speed. Of the 11 patients who received Dobutamine, eight (73%) had a BCW during RV systole at baseline and of these, seven (88%) continued to display a BCW following dobutamine. In one (12%) patient, the BCW was no longer discernible following Dobutamine. None of the three patients who did not display a BCW at baseline developed a BCW after Dobutamine.

4.5.2. Sodium Nitroprusside

Five (25%) patients received SNP following baseline heamodynamic assessment. Table 7 shows the haemodynamic and WIA parameters before and after SNP. Following SNP administration, the MPAP, PCWP, PVR, PVRi and RVSWi were significantly lower and PAC and SV were significantly higher. Interestingly, the forward compression wave intensity during early right ventricular systole, backward wave intensity and the wave reflection index did not reach statistical significance. Prior to SNP challenge, four (80%) patients displayed a backward compression wave at RV systole at baseline and of these one (25%) then did not display an early backward compression wave following SNP. The patient who did not display a backward wave at baseline also did not have a backward wave following SNP. Although the wave speed did not reach statistical significance, following SNP, in four (80%) patients the wave speed was slower.

Table 6. Haemodynamic parameters pre- and post-Dobutamine challenge.

Variables	Pre-Dobutamine (N= 11)	Post-Dobutamine Challenge (N=11)	P
RAP, mmHg	16+/-5.10	17+/-7.36	1
SPAP, mmHg	46+/-13.4	53+/-15.6	0.212
DPAP, mmHg	23+/-4.99	25+/-8.17	0.753
MPAP, mmHg	33+/-7.63	36+/-10.5	0.515
PCWP, mmHg	23+/-5.28	23+/-6.95	0.44
TPG, mmHg	10+/-4.73	13+/-5.46	0.5
PVR, WU	2.92+/-1.4	2.49+/-1.00	0.155
Indexed PVR, WU/m^2	4.94+/-2.14	4.7+/-1.66	0.375
PAC, ml/mmHg	2.44 (1.92)	2.45 (1.39)	0.878
PAPI	1 (1.40)	1.77 (1.42)	0.11
SV, ml	48.1+/-20.1	65+/-20.9	0.001*
HR, bpm	77+/- 15.4	83.5+/-21.2	0.128
CO, L/min	3.6 (1.55)	5.47 (1.37)	0.004*
CI, L/min/m^2	1.8 (0.63)	2.69 (0.97)	0.004*
Indexed RVSW, mmHg.ml/m^2	4.96 (3.76)	8.93 (8.54)	0.005*
FCW Intensity, 10^4 W/m2	2.7 (2)	3.73 (2.13)	0.033*
BCW Intensity, 10^4 W/m2	0.69 (1.81)	1.15 (1.31)	0.612
WRI, %	31.4 (40.6)	29.2 (7.6)	0.866
Wavespeed, cm/s	2.77 (5.11)	4.71 (2.49)	0.477

*denotes statistical significance with $p<0.05$.

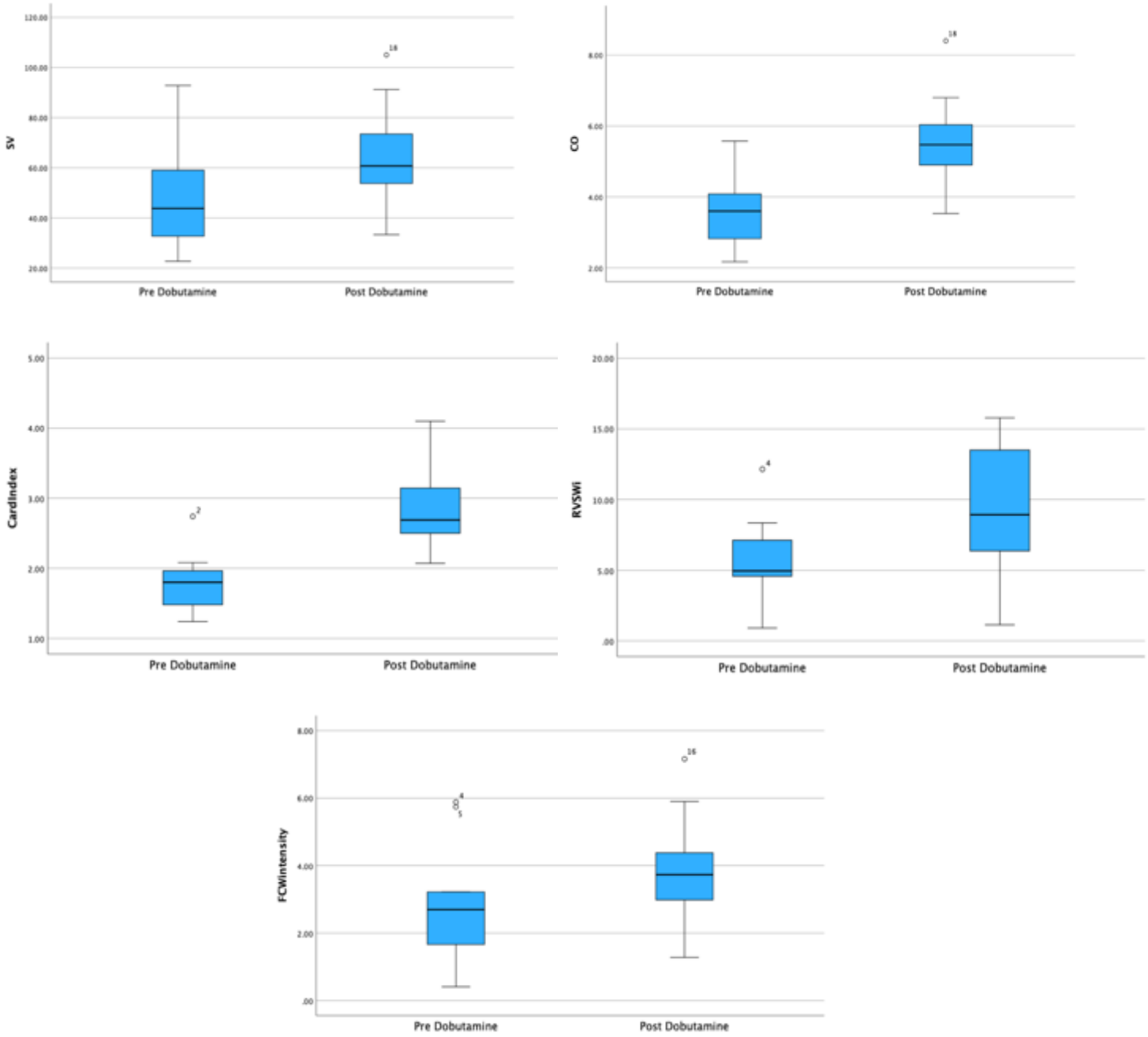

Figure 8. Box plots of Haemodynamic parameters Pre and Post Dobutamine. Forward Compression Wave (FCW) intensities were significantly increased following Dobutamine administration.

Table 7. Haemodynamic parameters pre- and post-SNP challenge.

Variables	Pre-SNP (n=5)	Post SNP (n=5)	P
RAP, mmHg	12 (10.5)	9 (9.5)	0.131
SPAP, mmHg	70 (16.5)	41 (16)	0.042*
DPAP, mmHg	27 (7)	19 (10)	0.08
MPAP, mmHg	43 (8.5)	31 (10.5)	0.043*
PCWP, mmHg	27 (10)	16 (9)	0.043 *
TPG, mmHg	16 (8.5)	10 (13)	0.343
PVR, WU	2.6 (3.11)	1.43 (3.93)	0.043*
Indexed PVR, WU/m^2	5.76 (3.96)	1.63 (4.43)	0.043*
PAC, ml/mmHg	2.22 (1.08)	4.57 (2.75)	0.043*
PAPI	2.6 (2.69)	2.25 (1.76)	0.08
SV, ml	62 (46.0)	83.3 (39.0)	0.042*
HR, bpm	75 (22)	75 (7)	0.892
CO, L/min	4.65 (4.04)	6.75 (2.92)	0.345
CI, L/min/m^2	2.68 (1.64)	3.14 (0.92)	0.345
Indexed RVSW, mmHg.ml/m^2	10.4 (5.76)	6.66 (3.56)	0.043*
FCW Intensity, 10^4 W/m2	3.78 (6.15)	3.8 (3.24)	0.138
BCW Intensity, 10^4 W/m2	0.7 (2.35)	0.30 (3.2)	1
WRI, %	28.1 (17.7)	7.63 (98.6)	0.715
Wavespeed, cm/s	3.78 (4.83)	3.61 (3.15)	0.08

*denotes statistical significance with $p<0.05$.

4.6. Discussion

This is the first study to characterise wave propagation in the pulmonary circulation in left sided heart failure. The main findings of this study are, i.) the pattern of wave propagation in the pulmonary circulation in the context of heart failure is comparable to that of the systemic circulation (Wang et al., 2011), with a dominating FCW during late systole followed by a FDW in diastole and wave reflection in both systole and diastole ii.) Wave reflection during systole is associated with higher pressures in the pulmonary circulation and lower pulmonary arterial capacitance. iii.) Forward compression wave intensity positively correlates with right ventricular stroke work.

WIA has been previously performed in the pulmonary circulation in healthy subjects, patients with primary pulmonary arterial hypertension and chronic thromboembolic pulmonary hypertension by Su et al (Su et al., 2017a). The pattern of wave propagation in this study is similar to what they have reported. Importantly, even in healthy control subjects, backward wave reflection in both systole and diastole were observed and therefore it is not exclusive in disease states where the pressures in the pulmonary circulation or the left side of the heart are elevated. In the systemic circulation in the human ascending aorta, wave reflection during mid-systole have also previously been reported (Koh et al., 1998).

We found that the MPAP, SPAP, DPAP were higher and PAC was lower in patients with an early BCW during systole while there was no difference in the PVR between the two groups. Currently, the definition of pulmonary hypertension is a MPAP of >20mmHg and a PVR of 3WU and above is used to differentiate between all forms of pre-capillary PAH with isolated

post capillary PAH (Simonneau et al., 2019b). However, PAC had been shown to be a superior prognostic indicator in both primary pulmonary arterial hypertension (Mahapatra et al., 2006b, 2006a) and in advanced heart failure (Dupont et al., 2012), this may be due to PAC combining the effects of PVR and the pressure in the left side of the heart. Our results suggests that wave reflection is determined by the compliance of the pulmonary arterial system and therefore WIA may be used in conjunction with conventional haemodynamic parameters in the assessment of pulmonary hypertension.

Indexed RVSW is calculated by the following formula: (MPAP – RAP) x SV Index x 0.0136. It has been shown to be a predictor of negative outcomes in advanced heart failure (Bayram et al., 2022; Ozenc et al., 2020), lung transplantation (Armstrong et al., 2013) and also an independent predictor of RV failure following LVAD implantation (Bellavia et al., 2017). RVSW is a surrogate marker for right ventricular work load taking into account RV contractility and the stroke volume generated. It is therefore intuitive that RVSW positively correlates with the FCW intensity, this relationship has not been shown before. Su et al had shown there were insignificant and weak correlation between the FCW intensity and other right ventricular parameters such as right ventricular stroke volume index (RVSVi), RV fractional area change and tricuspid annular plane systolic excursion (TAPSE) (Su et al., 2017a). This implies that the FCW intensity generated from WIA can also be used as a marker for RV performance.

The effect of inotropy on wave propagation has not been studied in humans. Jones et al reported the effects of Dobutamine on WIA in the canine ascending aorta (Jones et al., 2002). In the canine systemic circulation, Dobutamine was found to greatly increase the peak FCW but had no effect on the FDW. In concordance, we found that Dobutamine significantly increased the

FCW intensity. This was secondary to an increase in cardiac output from an increase in stroke volume but not heart rate; subsequently the indexed RVSW also significantly increased. This is the first study to report on the effects of inotropic agents on WIA in the human pulmonary circulation, this suggests that WIA can be used to monitor response of inotropic therapy in the clinical setting.

The effects of SNP on the pulmonary arterial pressures, the pulmonary capillary wedge pressure and pulmonary vascular resistance were as expected. However, it reduced the indexed right ventricular stroke work (RVSWi) significantly without any significant change to the cardiac output or the cardiac index. As stated in the previous chapter, RVSWi is calculated by: (MPAP – RAP) x SV Index x 0.0136. SNP reduced the RVSWi perhaps by disproportionately reducing the MPAP without any significant reduction in the right atrial pressure.

The effects of SNP on the wave intensity analysis parameters did not reach statistical significance. This may be due to the small number of patients in the SNP group. The wave speed was consistently lower after SNP in all bar in one patient, and can be explained by significant vasodilatation in the pulmonary vasculature in both the arterial and venous systems and therefore the reduction in vascular tone results in a reduction in velocity. Again the wave reflection index was not significantly different following SNP, however there was a very wide range in the WRI following SNP with an IQR of 98.6%.

4.7. Study limitations

The study number of study patients was small, therefore some of the statistical analyses may not have adequate power. In this cohort of patients, we had a majority of men just like in Su et al's study (Su et al., 2017a) but we don't expect this to have caused any significant differences in the wave propagation characteristics in our results.

Acquiring a 'clean' velocity trace was not always easy and often the data was noisy depending on the catheter and/or Combowire tip position. In some cases, significant time was required to adjust the catheter and Combowire tip position before an acceptable velocity trace was observed. This manipulation process takes a degree of experience and patience as acquiring a clean velocity trace is of paramount importance to the WIA analysis. At the beginning of the study, we acquired data from both the right and main pulmonary arteries (PA) but we found that the velocity data can be especially noisy or dampened in the right PA, therefore all our data reported were acquired from the main PA. This could be because in the right PA, the Combowire tip has a higher chance of being in contact with the arterial wall as the branch PAs have a smaller cross-sectional area compared to the main PA. However, this same problem can still occur in the main PA and distance from the pulmonary valve cannot be documented nor confirmed as we only had fluoroscopic guidance during the study. This could have been confirmed by echocardiography but this is not part of routine right heart catheterisation and the pulmonary valve and pulmonary arteries are not always easily visible on echocardiography.

4.8. Conclusion

This is the first study to report WIA in the context of advanced left heart failure. Wave reflection during right ventricular systole was associated with higher pressures in the pulmonary circulation and lower pulmonary arterial capacitance. Although the PCWP was higher in the group with wave reflection it did not reach statistical significance and there was no difference in the LVEF between the two groups. This implies that in the context of left heart failure, wave reflection is due to vascular impedance mismatch rather than elevated pressures from the left side of the heart.

5. Results: WIA in Left Ventricular Assist Device Therapy

In the previous chapter I reported the findings of WIA in the heart failure cohort and also the effects of Dopamine and SNP on wave propagation and wave reflection. In this chapter I report the results of WIA in patients with durable LVAD therapy and the effects of pump speed change on wave propagation and reflection.

5.1. Introduction

The indications for durable left ventricular assist device therapy (LVAD) are i. maintain cardiac output in advanced heart failure, ii. bridge to transplantation, iii. bridge to recovery and iv. destination therapy. The optimal pump speed should maintain cardiac output required whilst ensuring the interventricular septum is as central as possible to ensure right ventricular function is preserved. The current widely adopted technique for setting pump speeds are based on established ramp protocols with echocardiographic guidance and expert opinion (Uriel et al., 2012; Slaughter et al., 2010). LVAD therapy has been shown to reduce pulmonary arterial pressures in both pulsatile and continuous flow devices (Saidi et al., 2018; Haft et al., 2007), furthermore, pulmonary vascular resistance has been shown to decrease and pulmonary arterial compliance increases significantly as soon as 72 hours following LVAD implantation (Masri et al., 2017). This led to the hypothesis that by changing the pump speed and therefore LV loading conditions, this may affect pulmonary haemodynamics and therefore wave propagation in the pulmonary arteries.

Wave intensity analysis was first introduced by Parker and Jones in 1990 (Parker and Jones, 1990b) to assess the changes in arterial pressure and velocity simultaneous in order to ascertain

the origin, energy, type and timing of travelling waves in the circulation. It has the unique advantage over other impedance-based methods in that it analyses the pressure and velocity waveforms as successive wavefronts and not sinusoidal wavetrains (Parker, 2009). In the previous chapter, I have reported the findings of WIA in the pulmonary circulation in the setting of advanced heart failure in patients without durable LVAD therapy; wave propagation was similar in the pulmonary arteries when compared to the systemic circulation and that wave reflection was more likely at higher pulmonary artery pressures and in lower arterial compliance conditions.

The objective of this part of the study was to characterise wave propagation with WIA in the pulmonary arteries in patients with durable LVAD therapy, and the effect of acute pump speed changes. I hypothesise that wave propagation and reflection will be affected by acute changes in LVAD pump speeds.

5.2. Cohort Characteristics

Of the twenty patients included in the study, the velocity data were unusable in six cases, due to excessive noise in the data; hence, these patients were excluded from analysis. Characteristics of the remaining fourteen patients are summarised in Table 8. Twelve (86%) patients had Heartmate 3 devices in-situ and two (14%) had Heartmate 2 devices. The median baseline pump speed was 5,600rpm (IQR: 5,400-6,025), which was varied by ±300rpm (or ±400rpm for the HMII LVADs), with comparisons between the three pump speeds reported in Table 9.

5.3. Characterisation of Wave Propagation

At baseline pump speeds, as reported in the last chapter, the WIA characteristics are similar to those seen in the systemic circulation. The typical trace is characterised by a dominant forward compression wave related to RV contraction followed by an by a forward decompression wave (Figure 9). In some cases, immediately following the FCW, a BCW is present signifying wave reflection and also a BDW during diastole. In our cohort, all cases displayed a FDW, five (36%) had an early BCW and six (43%) displayed a BDW.

When the pump speeds were changed by ± 300rpm for those with a HM3 device and ± 400rpm for those with a HM2 in situ, there were no consistent nor significant changes in the WIA parameters or wave reflection. In eight patients (57.1%), the WIA waveform characteristics remained the same relative to baseline (Figure 10). In three (21%) patients, at baseline pump speed there was no BCW but when the pump speed was increased and decreased by 300rpm, a BCW was observed (Figure 11). In one (7%) patient a BCW was present at baseline and after pump speed change the BCW was no longer present. Increasing pump speeds was associated with significant increases in flow and pump power, and significant decrease in pulsatility index ($p<0.001$). FCW intensity was not found to vary significantly with pump speed change ($p=0.607$), with medians of 1.82 (IQR: 1.15-3.16) at the baseline speed, compared to 1.95 (IQR: 0.99-2.27) and 1.63 (IQR: 1.23-2.88) at minus and plus 300rpm respectively (Figure 12). No significant associations with pump speed were identified for any of the other parameters assessed. The changes in FCW intensity and early BCW representing wave reflection for each individual case is displayed in table 10 along with the different pump speeds and pump flows. This shows the high variability between each individual patient.

Table 8. Cohort characteristics

N=14	
Age, y	63 (52, 65)
Sex (% Male)	14 (100%)
Body mass index (BMI), kg/m^2	29.2 ± 2.5
Body surface area (BSA), m^2	2.09 ± 0.10
LVAD Type	
Heartmate 2	2 (14%)
Heartmate 3	12 (86%)
Diagnosis	
Idiopathic Dilated Cardiomyopathy	4 (29%)
Ischaemic Cardiomyopathy	10 (71%)
NYHA	
Class I	2 (14%)
Class II	12 (86%)
Mitral Regurgitation	
Nil	9 (69%)
Trivial	2 (15%)
Mild	2 (15%)
Moderate	0 (0%)
Tricuspid Regurgitation	
Nil	5 (36%)
Trivial	2 (14%)
Mild	5 (36%)
Moderate	2 (14%)
CVP/RAP, mmHg	8 (6, 15)
sPAP, mmHg	30 (22, 42)
PPP, mmHg	16 (11, 20)
PCWP, mmHg	13 (10, 22)
PAC, ml/mmHg	3.33 (2.98, 4.92)
TPG, mmHg	7 (5, 9)
PVR, WU	1.42 (1.03, 1.89)
PAPI	1.51 (1.33, 2.14)
Heart Rate, bpm	66 (60, 84)
Stroke Volume, ml	61.0 (45.0, 83.6)
dPAP, mmHg	16 ± 8
mPAP, mmHg	22 ± 9
CO, L/min	4.3 ± 1.0
CI , L/min/m^2	2.1 ± 0.4
Haemoglobin, g/L	139 (128, 151)
eGFR, ml/min/1.73m^2	69 (58, 89)
Creatinine, micromol/L	101 (79, 115)

Table 8. LVAD: left ventricular assist device, NYHA: new York heart association, CVP: central venous pressure, RAP: right atrial pressure, sPAP: systolic pulmonary arterial pressure, PPP: pulmonary pulse pressure, PCWP: pulmonary capillary wedge pressure, PAC: pulmonary arterial capacitance, TPG: transpulmonary gradient, DPG: diastolic pulmonary gradient, PVR: pulmonary vascular resistance, PAPI: pulmonary arterial pulsatility index, HR: heart rate, dPAP: diastolic pulmonary arterial pressure, mPAP: mean pulmonary arterial pressure, CO: cardiac output, CI: cardiac index, eGFR: estimated glomerular filtration rate.

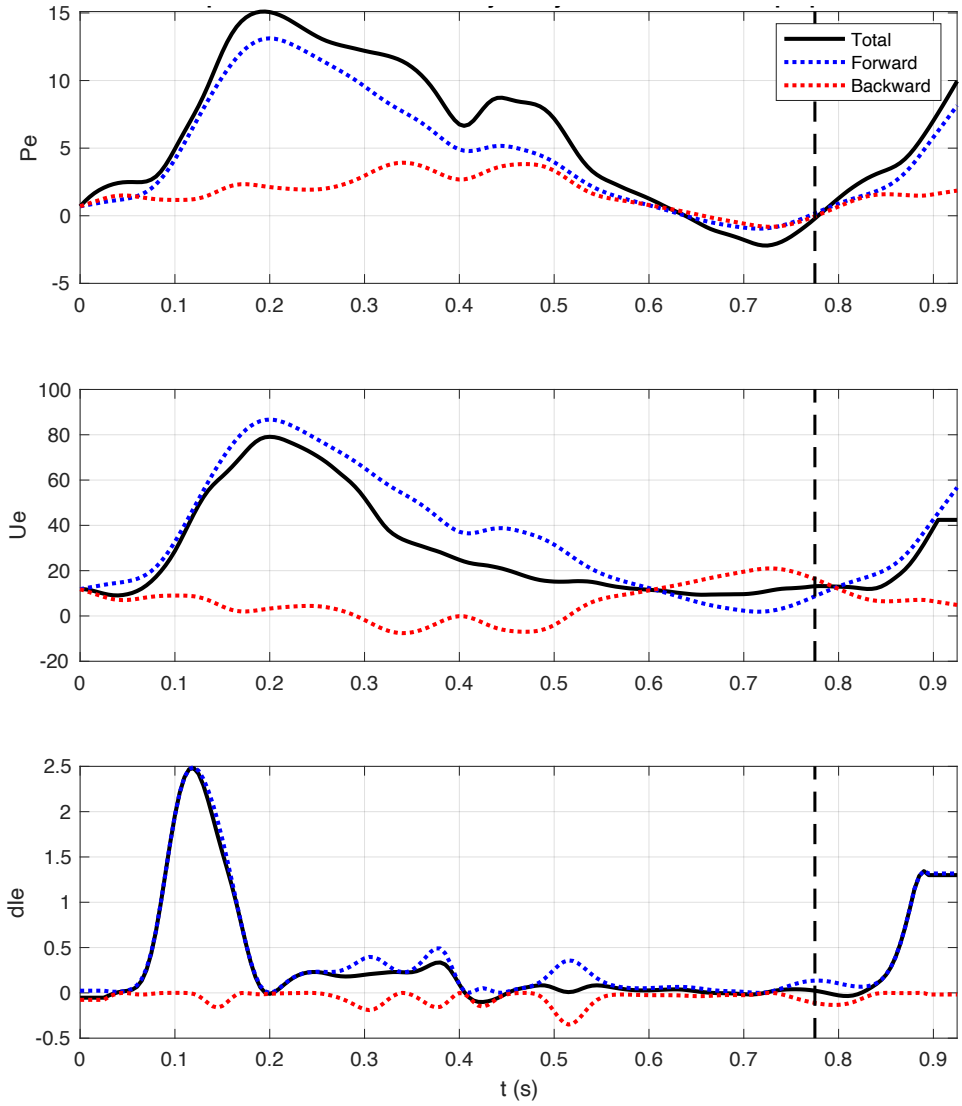

Figure 9. Representative WIA traces at baseline pump speed. The top panels display ensemble averaged pressure data (P, mmHg), the middle panel display ensembled average velocity data (U, cm/s) and the bottom panel display wave intensity (dI, 104W/m2). Black line represents the net P, U and dI, blue line denotes the forward component and red line represents the backward component. It is the net P, U and Wave Intensity that is used for data analysis. The wave intensity shows a dominant forward compression wave (FCW) in early systole followed by a forward decompression wave in diastole related to the dicrotic notch.

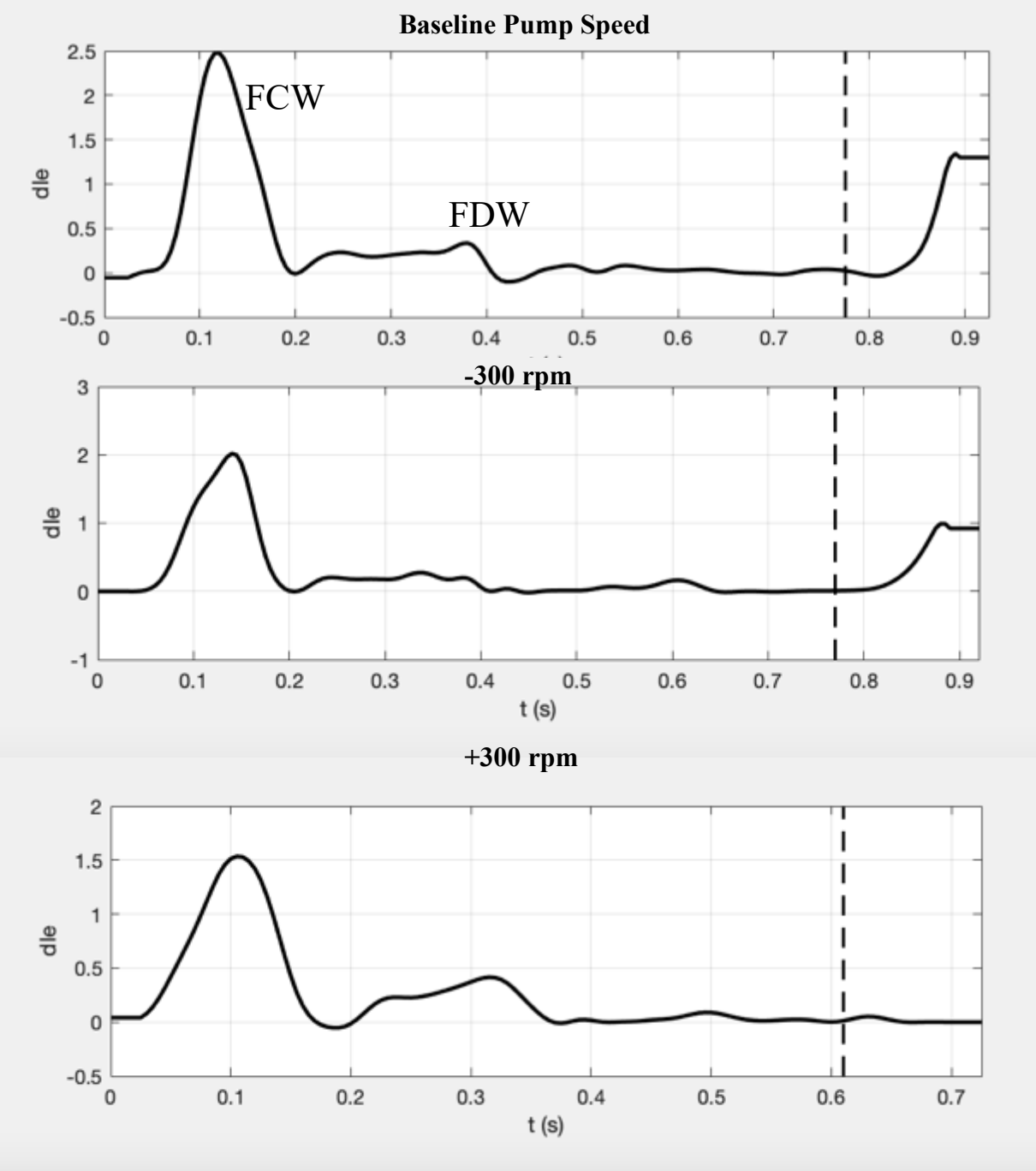

Figure 10. Displaying no change in wave intensity characteristics and pattern at different pump speeds.

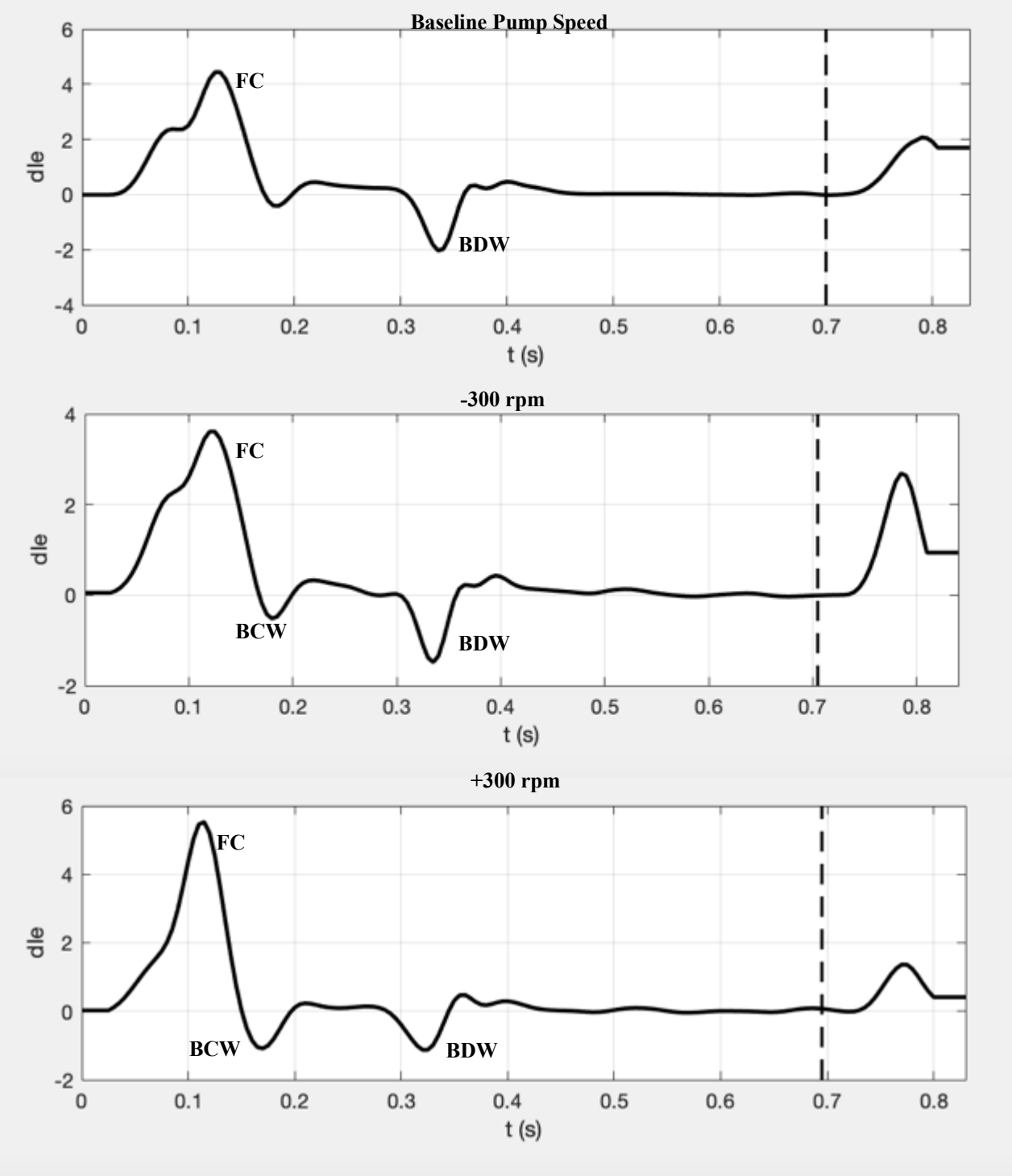

Figure 11. Displaying the increase of the BCW during systole when pump speeds increased and decreased by 300rpm.

Table 9. Changes in flow and WIA parameters with pump speed changes +/- 300rpm.

Parameter	Pump Speed *Minus 300rpm*	*Baseline*	*Plus 300rpm*	p
Pump Speed				*N/A*
Median (IQR)	5300 (5100, 5725)	5600 (5400, 6025)	5900 (5700, 6325)	
Flow, L/min				**<0.001**
Median (IQR)	4.5 (4.1, 5.1)	5.1 (4.7, 5.5)	5.4 (5.1, 5.7)	
Decrease (vs. Baseline)	13	-	2	
Increase (vs. Baseline)	0	-	11	
Pulse Index,				**<0.001**
Median (IQR)	5.5 (3.4, 5.9)	3.6 (3.2, 5.6)	3.3 (2.7, 4.4)	
Decrease (vs. Baseline)	4	-	10	
Increase (vs. Baseline)	9	-	3	
Pump Power				**<0.001**
Median (IQR)	4.0 (3.6, 4.4)	4.5 (4.1, 5.2)	4.8 (4.4, 5.5)	
Decrease (vs. Baseline)	12	-	0	
Increase (vs. Baseline)	0	-	12	
FCW Intensity, $10^4 W/m^2$				0.607
Median (IQR)	1.95 (0.99, 2.27)	1.82 (1.15, 3.16)	1.63 (1.23, 2.88)	
Decrease (vs. Baseline)	7	-	8	
Increase (vs. Baseline)	7	-	6	
BCW Intensity**, $10^4 W/m^2$				0.690
Median (IQR)	-0.26 (-0.53, 0.00)	0.00 (-0.63, 0.00)	-0.25 (-0.86, 0.00)	
Decrease (vs. Baseline)	5	-	6	
Increase (vs. Baseline)	4	-	3	
WRI**, %				0.368
Median (IQR)	9.1 (0.0, 28.6)	0.0 (0.0, 21.5)	13.0 (0.0, 26.5)	
Decrease (vs. Baseline)	4	-	2	
Increase (vs. Baseline)	5	-	7	
Wavespeed, cm/s				0.946
Median (IQR)	1.80 (1.30, 3.39)	2.25 (1.33, 4.64)	1.63 (1.17, 4.20)	
Decrease (vs. Baseline)	7	-	7	
Increase (vs. Baseline)	6	-	6	

FCW: forward compression wave, BCW backward compression wave, WRI: wave reflection index.

Table 10. Data for each individual case at each pump speed.

Case		Pump Speed		
		Minus 300rpm	***Baseline***	***Plus 300rpm***
1		5300rpm, 3lpm	5600rpm, 4.2lpm	5900rpm, 4.9lpm
	FCWi	2.01	2.48	1.53
	BCW	No	No	No
2		5000rpm, 4.7lpm	5300rpm, 5.4lpm	5600rpm, 5.6lpm
	FCWi	2.54	2.89	2.7
	BCW	Yes (-0.26)	Yes (-0.31)	Yes (-0.26)
3		5100rpm, 4.5lpm	5400rpm, 4.9lpm	5700, 5.1lpm
	FCWi	1.85	1.37	1.47
	BCW	Yes (-0.52)	No	Yes (-0.24)
4		5700rpm, 4.4lpm	6000rpm, 5.6lpm	6300rpm, 5.1lpm
	FCWi	2.18	2.04	1.8
	BCW	Yes (-0.8)	Yes (-1.46)	Yes (-1.27)
5*		9200rpm, 5lpm	9600rpm, 4.5lpm	10000rpm, 4.4lpm
	FCWi	3.67	3.97	3.58
	BCW	Yes (-0.29)	Yes (-0.62)	Yes (-1.02)
6		5300rpm, 3.9lpm	5600rpm, 4.5lpm	5900rpm, 4.4lpm
	FCWi	1	1.42	1.39
	BCW	No	No	No
7		5100rpm, 5.8lpm	5400rpm, 6.1lpm	5700rpm, 6.6lpm
	FCWi	2.09	5.36	2.49
	BCW	Yes (-1.37)	Yes (-1.21)	Yes (-0.64)

8	5100rpm, 3.7lpm	5400rpm, 4.1lpm	5700rpm, 4.5lpm
FCWi	1.69	1.59	1.37
BCW	No	No	No
9	5400rpm, 4.5lpm	5700rpm, 5.1lpm	6000rpm, 5.3lpm
FCWi	0.68	0.58	0.43
BCW	No	No	No
10	5000rpm, 4.5lpm	5300rpm, 5.1lpm	5600rpm, 5.4lpm
FCWi	0.97	0.71	0.81
BCW	Yes (-0.29)	Yes (-0.15)	Yes (-0.25)
11	5400rpm, 4.2lpm	5700rpm, 5.1lpm	6000rpm, 5.5lpm
FCWi	1.89	2.81	3.42
BCW	No	Yes (-0.64)	Yes (-0.81)
12*	9400rpm, 5.1lpm	9800rpm, 5.2lpm	10200rpm, 5.8lpm
FCWi	2.13	1.29	1.73
BCW	Yes (-0.26)	No	Yes (-0.16)
13	5300rpm, 4lpm	5600rpm, 4.5lpm	5900rpm, 5.1lpm
FCWi	3.61	4.43	5.53
BCW	Yes (-0.54)	No	Yes (-1.09)
14	5800rpm, 5.5lpm	6100rpm, 6.3lpm	6400rpm, 6.5lpm
FCWi	0.91	0.75	0.78
BCW	No	No	No

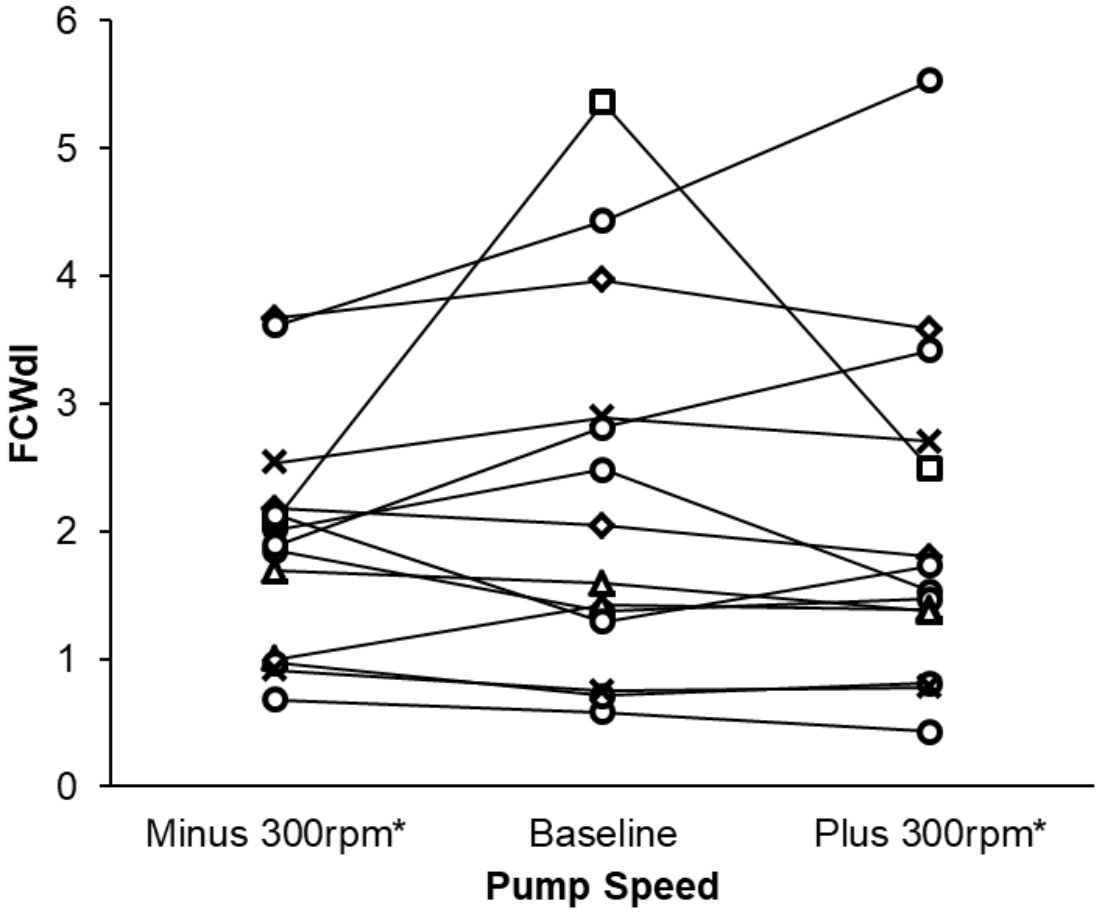

Figure 12. Individual FCW intensity response to pump speed changes. Points represent individual assessments, with different symbols used to ease differentiation between the N=14 patients. *For the N=2 patients with a Heartmate 2, alternative pump speeds of ±400rpm were used.

5.4. Discussion

This is the first study to characterise wave propagation in the pulmonary artery in patients with durable LVAD therapy. The main findings are: i.) the pattern of wave propagation in the pulmonary circulation in durable LVAD therapy is similar to patients without LVAD; with a dominating FCW during systole followed by a FDW in diastole and wave reflection in both systole and diastole. ii.) Acutely changing the pump speed by +/- 300rpm or 400rpm were not associated with a significant change in wave reflection in the pulmonary circulation, however there was a variable response across the cohort. iii.) Changing the pump speed did not cause the forward compression wave intensity to change significantly.

It has been demonstrated that left ventricular unloading can be achieved during ramp testing with significant reduction in left ventricular end diastolic diameter without causing RV dysfunction (Najjar et al., 2020), therefore as the pump speed changes it may have the potential to change wave propagation in the pulmonary circulation. However, in this study pump speed changes did not significantly affect WIA parameters nor wave reflection. This could be due to the baseline PVR (1.42 (1.03, 1.89)) and PAC (3.33 (2.98, 4.92)) were relatively optimised already and therefore further LV unloading or increasing the filling pressures by reducing the pump speeds did not cause wave reflection in the pulmonary circulation. It is also possible that by increasing and decreasing the pump speeds by 300rpm was not enough to effect a large enough change in the loading conditions for WIA to be able to detect changes in wave propagation. Various established ramp protocols in the literature for both HM2 and HM3 devices advocate adjusting pump speeds by over 1000rpm (Uriel et al., 2017; Addetia et al., 2018; Slaughter et al., 2009) and perhaps if we had changed the pump speeds by that magnitude we may have observed a change in wave propagation; however we did not have the resources

to do this in the cath lab during the RHC procedure. Furthermore, this was a point of discussion during the ethics application as we had to ensure we used similar ranges of pump speed changes following our usual protocol for pump speed optimisation post implant of Heartmate 3 devices.

Uriel et al have shown that on 3D echocardiography, at low pump speeds, the RV volumes and function remain stable but this deteriorates at higher pump speeds (Uriel et al., 2019), this may explain why there was no observed change in the forward compression wave intensity at all three pump speeds as the RV stroke volume and function were unaffected. In the previous chapter I have shown that the FCW intensity is directly proportional to the right ventricular stroke work index (RVSWi). Hence, if there is no change in the RVSWi then the FCW intensity is unlikely to be affected.

5.5. Limitations

The study included only a small number of patients, which limits the statistical power of the analyses. Pump speed changes of +/-300 rpm in HM3 and +/-400 in HM2 may not have changed the LV loading conditions enough to effect a change in the pulmonary circulation, however changes of 300rpm may avoid any excessive risk to patients as this point was specifically mentioned and discussed with the ethics committee review board. This study protocol affects acute changes only, longer term changes are unknown. It was not possible to acquire pulmonary arterial wedge pressure simultaneously during the pump speed changes to further assess LV filling pressure changes.

5.6. Conclusion

Wave propagation characteristics and pattern are similar in those with a durable LVAD compared to those who do not; this is the first study of WIA in the LVAD population. Changing the pump speeds by +/- 300rpm in HM3 and +/- 400rpm in HM2 devices did not change WIA parameters, and future studies in the LVAD cohort utilising WIA should consider a wider range of pump speed changes.

6. Results: Predictors of Mechanical Circulatory Support Following Heart Transplantation

In the previous chapter I reported my findings on WIA in patients with durable LVAD devices in situ. In this chapter, I investigated haemodynamic predictors of mechanical circulatory support following orthotopic heart transplantation and I report my findings below.

6.1. Introduction

Early graft dysfunction (EGD) whether primary or secondary (eg: related to surgical/ technical factors, immunological response or pulmonary hypertension) within 24 hours of heart transplantation is associated with significant morbidity and mortality. Severe EGD is defined as the use of mechanical circulatory support (MCS) occurring within 24 hours of being weaned from cardiopulmonary bypass and transfer to intensive care (Kobashigawa et al., 2014). The incidence of EGD following heart transplantation has been reported to be between 2.3% - 28.2% and in recipients who develop EGD, the overall mortality have been reported to be 28.4% and 38% and 45.8% at 30 days, 1 year and 5 years respectively (Smith et al., 2022).

In most cases, early mechanical circulatory support is deployed for severe graft dysfunction due to failure to separate from cardiopulmonary bypass or immediate haemodynamic instability. However, in some cases, graft dysfunction may evolve over hours after transplantation, possibly compounded by other hemodynamic insults such as vasoplegia, leading to ‘delayed’ use of MCS. There are little published data on the evolution of EGD and ‘delayed’ MCS following heart transplantation.

Low pulmonary artery pulsatility index (PAPI, ratio of pulmonary artery pulse pressure to right atrial pressure) has been shown to be associated with an increased rate of adverse cardiac events which including left ventricular assist device (LVAD) implantation in patients with advanced heart failure (Bayram et al., 2022; Yim et al., 2023; Cesini et al., 2020). Low PAPI prior to heart transplantation from RHC (median of 31 days for those with pulmonary hypertension and 41 days for those without pulmonary hypertension preceding heart transplantation) was also associated with graft failure following transplantation (Wagner et al., 2022).

I therefore analysed data from two heart transplant centres in the UK to characterise the haemodynamic changes and tuse of 'delayed' use of MCS following heart transplantation. I hypothesise that a low PAPI is associated with delayed MCS use following heart transplantation.

6.2. Methods

A retrospective analysis was performed on 216 consecutive heart transplant recipients from two UK transplant centres, Queen Elizabeth Hospital Birmingham and Royal Papworth Hospital, Cambridge, between 10th May 2018 to 20th December 2022. Patients who required MCS immediately at the end of the operation either because it was planned or because of haemodynamic instability were excluded. 28 recipients were excluded from centre 1 and 15 recipients were excluded from centre 2, therefore analysis was performed on 173 recipients. Transplant related data and postoperative haemodynamic data were obtained from both centres with a full data set available. Haemodynamic data were obtained at T0 (immediately post-transplant) and at T6 (six hours following transplant) and we compared the recipients who

required delayed MCS to those who did not. PAPI was derived from the ratio of pulmonary arterial pulse pressure to the right atrial pressure.

For all variables, descriptive statistics were computed with histograms and Q-Q plots performed. Normally distributed data are presented as means and standard deviations and non-parametric data are displayed as medians and interquartile range. Paired T-test was used for normally distributed data and the Wilcoxon signed rank test was used for non-parametric related data. Independent T Test was used for independent normally distributed data and the Mann Whitney U test was employed for independent non-parametric data. Two tailed tests of significance were considered to be significant at $p < 0.05$. PAPI were analysed with receiver operating characteristic (ROC) curves, the total area under the ROC curve (AUC) values were considered to assess the performance of the variable.

Univariate logistic regression and the Hosmer and Lemeshow goodness of fit tests were performed. If the Hosmer and Lemeshow goodness of fit test was significant, then the variable underwent log transformation prior to being included in the multivariable analysis. The models were built including PAPI, total ischaemic time and short term MCS bridge to transplantation as these are widely reported to predict post-transplant MCS requirement. In view of the low number of patients who required MCS (n=24), I limited the number of variables to three to avoid over-fitting. Multivariable logistic regression models were performed with both T0 and T6 PAPI as separate models. All statistical analyses were performed using SPSS (IBM Corp. SPSS Statistics for Macintosh, Version 29.0, Armonk, NY).

6.3. Results

Patients who had 'immediate' MCS were excluded at the end of the operation, (n=43), therefore analysis was performed on 173 recipients (Figure 13). In this cohort of heart transplant recipients, 19.9% underwent 'immediate' MCS and 13.9% of patients underwent 'delayed' MCS. The median recipient age was 49 years, 69.4% were male and the most common pathology was idiopathic dilated cardiomyopathy. The median total ischaemic time was 179 mins and median cardiopulmonary bypass (CPB) time was 189 minutes (Table 11). There were no deaths at or before 30 days in this cohort of patients. There were no significant differences in cold ischaemic time, warm ischaemic time, total ischaemic time or cumulative CPB time between the two groups.

Twenty-four recipients (13.9%) required 'delayed' MCS following heart transplantation (4 central ECMO, 8 peripheral ECMO, 11 percutaneous RVAD, 1 central RVAD). Right atrial pressure (RAP) was significantly higher in the 'delayed' MCS group at both T0 and T6, compared to the no 'delayed' MCS group (Table 12), and increased significantly from T0 to T6 in the 'delayed' MCS group ($p= 0.026$). As a result, PAPI was significantly lower in the 'delayed' MCS group at both T0 and T6 (T0: 1.67 vs 1.21 ($p= 0.001$) and T6: 1.44 vs 0.77 ($p<0.001$) (Figure 14). Cardiac indices were comparable between the two groups at both time points, but cardiac index dropped significantly in the 'delayed' MCS group at T6 relative to T0, $p=0.007$. Right ventricular stroke work index was similar between the two groups at T0 but was significantly lower at T6 (3.53 (2.34) vs 1.80 (1.93), $p<0.001$) which suggests the cause for EGD and the need for MCS is due to right ventricular failure.

Table 11. Donor and Recipient characteristics, by those requiring delayed MCS in the early perioperative period compared with those who did not.

N= 173	All	No MCS N=149	MCS N=24	P
Recipient Sex (male %)	69.4	70.5	62.5	0.433
Recipient Age (years)	49 (21)	50 (20.5)	47.5 (24.3)	0.735
Recipient Height (m)	1.71 +/- 0.1	1.71 +/- 0.1	1.69 +/-0.1	0.319
Recipient Weight (Kg)	75.7 +/- 14	75.5 +/-14.2	77.3 +/- 13.1	0.57
Recipient BMI (kg/m2)	25.9 +/- 4.33	25.7 +/- 4.34	27.2 +/- 4.14	0.128
Recipient BSA(m2)	1.87 +/- 0.20	1.87 +/- 0.20	1.88 +/- 0.19	0.982
Recipient LV Mass (g)	147 +/- 26.6	147 +/- 26.7	146 +/- 26.5	0.838
Recipient RV Mass (g)	23.4 (5.41)	23.9 (5.43)	24.0 (5.48)	0.902
Recipient Ventricular Total Mass (g)	171 +/- 29.5	171 +/- 29.7	170 +/- 29.1	0.865
Donor Sex (male %)	60.7	61.7	58.3	0.799
Donor Age (years)	36(20)	36 (12.8)	38.5 (15.5)	0.514
Donor Height (m)	175 +/- 9.1	176 +/- 8.92	171 +/-9.71	0.06
Donor Weight (Kg)	80 +/- 15.2	79.5 +/- 14.4	83.8 +/-19.6	0.2
Donor BSA(m2)	1.95 +/- 0.19	1.95 +/- 0.19	1.96 +/- 0.23	0.858
Donor LV Mass (g)	155 (41.1)	154 (41.0)	166 (36.2)	0.546
Donor RV Mass (g)	27.0 (7.15)	27.0 (7.43)	26.3 (5.34)	0.315
Donor Ventricular Total Mass (g)	184 (47)	183 (48.0)	193 (45.0)	0.696
Donor Status DCD (n, %)	26 (15)	25 (16.8)	1 (4.2)	0.109

N= 173	**All**	**No MCS N=149**	**MCS N=24**	**P**
Cold Ischaemic Time (mins)	126 +/- 39.9	126 +/- 38.5	131 +/- 47.0	0.549
Warm Ischaemic Time (mins)	58 (20.5)	58 (21.5)	58.5 (21.5)	0.245
Total Ischaemic Time (mins)	179 (70.5)	175 (70)	197 (64)	0.058
Cardiopulmonary Bypass Time (mins)	189 (88.5)	190 (87.5)	186 (117)	0.814
Recipient Aetiology				
Dilated Cardiomyopathy (%)	53.8	53	54.2	
Ischaemic Cardiomyopathy (%)	23.1	23.5	20.8	
Hypertrophic Cardiomyopathy (%)	12.7	12.8	12.5	
Other	10.4	10.7	12.5	

At T0, the ‘delayed’ MCS group were treated with significantly higher levels of Epinephrine, Norepinephrine, Phosphodiesterase inhibitors (PDEi) and Vasopressin, resulting in significantly higher Vasoactive inotropic scores (VIS) to maintain comparable blood pressure (Table 13). Both SVR and SVRi were lower in the ‘delayed’ MCS group at both time points, albeit not statistically significant (p=0.100 and 0.066 for SVR and SVRi respectively at T0 and p=0.235 and 0.332 at T6)), and with significantly higher vasopressor use. At T6, the MCS group continued to require significantly higher levels of Norepinephrine and had a higher VIS. The changes in the inotropic/vasoconstrictor levels and the VIS score from T0 to T6 in the ‘delayed’ MCS group was not statistically significant.

On multivariable logistic regression analysis, both PAPI at both T0 and T6 was associated with ‘delayed’ MCS following transplantation independent of donor organ total ischaemic time and short term MCS bridge to transplantation (p= 0.03 and p<0.01 respectively) (Table 14). Receiver operator characteristics were performed for PAPI, CVP and RVSWi and T6 PAPI was found to be the best predictor for MCS with an AUC of 0.868. T0 CVP AUC 0.660, T6 CVP AUC 0.779, T0 RVSWi AUC 0.595, T6 RVSWi 0.810. The optimal cut-off for T6 PAPI was determined as 1.22 for predicting MCS following heart transplantation with a sensitivity of 81% and 65% specificity (Figure 15).

Table 12. Haemodynamic parameters for the entire cohort, those who did not require MCS and for those who had delayed MCS.

T0 Haemodynamic Parameters (N= 173)	**T0 All**	**T0 No MCS N=149**	**T0 MCS N=24**	**P**
RAP (mmHg)	10.3 +/- 3.7	9.9 +/-3.7	12.1 +/-3.1	0.009*
SPAP (mmHg)	33.3 +/- 6.5	33.5 +/- 6.7	31.9 +/- 5.4	0.281
DPAP (mmHg)	16.7 +/- 4.6	16.7 +/- 4.7	17.0 +/- 3.8	0.786
MPAP (mmHg)	22.2 +/- 5.0	22.3 +/- 4.8	21.1 +/- 5.9	0.256
MAP (mmHg)	69.3 +/- 9.2	69.9 +/- 9.0	65.5 +/- 9.9	0.03*
PAPi	1.64 (1.19)	1.67 (1.23)	1.21 (1.21)	0.001*
TPG (mmHg)	5 (3)	5 (3)	5 (2)	0.120
PVR (WU)	1.05 (0.53)	1.11 (0.59)	0.92 (0.28)	0.122
RVSWi (g/m^2/beat)	3.83 (3.01)	3.85 (2.79)	3.02 (3.01)	0.115
CO (L/min)	5.10 (2.48)	5.10 (2.50)	5.60 (1.89)	0.704
CI (L/min/m2)	2.67 (2.48)	2.67 (1.27)	2.87 (0.94)	0.596
SVR (dynes.sec.cm-5)	948 (472)	959 (481)	831 (579)	0.1
SVRi (dynes.sec.cm-5.m2)	1770 (869)	1842 (930)	1597 (750)	0.066
T6 Haemodynamic Parameters (N=173)	**T6 All**	**T6 No MCS N=149**	**T6 MCS N=24**	**P**
RAP (mmHg)	11.3 +/- 3.5	10.8 +/- 3.1	14.7 +/- 4.4	<0.001*
SPAP (mmHg)	31.7 +/- 6.6	32.0 +/- 6.8	29.5 +/- 4.7	0.038*
DPAP (mmHg)	16.5 +/- 4.4	16.3 +/- 4.4	17.8 +/- 3.9	0.12
MPAP (mmHg)	21.3 +/- 5.2	21.5 +/- 4.8	19.9 +/-7.2	0.164
MAP (mmHg)	68.4 +/- 8.4	69.3 +/- 8.3	63.0+/- 6.5	<0.001*
PAPi	1.38 (0.88)	1.44 (0.82)	0.77 (0.52)	<0.001*
TPG (mmHg)	5 (2)	5 (2)	4 (1.25)	<0.001*

T6 Haemodynamic Parameters (N=173)	T6 All	T6 No MCS N=149	T6 MCS N=24	P
PVR (WU)	0.99 (0.51)	1.02 (0.5)	0.83 (0.23)	0.018*
RVSWi (g/m^2/beat)	3.36 (2.39)	3.53 (2.34)	1.80 (1.93)	<0.001*
CO (L/min)	4.77 (1.90)	4.80 (1.90)	4.60 (1.91)	0.17
CI (L/min/m2)	2.55 (0.88)	2.60 (0.91)	2.40 (0.82)	0.06
SVR (dynes.sec.cm-5)	947 (347)	949 (346)	858 (341)	0.235
SVRi (dynes.sec.cm-5.m2)	1797 (589)	1802 (622)	1622 (558)	0.332

RAP: right atrial pressure, SPAP: systolic pulmonary arterial pressure, DPAP: diastolic pulmonary arterial pressure, MPAP: mean pulmonary arterial pressure, MAP: mean arterial pressure, PAPi: pulmonary arterial pulsatility index, TPG: transpulmonary gradient, PVR: pulmonary vascular resistance, RVSWi: right ventricular stroke work index, CO: cardiac output, CI: cardiac index, SVR: systemic vascular resistance, SVRi: indexed systemic vascular resistance.

Table 13. Inotropic and Vasoconstrictor data.

T0 Inotropes/Vasoconstrictors	T0 All	T0 No MCS N=149	T0 MCS N=24	P
Epinephrine (micrograms/kg/min)	0.04 (0.05)	0.04 (0.05)	0.03 (0.07)	0.910
	77.5%	78.5%	70.8%	0.403
Norepinephrine (micrograms/kg/min)	0.07 (0.09)	0.06 (0.07)	0.15 (0.15)	<0.001*
	83.2%	80.5%	100%	0.018*
Dopamine (micrograms/kg/min)	3.8 (5)	4 (5)	0 (5)	0.178
	64.2%	67.8%	41.7%	0.013*
Milrinone (micrograms/kg/min)	0 (0.17)	0 (0.15)	0.225 (0.18)	<0.001*
Enoximone (micrograms/kg/min)	0 (0)	0 (0)	0 (0)	0.116
PDEi (Enoximone or Milrinone)	57.2%	53.0%	83.3%	0.005*
Vasopressin	34.7%	31.5%	54.2%	0.031*
Vasoactive Inotropic Score	16 (11.4)	15.4 (9.88)	23.8 (16.8)	<0.001*

T6 Inotropes/Vasoconstrictors	T6 All	T6 No MCS N=149	T6 MCS N=24	P
Epinephrine (micrograms/kg/min)	0.03 (0.06)	0.03 (0.06)	0.04 (0.07)	0.229
	71.7%	70.5%	79.2%	0.380
Norepinephrine (micrograms/kg/min)	0.07 (0.11)	0.06 (0.09)	0.17 (0.10)	<0.001*
	82.1%	79.2%	100%	0.014*
Dopamine (micrograms/kg/min)	4.2 (5)	4.4 (5)	0 (5.07)	0.146
	64.7%	69.1%	37.5%	0.003*
Milrinone (micrograms/kg/min)	0 (0.15)	0 (0.14)	0.14 (0.23)	0.005*
Enoximone (micrograms/kg/min)	0 (0)	0 (0)	0 (0)	0.640
PDEi (Enoximone or Milrinone)	57.8%	56.4%	66.7%	0.343
Vasopressin	35.8%	33.6%	50%	0.119
Vasoactive Inotropic Score	16.7 (11.7)	16.2 (11.7)	26.0 (15.8)	<0.001*

Doses given in micrograms/kg/min and percentages represent the proportion of patients who were on each drug. PDEi= phosphodiesterase inhibitors (either Milrinone or Enoximone)

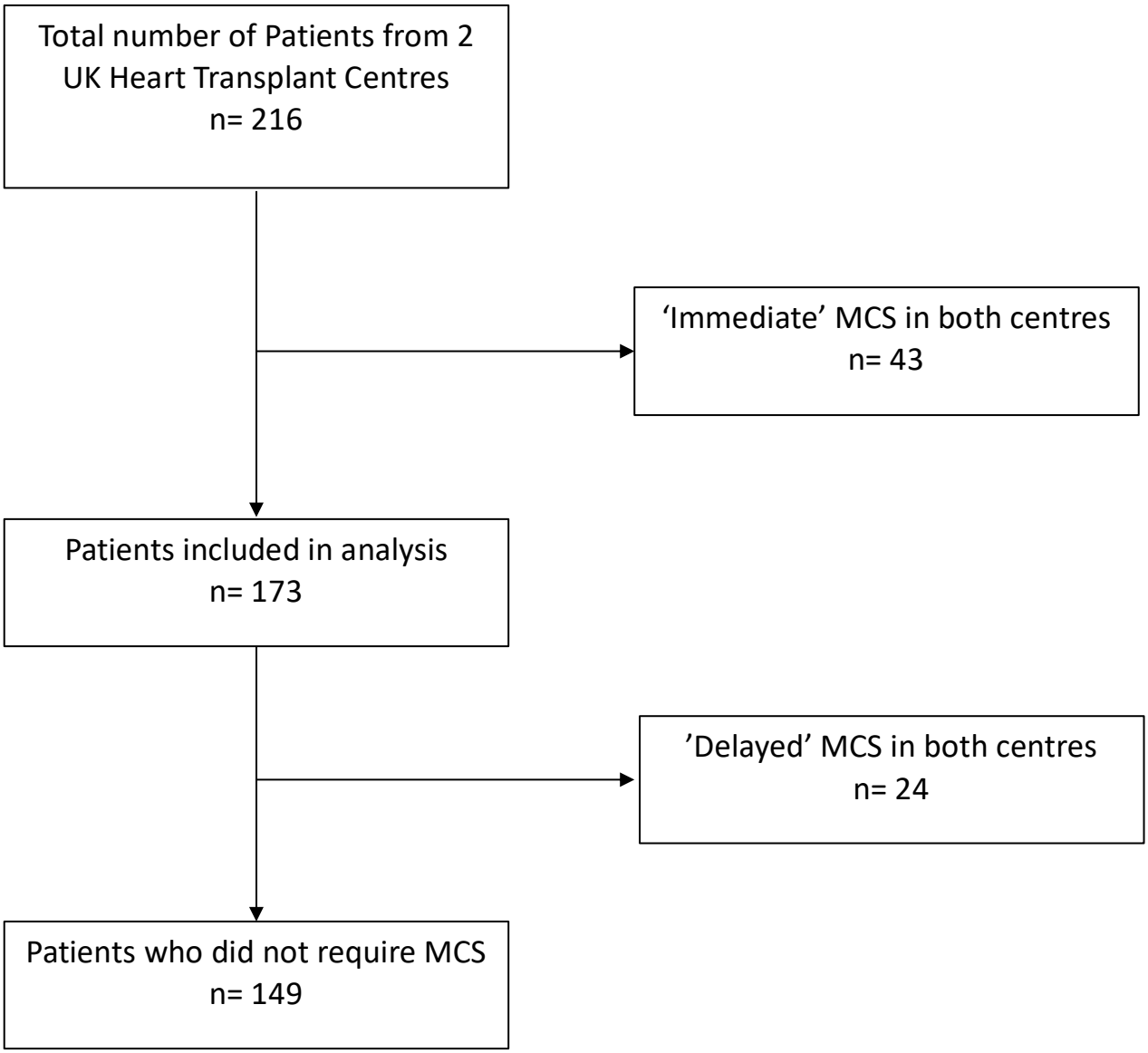

Figure 13. Consort diagram displaying the number of patients excluded from analysis.

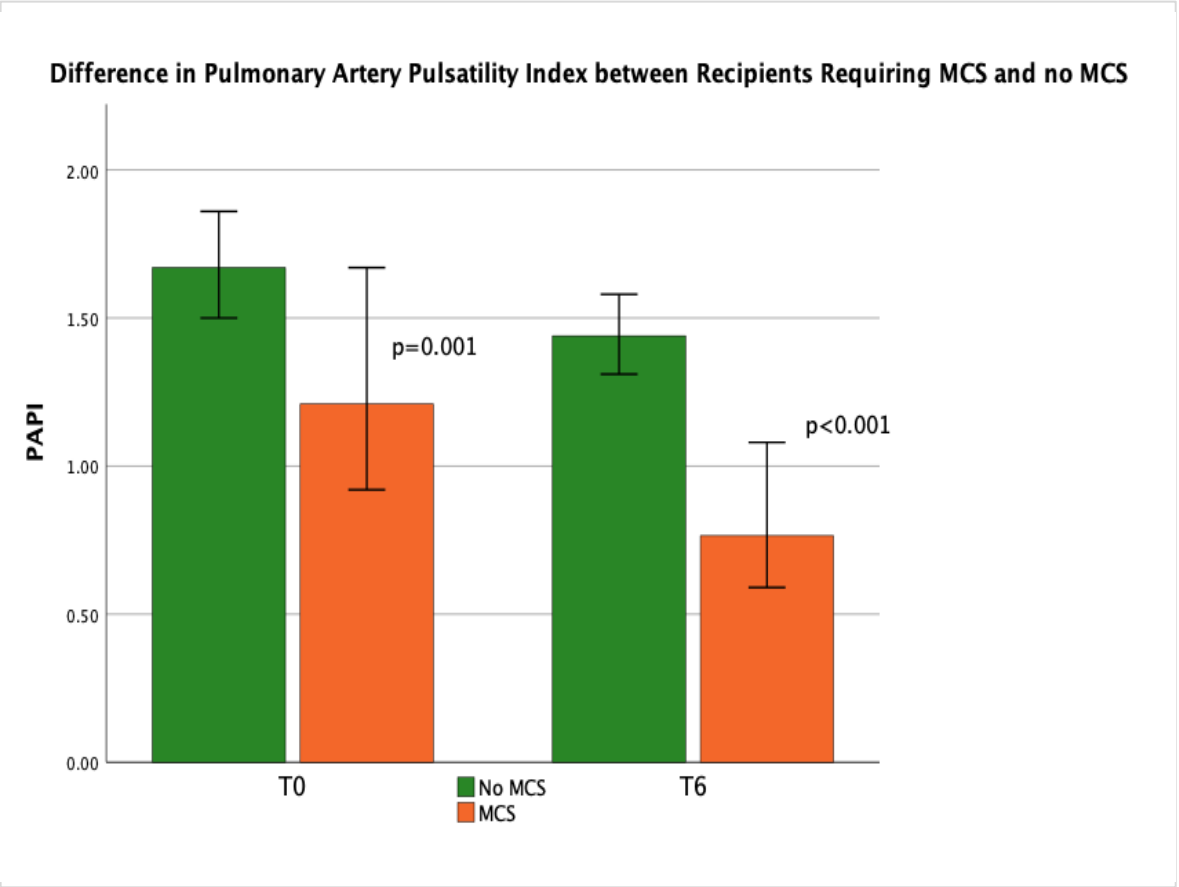

Figure 14. Histogram displaying the difference of PAPI between recipients who did and did not require MCS.

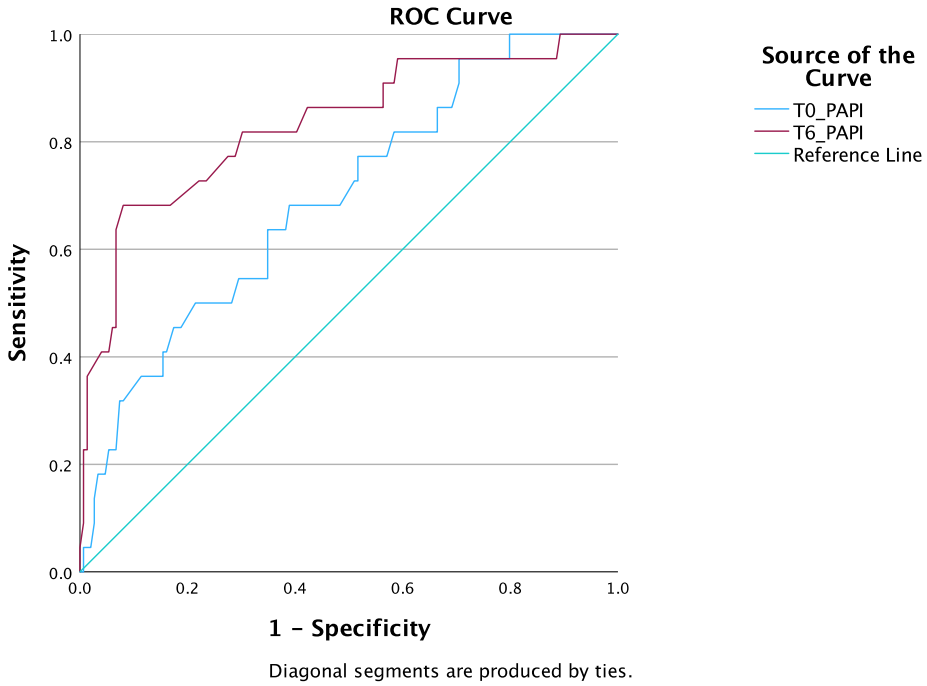

Figure 15. Receiver operating characteristics of T0 PAPI and T6 PAPI. T0 PAPI AUC= 0.694, T6 PAPI AUC= 0.832.

Table 14. Multivariable logistic regression analysis

T0	**Regression Coefficient**	**P**	**Odds Ratio**	**95% CI**
PAPi	-1.295	0.003*	0.274	0.117- 0.643
Total Ischaemic Time	0.008	0.125	1.008	0.998-1.018
Short term MCS Bridge	-0.391	0.476	0.676	0.231-1.982
Constant	-1.135	0.342	0.321	
T6	**Regression Coefficient**	**P**	**Odds Ratio**	**95% CI**
PAPi	-2.303	<0.001*	0.1	0.036-0.276
Total Ischaemic Time	0.007	0.193	1.007	0.996-1.018
Short term MCS Bridge	0.94	0.882	1.098	0.318-3.789
Constant	-2.956	0.005	0.052	

6.4. Discussion

In this study, I found that i.) 19.9% underwent immediate MCS and 13.9% of patients underwent 'delayed' MCS for EGD; ii.) A lower PAPi at both T0 and T6 were associated with 'delayed' MCS; iii.) PAPI <1.22 at T6 was independently associated with 'delayed' MCS, with sensitivity and specificity of 81% and 65% respectively.

Severe EGD, especially primary graft dysfunction often manifests at the time of surgery with difficulty in separating from cardiopulmonary bypass or low cardiac output syndrome shortly after separation from cardiopulmonary bypass. Vasoplegia is also a recognised cause of haemodynamic instability and may plausibly result in secondary graft dysfunction related to hypoperfusion. Secondary graft dysfunction in these cases may manifest over hours as progressive deterioration in right heart function. As such, an early measure of right heart function may identify patients at risk of severe graft dysfunction and 'delayed' MCS.

There has been great interest in employing PAPI to predict right heart failure (RHF) and indeed one original development of PAPI was in the context of cardiogenic shock following right ventricular infarction(Korabathina et al., 2012). In patients with durable left ventricular assist device (LVAD) a lower PAPI has been well documented to be associated with RHF and worse outcomes in the LVAD setting(Kang et al., 2016; Morine et al., 2016; Gudejko et al., 2019). In the advanced heart failure cohort of patients a lower PAPI has been shown to be associated with significant adverse cardiovascular events including death and rehospitalisation(Kochav et al., 2018). There are no previously published reports of PAPI and severe EGD post-heart transplantation.

Data from the Eurotransplant database suggested that a low pre-transplant PAPI and high PVR predicted graft failure, although PAPI alone did not have any prognostic implications(Wagner et al., 2022). Furthermore, pre-transplant haemodynamics of the right heart, i.e. RAP, pulmonary capillary wedge pressure (PCWP), RAP:PCWP ratio, MPAP and PAPI, have also been shown to predict post-transplant acute kidney injury(Guven et al., 2018). Pre-transplant RAP has been shown to be associated with primary graft dysfunction and it has been used as part of the RADIAL score which predicts primary graft failure following heart transplantation(Segovia et al., 2011; Cosío Carmena et al., 2013). However, pre-transplant hemodynamic data have limited utility in guiding the use of post-transplant MCS, as post-heart transplant management is primarily guided by post-transplant hemodynamic data. This is the rationale for studying the evolution of hemodynamic parameters in the hours following heart transplantation, and emphasises the value of serial hemodynamic assessment in guiding MCS use. Mortality was low (2/24, 8%, both deaths were >120days following transplant) in this cohort of patients undergoing 'delayed' MCS, suggesting that a strategy of close hemodynamic monitoring and hemodynamic-guided MCS use may not compromise early post-transplant survival.

Pulmonary arterial pulsatility index has been used as an indicator of right heart function and it assumes that the failing right heart results in congestion (high RAP) and reduced stroke volume (reduced pulmonary artery pulse pressure). Pulmonary arterial pulse pressure is also intricately linked to pulmonary arterial capacitance (PAC) and pulmonary vascular resistance, as PAC decreases as MPAP increases (Lim and Gustafsson, 2020). In this study, the lower PAPI in the 'delayed' MCS group was related to a combination of higher RAP and lower pulmonary artery pulse pressure at both T0 and T6. The ROC analysis showed that PAPI was a good predictor of

delayed MCS use following heart transplantation, especially at T6. The median PAPI was 1.21 at T0 and significantly dropped to 0.77 at T6 (p=<0.001). In our cohort, a PAPI at T6 of 1.22 was the optimal cut-off for predicting impending MCS. It should be noted that PAPI threshold is highly dependent on the patient population under study, as PAC and pulmonary vascular resistance are determinants of PAPI. Thus, the PAPI cut-off cannot be extrapolated from studies of other patient groups.

6.5. Study limitations

This was an observational study without randomised data and we had relatively small numbers in our cohort. Our data is only relevant in the setting of heart transplantation without wider application. Finally, we only had data from 2 time points, at T0 and at T6. It would have been desirable to have had data from more additional time points at one, three and beyond six hours.

6.6. Conclusions

In this chapter, I have shown that a lower PAPI in the early postoperative period following heart transplantation is associated with delayed MCS, especially measured at 6 hours post-operation. A T6 PAPi below 1.22 was associated with MCS implantation and this would suggest that PAPI could be used to predict impending PGD and signal the need for early MCS. The use of PAPI in this setting requires further validation but should be considered to be incorporated into future risk scores for predicting PGD in cardiac transplantation.

7. Results: Stroke Volume Calculator Utilising Pulmonary Haemodynamics

In the previous chapter, I have shown that a low PAPI and a high RAP are associated with mechanical circulatory support following orthotopic heart transplantation. Using the data from the previous chapter, I then investigated if the stroke volume can be estimated utilising pulmonary haemodynamic data and I will present my findings in this chapter.

7.1. Introduction

On intensive care and intraoperatively, it is often desirable to have stroke volume (SV) data to aid fluid management, optimisation of preload and to guide inotropic and vasoconstrictor therapy especially in the setting of Cardiac Surgery. The most widely used method of calculating stroke volume is by using a pulmonary arterial catheter (PAC) and performing cardiac output (CO) studies either by thermodilution or by using Fick's principle. The thermodilution method requires repeated and multiple injections of cold fluid which can be undesirable and have its limitations. Firstly the results are dependent on the volume, rate and temperature of the injectate as shown by the Steward-Hamilton equation (Bootsma et al., 2022), and secondly there are different clinical states which over or underestimates the CO such as tricuspid regurgitation and high flow states (Kubo et al., 1987; Renner et al., 1993). There are contemporary PACs which can continuously monitor CO and therefore SV, utilising the area under the thermodilution waveform and this has been validated against the intermittent bolus method (Mihaljevic et al., 1995; Yelderman et al., 1992; Sun et al., 2002). However, there are

drawbacks to continuous CO monitoring PACs mainly surrounding the cost and also the delayed response of these catheters as the CO data produced reflects the haemodynamic status from the previous 4-12 minutes, making the impact of interventions, such as fluid boluses or increased inotrope infusion, more difficult to assess, and therefore it has not been widely adopted.

Non-invasive CO devices such as the LiDCO™, PiCCO™ and FloTrac™ have been developed to estimate CO utilising arterial wave form analysis. However, there are few validation studies comparing these devices with PAC and the power of the studies are often limited (Mora et al., 2011; Hadian et al., 2010; Lamia et al., 2018), hence they have not been widely adopted following cardiac surgery. PAC is still the current gold standard of cardiac output monitoring on cardiac intensive care units (ITU). Using the data collected in this projected, I have devised a calculator which estimates the SV utilising pulmonary haemodynamics only and negates the need for multiple cold fluid bolus injections.

Pulmonary artery pulse pressure (PAPP) is directly related to SV, a relationship that is modified by pulmonary vascular resistance (PVR). The purpose of this study was to develop a SV calculator from PAPP to allow continuous monitoring of SV and CO from PAPP based on this relationship between PAPP and SV. I evaluated this calculator in a cohort of patients who underwent heart transplantation. From the results of the previous chapter, I noted no significant changes in PVR from admission into intensive care unit post-heart transplantation (T0) to six hours post-admission into the intensive care unit (T6).

7.2. Methods

Analogous to the charging of capacitors, a significant proportion of the right ventricular SV 'charges' the reservoir volume and increases pressure in the compliant pulmonary arteries in systole, which discharges during diastole. Total pulmonary arterial capacitance (C) defines this relationship between volume and pressure as the increase in blood volume (ΔV) in the arterial system that produces a unit increase in arterial transmural pressure. In practice, C is difficult to measure because direct measurement of ΔV is not possible due to the continuous outflow from the arterial system. Therefore, the ratio of SV/PAPP has been used to determine C, accepting that this equation overestimates the true C.

PAPP = SV/C

Rearranging this equation: PVR x SV = RC x PAPP

RC is related to pulmonary arterial wedge pressure (PAWP) as previously described by Tedford et al (Tedford et al., 2012) and Lankhaar et al (Lankhaar et al., 2006, 2008):

RC= -0.0063 x PAWP + 0.46

Therefore: SV = (-0.0063 x PAWP + 0.46) x PAPP/PVR, or

SV = (-0.0062 x PAWP + 0.46) x PAPP/ (PVR x 60/1000), will derive SV in ml.

Based on this equation, SV is predominantly related to PAPP and PVR. Changes in absolute levels of PAWP have modest effect on absolute SV. For example, at a constant PVR of 2.0WU and PAPP of 20mmHg, doubling PAWP from 12mmHg to 24mmHg is associated with a decrease in SV from 64ml to 51ml. However, at PAWP of 12mmHg and PAPP of 20mmHg, SV increases from 64ml to 85ml if PVR is reduced from 2.0 to 1.5WU.

In the absence of significant changes in PVR, PAPP is predominantly related to absolute SV. We hypothesized that changes in PAPP can be used to track changes in SV and CO in acute settings where PVR is unchanged.

Haemodynamic data on 169 patients following orthotopic heart transplantation was used at two separate time points, immediately following return to intensive care (T0) and at six hours post-transplant (T6), therefore 338 data points were used in this analysis. Haemodynamic data were all recorded from standard PACs. This study has two parts:

Firstly, I tested the agreement between the calculator-derived SV (ie: calculator SV) and the SV derived from conventional thermodilution CO (ie: thermodilution SV) studies at T0.

Secondly, I simulated the condition where repeat thermodilution and wedge studies were not available, so the pulmonary vascular resistance was assumed to be unchanged from baseline. For this simulation, we used baseline (T0) R to 'calibrate' the calculator and pulmonary artery diastolic pressure (PADP) at T6 to replace PAWP at T6. The calculator SV using these assumptions were compared against the 'true' thermodilution SV. To further expand on the calibration process, linear regression analysis between the calculator derived stroke volumes and thermodilution derived stroke volumes was performed and with the coefficient and constant obtained, this was then applied to the calculator stroke volumes before performing the Bland-Altman analysis. For example Figure 16 shows the linear regression analyses with a $r=0.920$, $p<0.001$, and obtaining the coefficient of 0.539 and the constant of 2.06 which was then applied to the calculator stroke volumes.

Statistical Analysis

All data were analysed for normality with histograms and the Shapiro-Wilk test. Normally distributed data are expressed as mean and standard deviation and non-parametric data are expressed as median and interquartile range (IQR). The Mann Whitney U test was employed to compare non-parametric data. A $p<0.05$ was considered statistically significant.

Correlation and linear regression analyses were performed comparing the calculator derived SV and the thermodilution-derived SV and SV index (SVi, indexed to body surface area). The calculator SV were adjusted based on the coefficient and constant. The differences, percentage change and mean between the calculator and thermodilution-derived SV were then calculated and Bland-Altman plots were constructed. The percentage error (ie, accuracy), derived by the Bland–Altman analysis, is the difference between the measured value and that calculated using the reference method.

There is inherent error in cardiac output measurements by thermodilution (limits of precision of ±10-20%). When comparing the current calculator against this reference method (thermodilution), the limits of agreement will inevitably be larger than the limits of precision of the reference method (combining the errors of the test and reference methods). On the basis of an analysis of 25 studies, Critchley et al (Critchley and Critchley, 1999) suggested that a value of up to 30% is considered clinically acceptable, and this is the limit that I have adopted in this study.

Pearson correlation was performed comparing the raw calculator SV with CO derived SV and the coefficient and constant yielded was used to adjust the raw calculator SV data. All statistical

analyses were performed on IBM SPSS Statistics for Mac, Version 29.0. Armonk, NY: IBM Corp.

7.3. Results

This study included 169 patients who underwent orthotopic heart transplantation at either Queen Elizabeth Hospital Birmingham or Royal Papworth Hospital, Cambridge from 2019 to 2022, and the cohort characteristics are displayed in Table 15. Haemodynamic data at T0 and T6 are displayed in Table 16. The median thermodilution-derived SV was 47.9ml (37.5-61.0ml) and the median calculated SV was 87.4ml (66.1, 110.1). Calculator SV correlated with thermodilution-derived SV at T0 ($r=0.920$, $p<0.001$, coefficient of 0.539 and the constant of 2.06) (Figure 16a). After applying the coefficient and constant to the calculator SV, the adjusted median calculator SV was 49.1 (IQR 37.4-63.1) ml. There was no significant difference between the adjusted calculator SV compared with the CO derived SV: 49.1ml (IQR 37.4- 63.1) vs 48ml (37.0-62.8), respectively ($p= 0.780$).

The median difference at T0 between the adjusted calculator SV and thermodilution-derived SV was -0.052ml (IQR -4.12-4.46), the median percentage change was -0.078% (IQR -8.86-11.6). The difference between the calculator SV and thermodilution-derived SV was not statistically significant (mean: -0.04, SD: 7.97, $p=0.944$). The absolute difference between the adjusted calculator SV and the CO derived SV at T0 was plotted against the mean on Bland-Altman plot in Figure 17a, with the red line denoting the mean difference of -0.043ml and the black lines representing the 95% confidence interval (95% CI -15.6 – 15.6). The mean percentage change between the adjusted calculator SV and thermodilution-derived SV was 1.83% and 95% CI -27.2 – 30.8 (Figure 18a).

A.

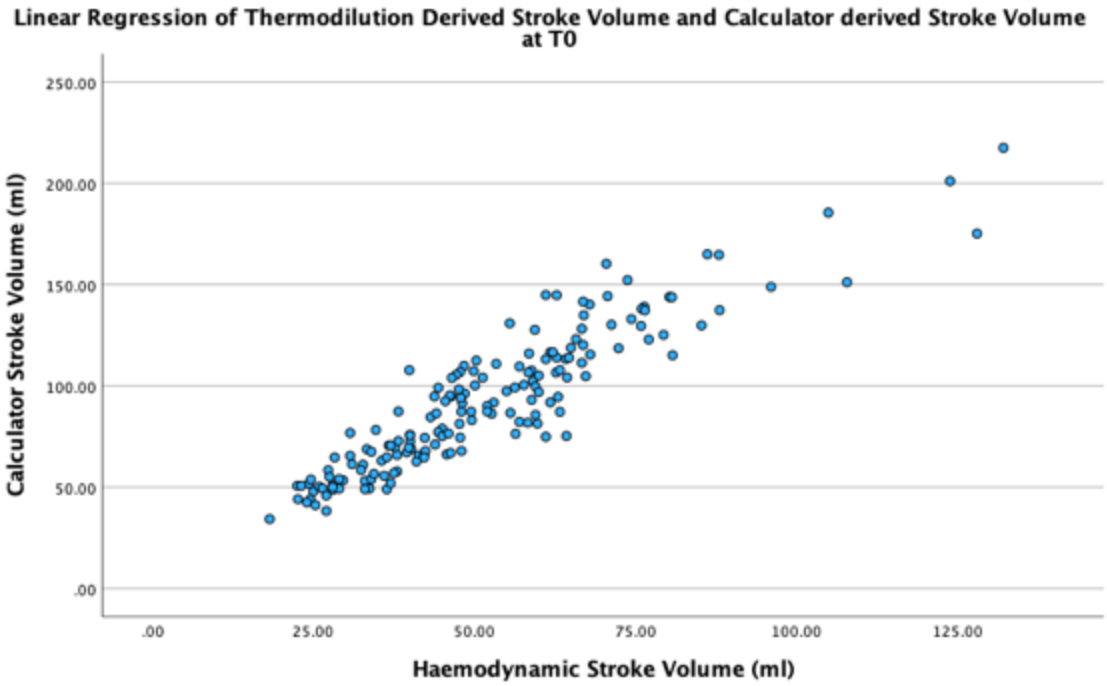

B.

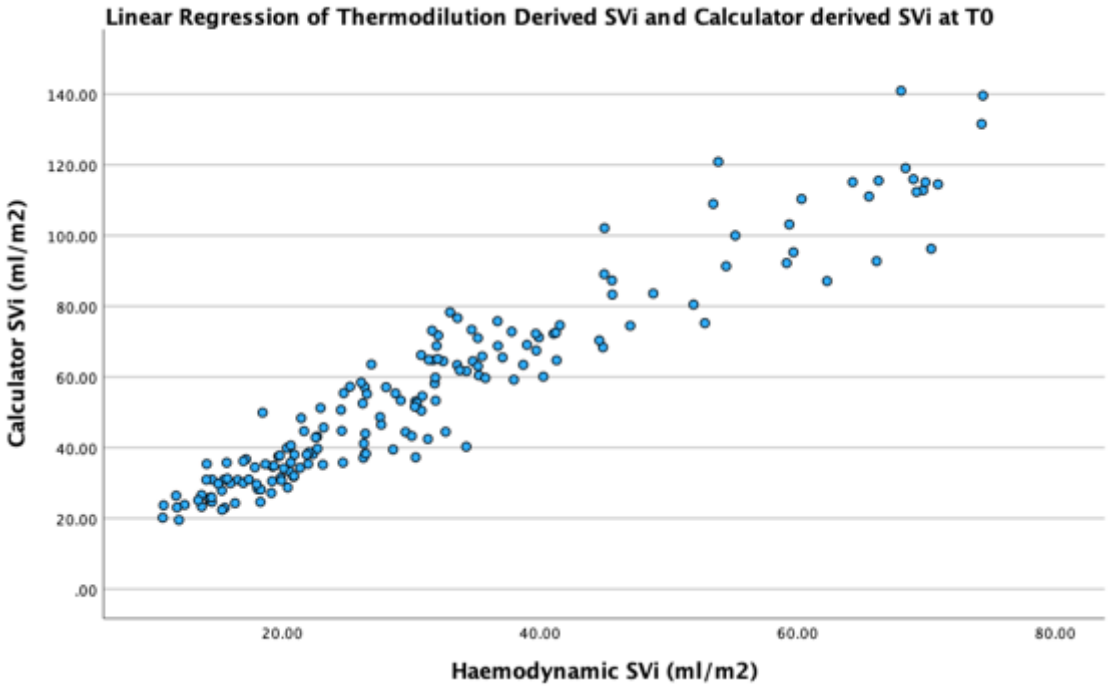

Figure 16. Correlation analysis of the calculator stroke volume (SV) with thermodilution-derived stroke volume, using A) unadjusted SV, and B) indexed SV (SVi).

A.

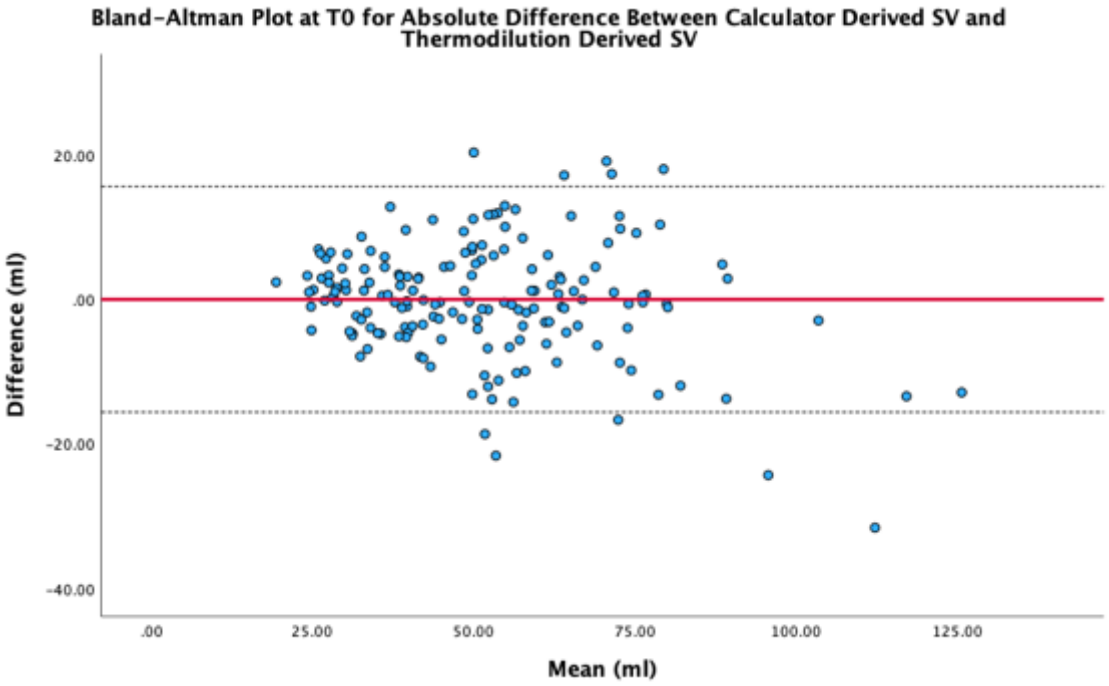

B.

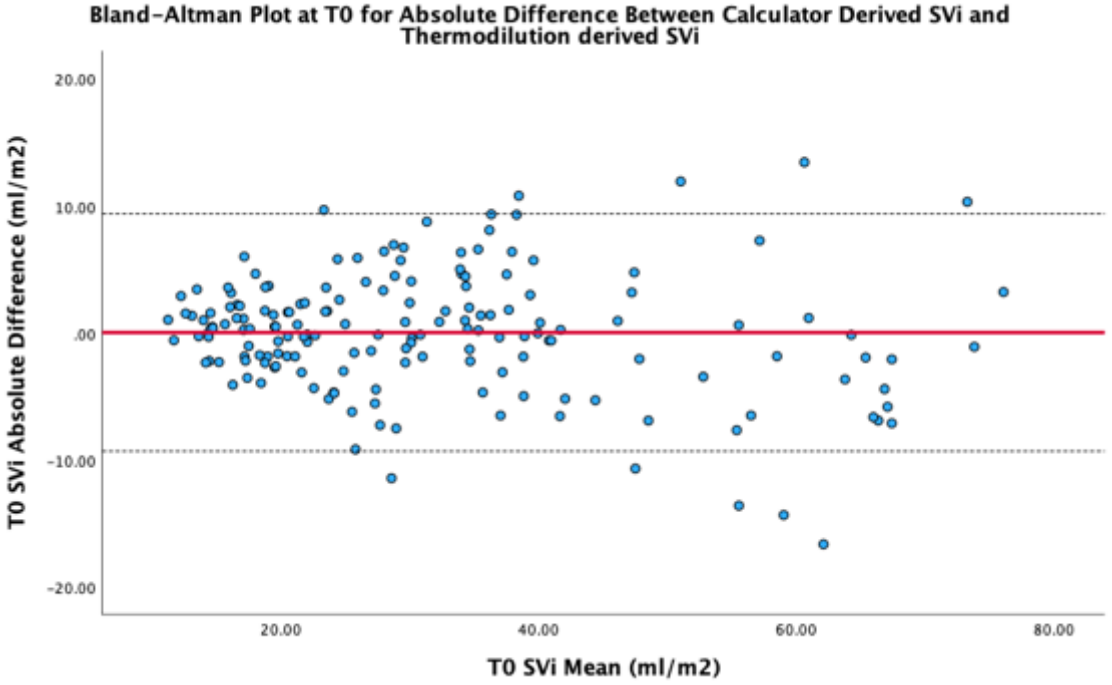

Figure 17. Bland-Altman plots of absolute difference between the adjusted calculator stroke volumes (SV) and thermodilution-derived stroke volumes at T0, using A) adjusted SV, and B) indexed SV (SVi). The red lines denote the mean (-0.04ml in A, 0.025ml in B) and the dotted black lines denote the 95% confidence interval (-15.6 - 15.6 in A, -9.33-9.38 in B).

A.

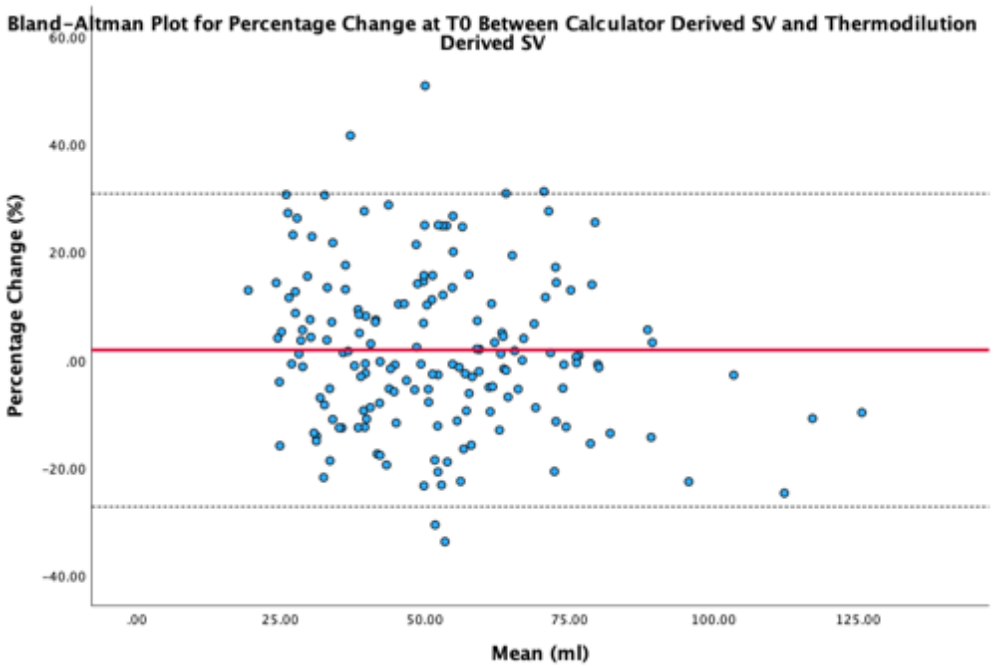

B.

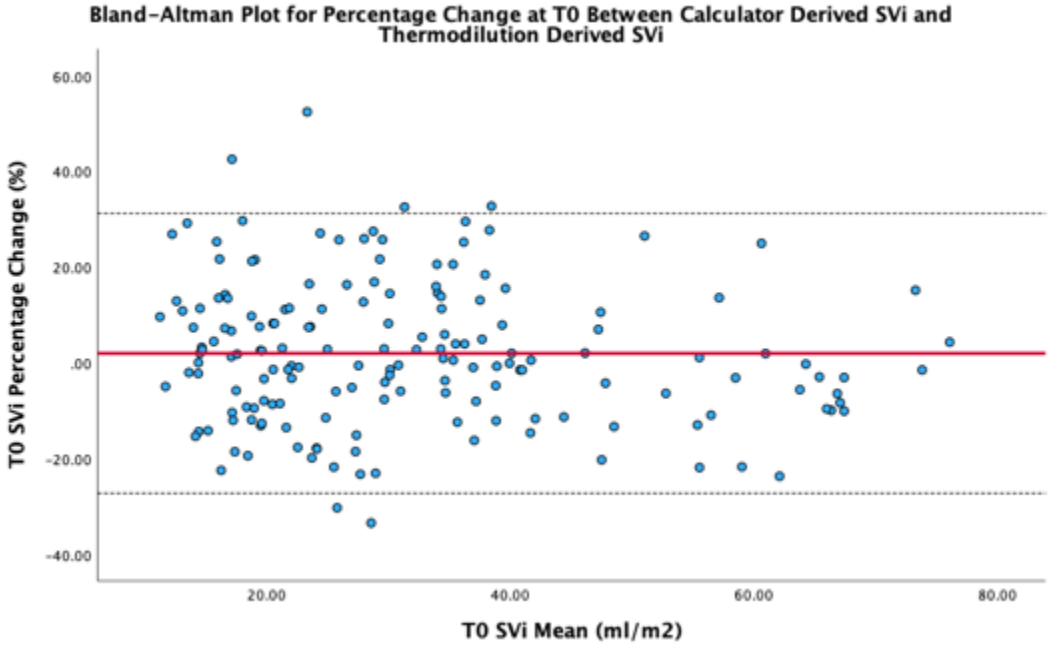

Figure 18. Bland-Altman plots of percentage difference between the calculator stroke volumes (SV) and the thermodilution-derived stroke volumes at T0, using A) adjusted SV, and B) indexed SV (SVi). The red lines denote the mean (1.83% in A, 1.96% in B) and the dotted black lines denote the 95% confidence interval (-27.2 - 30.8 in A, -27.2-31.2 in B).

For indexed stroke volume (stroke volume index, SVi), the median thermodilution-derived SVi was 28.1ml (19.7, 38.7) and the median calculator SVi was 51.2ml (34.7, 71.2). Correlation and linear regression analysis showed strong correlation with an R2 of 0.911, and a coefficient and constant of 0.552 and 0.6 respectively. The median adjusted calculator SVi was 28.9ml (19.7, 39.9) compared to the CO derived SVi of 28.1ml (19.7, 38.7), and there was no significant difference (p= 0.781). Bland-Altman plots for SVi are displayed in figures 17b and 18b. Over 95% of the calculator SV values were within the 30% limit of agreement with thermodilution-derived SV.

Stroke volume was calculated at T6, adjusted using the same coefficients and constants as above and compared to thermodilution-derived SV, using the simulated conditions where repeat pulmonary vascular resistance measurements were not available. Using the PVR at baseline (T0) to 'calibrate' the calculator and PADP at T6 (instead of PAWP at T6), we found no significant difference between the thermodilution-derived SV versus the calculator SV at T6: 47.7ml (IQR 37.6-58.9) vs 46.4ml (IQR 33.2-59.6), p= 0.251. The median thermodilution-derived SVi was 27.7ml (IQR 19.5-35.9) compared to the median adjusted calculator SVi of 26.1ml (IQR 17.7-37.7) and this was also not statistically significant (p= 0.203), suggesting that once 'calibrated' at baseline, PAPP can be used to estimate SV at T6. The Bland-Altman plots for T6 are displayed in Figures 19 and 20. With these assumptions under simulated conditions, there appeared to be greater scatter (about 25% of values exceeded the 30% limit of agreement), especially at higher SV.

Table 15. Cohort baseline characteristics.

Cohort Characteristics	
Male sex, n (%)	69.4
Age, years (SD)	49 (21)
Height (m)	1.71 +/- 0.1
Weight (Kg)	75.7 +/- 14
BMI (kg/m2)	25.9 +/- 4.33
BSA(m2)	1.87 +/- 0.20
Donor Organ Cold Ischaemic Time (mins)	126 +/- 39.9
Donor Organ Warm Ischaemic Time (mins)	58 (20.5)
Total Ischaemic Time (mins)	179 (70.5)
Cardiopulmonary Bypass Time (mins)	189 (88.5)
Diagnosis	
Dilated Cardiomyopathy (%)	53.8
Ischaemic Cardiomyopathy (%)	23.1
HOCM	12.7
Other	10.4
PCWP (mmHg)	16.6 +/- 4.48
PAPP (mmHg)	15 (7)
PVR (WU)	1.03 (0.52)
Stroke Volume (from CO studies) (ml)	47.9 (23.6)
Stroke Volume (from Calculator) (ml)	87.4 (44.1)
Stroke Volume (Adjusted Calculator) (ml)	48.8 (23.0)

BMI: body mass index, BSA: body surface area, HOCM: hypertrophic obstructive cardiomyopathy, PCWP: pulmonary capillary wedge pressure, PAPP: pulmonary arterial pulse pressure, PVR: pulmonary vascular resistance.

Table 16. Haemodynamic data

Haemodynamic parameters	**T0**	**T6**
RAP (mmHg)	10.3 +/- 3.71	11.3 +/- 3.5
SPAP (mmHg)	33.3 +/- 6.52	31.7 +/- 6.64
DPAP (mmHg)	16.7 +/- 4.56	16.5 +/- 4.38
MPAP (mmHg)	22.2 +/- 5	21.3 +/- 5.21
MAP (mmHg)	69.3 +/- 9.19	68.4 +/- 8.35
PAPi	1.64 (1.19)	1.38 (0.88)
TPG (mmHg)	5 (3)	5 (2)
PVR (WU)	1.05 (0.53)	0.99 (0.51)
RVSWi (g/m^2/beat)	3.83 (3.01)	3.36 (2.39)
CO (L/min)	5.1 (2.48)	4.77 (1.90)
CI (L/min/m2)	2.67 (2.48)	2.55 (0.88)
SVR (dynes.sec.cm^{-5})	948 (472)	947 (347)
SVRi (dynes.sec.cm^{-5}.m^2)	1770 (869)	1797 (589)

T0: immediately following orthotopic heart transplantation, T6: six hours following orthotopic heart transplantation, RAP: right atrial pressure, SPAP: systolic pulmonary arterial pressure, DPAP: diastolic pulmonary arterial pressure, MPAP: mean pulmonary arterial pressure, MAP: mean arterial pressure, PAPi: pulmonary arterial pulsatility index, TPG: transpulmonary gradient, PVR: pulmonary vascular resistance, RVSWi: right ventricular stroke work index, CO: cardiac output, CI: cardiac index, SVR: systemic vascular resistance, SVRi: indexed systemic vascular resistance.

A.

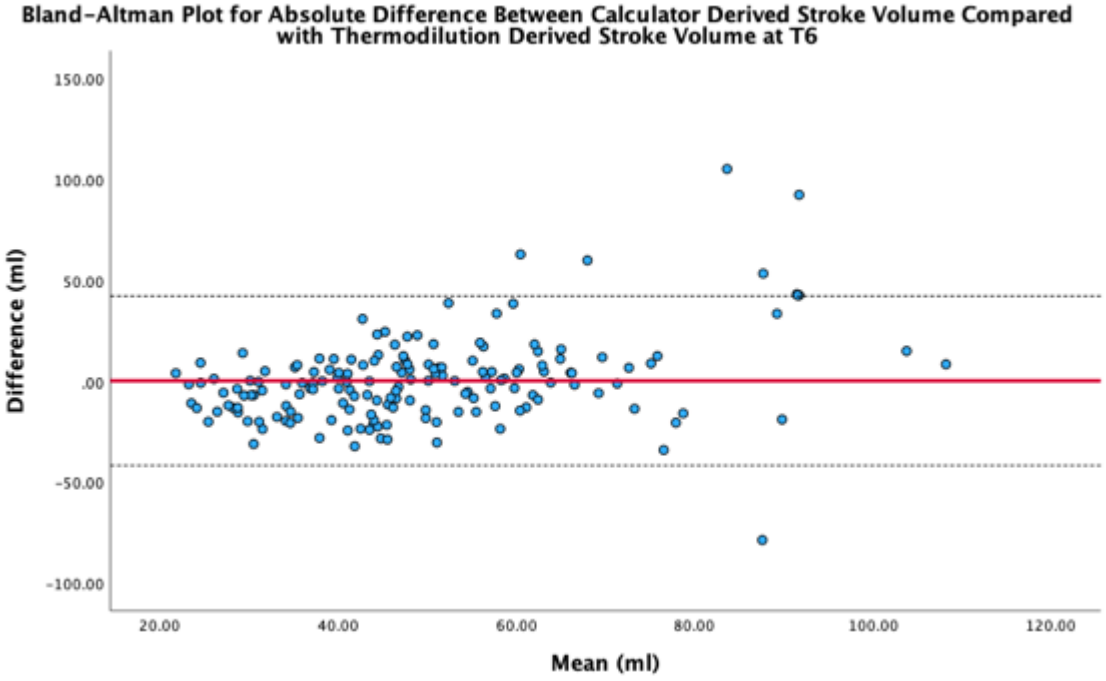

B.

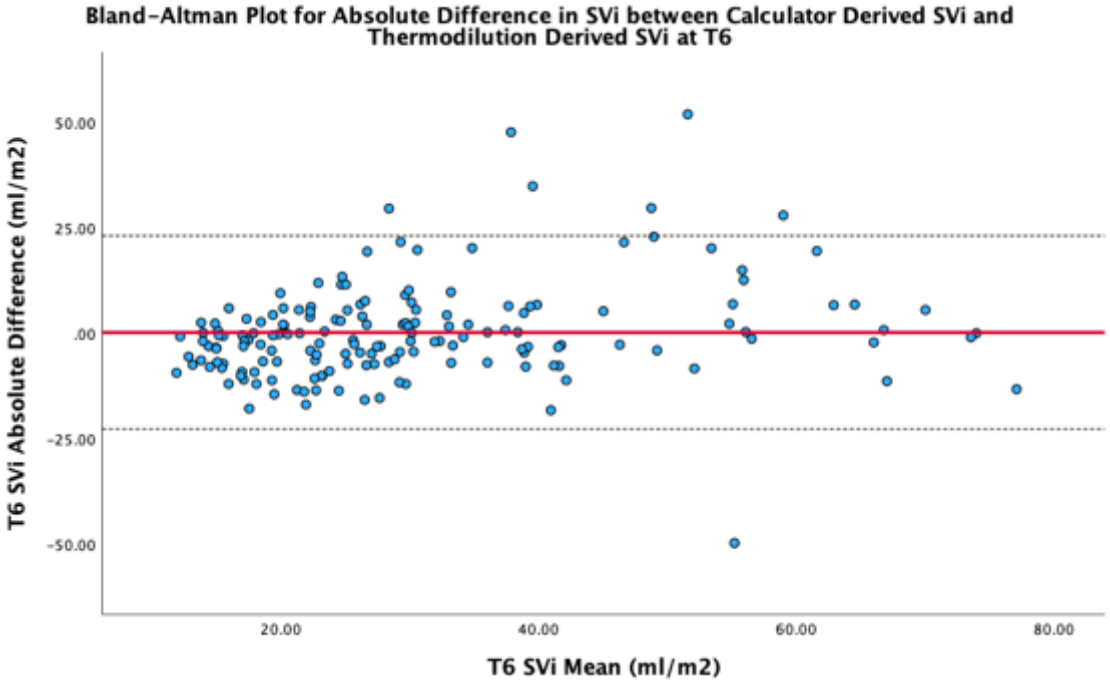

Figure 19. Bland Altman plots of absolute difference between calculator stroke volumes (SV) (simulated conditions) and thermodilution-derived stroke volumes at T6, using A) adjusted SV, and B) indexed SV (SVi). The red lines denote the mean (0.18ml in A, 0.16ml in B) and the dotted black lines denote the 95% confidence interval (-41.8 - 42.2 in A, -22.7-23.1ml in B).

A.

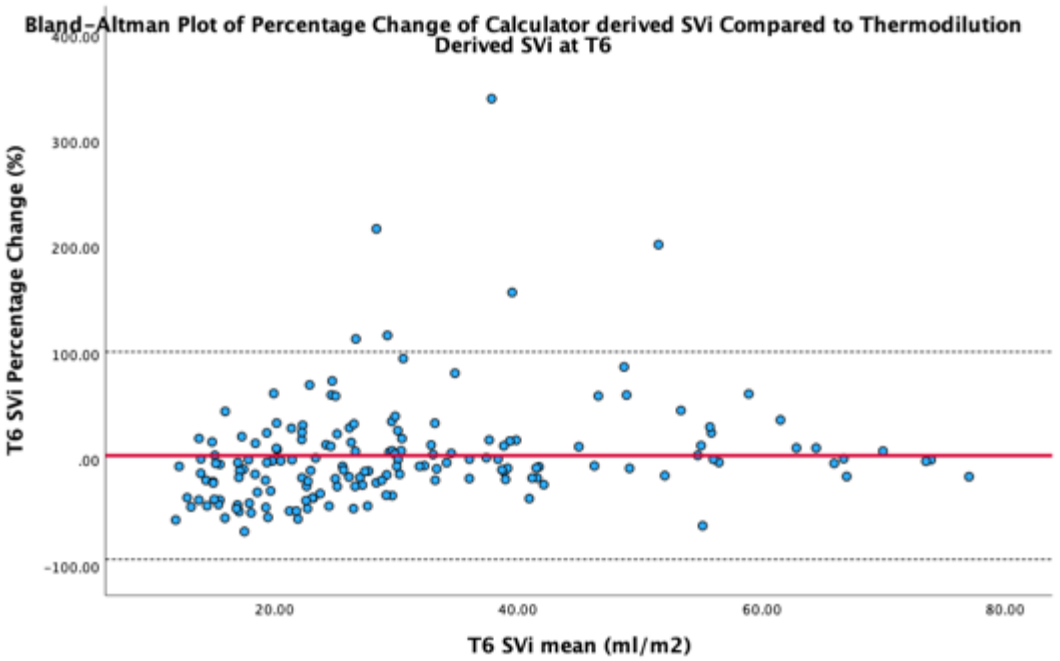

B.

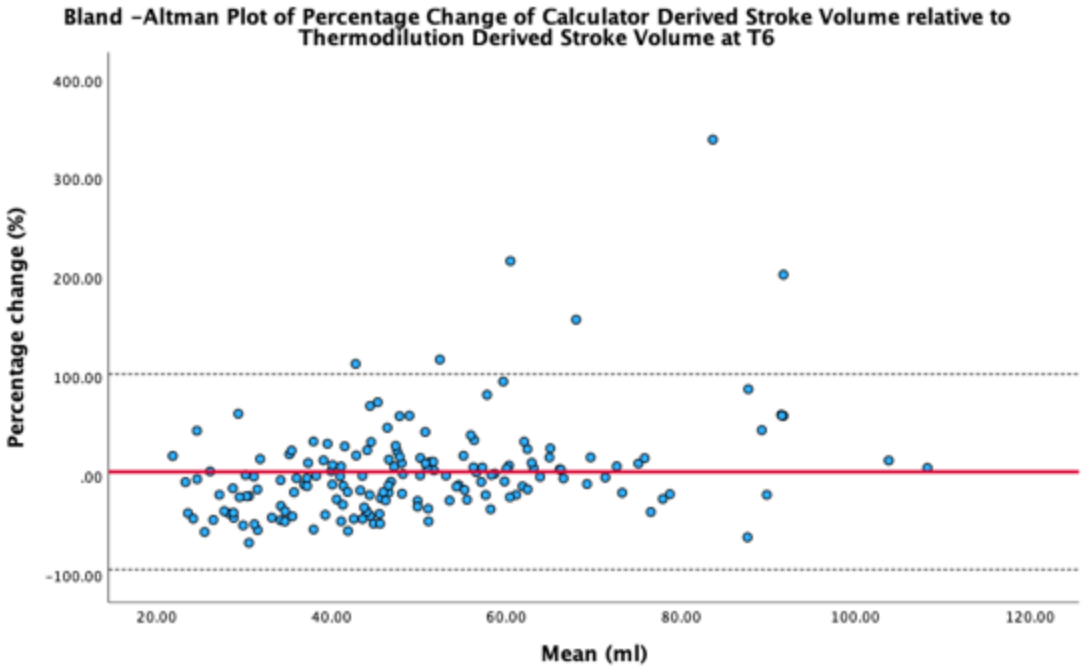

Figure 20. Bland-Altman plots of percentage difference between calculator stroke volume (SV) (simulated conditions) and the thermodilution-derived stroke volumes at T6, using A) adjusted SV, and B) indexed SV (SVi). The red lines denote the mean (4.07% in A, 4.03% in B) and the dotted black lines denote the 95% confidence interval (-94.7 - 102.9 in A, -93.7-101.8 in B).

7.4. Discussion

In this chapter, I have shown that in a cohort of patients who underwent heart transplantation at two centres, this calculator once 'calibrated' using baseline pulmonary vascular resistance, can track SV from PAPP within a six-hour interval with an acceptable level of agreement between the calculator-derived and thermodilution-derived SV. Over 95% of the calculator SVs were within the 30% limit of agreement with thermodilution-derived SV, although there was greater scatter (lower agreement) under the simulated conditions, especially at higher SV.

There are limitations to all CO monitoring devices and technology. The main limitation of using a calculator (other than the invasiveness of PAC) is the inherent assumptions. Firstly, the pulmonary artery capacitance is calculated as a simple ratio of SV to PAPP, which overestimates true capacitance. Secondly, the RC time constant reported by Tedford et al is derived from simple regression of hemodynamic data from a large, mixed cohort of patients. Nonetheless, this simple calculator appears to perform within acceptable limits. We further evaluated this calculator using published data. For example, taking pooled data from 47 publications (Kovacs et al., 2009) that described 72 individually evaluated populations comprising of 1,187 subjects, the calculator-derived SV of 91ml is close to the reported mean SV of 96ml.

Potential applications include the assessment of SV response to intravenous fluid administration or inotropes, as both are common interventions in cardiac intensive care units. Rapid intravenous fluid administration such as fluid challenges do not appear to have a significant effect on pulmonary vascular resistance. For example, the study by Fujimoto et al (Fujimoto et al., 2013) showed no significant changes in PVR with rapid saline infusions of 10-

15ml/kg in individuals without heart failure and 0.3-1.0L of normal saline in patients with heart failure. Similarly, Andersen et al (Andersen et al., 2015) reported no significant change in PVR with fluid administration in patients with heart failure. Indeed, this calculator-derived SV also appears to operate within acceptable limits compared to the hemodynamic data reported by Andersen et al.

One caveat is that the increase in PAWP could confound the relationship between PAPP and SV. Increase in PAWP would increase PAPP, even if SV is unchanged. There are two mitigating factors. Firstly, the effect of PAWP on PAPP and absolute calculator SV is modest. Secondly, PADP can be used to approximate PAWP in most cases in the absence of pulmonary vascular disease. Thus, once 'calibrated' with baseline PVR and using PADP, the changes in SV in response to fluid administration could be quantified:

SV = (-0.0062 x PADP + 0.46) x PAPP/ (PVR x 60/1000), to derive SV in ml.

Our data suggest that these assumptions reduced the agreement between calculator SV and thermodilution SV (about 25% exceeded the 30% limit of agreement), but was acceptable in the majority of patients within the first six hours of heart transplantation. It is likely that a more selected use of this calculator, by identifying conditions where these assumptions are valid, would improve the level of agreement.

Aside from the calculator, the physiologic considerations also allow the following 'rules-of-thumb' to be applied:

1. With acute intravenous fluid administration, at an unchanged PVR, the absence of an increase in PAPP with would suggest the absence of an increase in stroke volume in response to the fluid challenge.

2. With the administration of inotropes, the potential reduction in PVR and PAWP would be expected to PAPP. An increase in PAPP in response to inotropes must reflect an increase in SV.

7.5. Limitations

This study has notable limitations. First, I have only evaluated this calculator in patients who are in the early postoperative period following heart transplantation; the application of this calculator to other patients would need further study. Secondly, the measurements were not standardized. It is possible that standardization of PAPP measurement (eg: during the expiratory phase) may improve agreement between the calculator and thermodilution-derived SVi and CO. Thirdly, we have evaluated a PVR does not change significantly over this time interval. It is possible that the window may be extended in the absence of any significant changes in ventilatory parameters that could alter PVR. Alternatively, this calculator may be used to complement intermittent thermodilution studies (eg: six-hourly) to derive PVR and 're-calibrate' the calculator. Finally, although there was general agreement between calculator SV and thermodilution SV under simulated conditions at T6, the level of agreement was poorer and there were individuals with clinically significant deviations; implying that these assumptions are not valid in some patients. Future studies are needed to further examine the use of this calculator.

7.6. Conclusions

In this chapter I have described a calculator to derive SV from PAPP, as an adjunct to aid continuous haemodynamic monitoring following heart transplantation. Once ‘calibrated’ from baseline PVR, this calculator may be used to track SV from PAPP within a six-hour interval with an acceptable level of agreement with thermodilution-derived SV in a selected group of patients.

8. Discussion

8.1. Project Overview

In this thesis, I have presented my work which is centred upon pulmonary haemodynamics and heart failure. I have successfully recruited the target number of patients for the wave intensity analysis study and the project has been completed within the timeline set out at the beginning of the study.

In chapter 4, the first of the results chapters, I had presented my findings of WIA in the pulmonary circulation in patients with advanced left sided failure; this was the first study of WIA in this patient cohort. I had hypothesised that 1. higher pulmonary vascular resistance is associated with increased wave reflection, and 2. with administration of dobutamine, wave reflection will be reduced and it will increase the forward compression wave on WIA. The results showed that wave propagation in the pulmonary circulation in left sided failure was comparable to that of the systemic circulation. Wave reflection was more likely observed with higher pulmonary artery pressures and lower pulmonary arterial compliance, however there was no significant change in wave reflection with increasing PVR. Therefore the results do not support the first part of my hypothesis. Furthermore, the magnitude of the initial forward compression wave related to RV systole was directly correlated to the RV stroke volume which is also what I had anticipated to find. In the second part of the study, the effects of positive inotropy with Dobutamine was investigated and I found that Dobutamine did not significantly effect wave reflection, but it was associated with an increase in the FCW intensity; although the number of patients who had Dobutamine was relatively small. Therefore my results only partially support the second part of my hypothesis. I was somewhat surprised by the finding

that PVR did not significantly effect backward wave reflection as PVR is widely adopted as a marker of pulmonary vascular disease. This could be due to a relatively modest elevation of PVR in our patient cohort compared to patients with chronic thrombo-embolic disease in the pulmonary circulation and the effects of a low pulmonary arterial compliance may be more pronounced due to the PAC-PVR hyperbolic relationship.

Right ventricular stroke work has been used as a surrogate marker for RV performance and as the FCW intensity positively correlated to RVSWi, this would suggest that the magnitude of the FCW intensity could also be used as a surrogate marker for RV performance. This may be useful in the clinical setting if real time WIA can be developed using pulmonary artery catheter data on intensive care. However, with the current technology available, there are significant barriers to translating WIA to the clinical setting, chiefly the difficulty in acquiring a 'clean' velocity signal in the pulmonary artery. During the study, a significant amount of time was spent on each patient in positioning the combo wire in order to acquire an acceptable trace for the velocity and this was then subject to change. The offline analysis of the data was also dependent on which segment of the study was chosen to be used. Finally, Phillips who made the Combo wire used in this study no longer manufacture this product and therefore an alternate wire will have to be sought if this study were to be taken forward.

The results of WIA in patients with durable LVAD therapy are reported in chapter 5 in whom I investigated wave propagation. I had hypothesised that WIA can be used to identify an optimal LVAD pump speed based on optimal forward compression waves and changes in wave reflection. The main findings were that 1.) wave propagation was comparable in patients with LVAD vs those without, this was the first study to show this, 2.) changing the pump speeds of

the Heartmate 3 device by +/- 300rpm (+/-400rpm in Heartmate 2 devices) did not significantly effect wave reflection acutely and iii.) changing the pump speeds did not alter the magnitude of the FCW intensities. Therefore my results do not support my hypothesis and WIA could not be used to set optimal pump speeds for patients with durable LVAD therapy.

There was a highly variable response from patient to patient and there was no clear pattern of effect of either increasing or decreasing the pump speeds by 300rpm. All patients studied in this cohort were at least 6 months following LVAD implant and therefore their PVRs have all been well optimised, this could be a possible explanation for wave reflection being unaltered by changing the pump speeds. It is also possible that changing the pump speeds by 300/400rpm was not enough to elicit an effect on wave propagation or reflection, however, we were restricted to these pump speed changes as this was a point raised by the ethics committee to ensure patient safety. Furthermore, we would not have had the resources to have observed the patients for a longer period of time at each pump speed change due to the restriction on time in the catheter laboratory.

In the LVAD part of the study, data from six patients were not usable mainly due to the velocity trace. In the latter half of the patients recruited, we had the final batch of wires delivered from Phillips shortly before the combo wire was discontinued by the company; this coincided with a spate of poor velocity signals. Again, just like in the heart failure cohort of patients, a significant amount of time was necessary to adjust the wire positioning on fluoroscopy before an acceptable velocity signal was observed and frequently the wire required repositioning during a study. The original ambition was to potentially develop WIA into a useful clinical tool as an adjunct in setting optimal pump speeds for durable LVAD devices, however, I do not think this

is possible with the current available technology. A new wire which provides more stable velocity signals and requires less manipulation would need to be developed before WIA could be translated into a bedside tool. This may never be possible given the dynamic nature of the pulmonary artery and the propensity of the wire to come into contact of the side wall of the pulmonary artery.

In chapter 6, I investigated the pulmonary haemodynamics in heart transplant recipients to elucidate whether predictors of severe early primary graft dysfunction requiring mechanical circulatory support could be identified. I hypothesised that a low PAPI is associated with delayed MCS use following heart transplantation. Data from two UK Cardio-Thoracic transplantation units were collated, the Queen Elizabeth Hospital Birmingham and Royal Papworth Hospital in Cambridge. I found that RAP was significantly higher and PAPI was significant lower in patients who required MCS following transplantation, therefore supporting my hypothesis. As expected, the vasoactive inotropic score was higher in the MCS group relative to the group who did not require MCS. On multivariable logistic regression analysis, PAPI at both time points, immediately following return to intensive care and at six hours post-transplant were associated with MCS use independent of donor organ ischaemic time and pre-operative MCS bridge to transplantation. On ROC analysis, PAPI was found to be better than RAP and RVSWi in predicting MCS use following heart transplantation in this cohort of patients; it also suggested that a PAPI cut off of 1.22 can be used as a marker for impending MCS. There were no previously published reports of PAPI and severe early graft dysfunction following heart transplantation and the findings of this study will be relevant to clinicians in the international transplant community.

There has been great interest in PAPI in recent times and this study adds to the literature in support of the use of PAPI as a useful haemodynamic parameter. However, the PAPI cut off reported should be used with caution in different patient cohorts as it is highly dependent on the PAC and PVR. Early MCS use following heart transplantation has been shown to improve outcomes, therefore any predictor for impending need for MCS would be desirable. Future work including a significantly larger cohort of transplant recipients would add value by establishing the effectiveness of PAPI as a haemodynamic predictor for impending MCS, such as the Eurotransplant database or the ISHLT registry.

In chapter 7, using the haemodynamic data from the two transplant centres in chapter 6, I explored the relationship between pulmonary arterial pulse pressure, pulmonary arterial capacitance and stroke volume to see whether or not stroke volume derived from pulmonary haemodynamics would be accurate. Following initial results from the calculator, once 'calibrated' using the coefficients and constants from linear regression studies, the calculator values were within pre-set limits of precision. The Bland-Altman plots for each of the time points showed acceptable scattering and distribution when comparing the means and the differences of the calculator derived stroke volumes with the thermodilution derived stroke volumes. Although, there appeared to be greater scatter and therefore lower agreement at higher stroke volumes.

A potential uses of this calculator in the clinical setting would be to assess the response to intravenous fluid administration and the introduction of inotropic agents in intensive care. The calculator would have the additional benefit of not requiring repeat cardiac output thermodilution studies. However, the main limitation is that the calculator was evaluated on a

relatively small number of patients and only in the setting of post-heart transplant and it required ‘calibration’. Furthermore, the calculator was only evaluated in a 6 hour window and further validation studies will be required should this be translated into a widely applicable clinical tool.

8.2 Personal Reflections

Throughout the past few years, I have learnt a huge amount about clinical research through working on this project and thesis. At times, it had been immensely frustrating but ultimately delivering and finishing this thesis has been one of my most personally rewarding accomplishments. Prior to taking on this project, I had classed my academic and research knowledge as average or adequate but it very quickly became apparent that it was actually poor. This whole process has really allowed me to develop my academic knowledge and transferable skills which will be invaluable to me as a consultant surgeon in the future whether or not I pursue any academic elements in my practice.

Getting involved with the IRAS system, participating in writing grants and dealing with REC/R&D are all new experiences for me and these are wholly mandatory processes which were extremely important for me to have experienced first-hand. Unfortunately these are also, individually, frequent sources of great frustration and often out of the researcher's control. For example, recruitment for the WIA study was halted for circa 5 months because of an amendment that needed to be made and submitted to the HRA. The amendment on its own was trivial, but once the amendment form was sent to UHB's R&D department for sign off, the whole process then stalled. It was near impossible to get a reply from them and without them signing off the amendment and forwarding the form, there was no way to re-start recruitment. To add to the frustration, eventually when it was done, it became apparent that all the R&D administrator had to do was click a single button on the form and it took well over five months for that to happen. During this whole saga, I couldn't help but think some of the tedium which mainly revolved around the administrative side of research in the U.K. is a major barrier to clinicians performing research. When compared to some other countries, like the United States (hearing how

clinicians carry out research at international conferences), this level of bureaucracy just doesn't exist and in fact clinicians seem to be given a lot more resources to facilitate and encourage research and academia. Nonetheless, this period of 'down time' forced me to get on with other smaller projects and other parts of this thesis which didn't involve the WIA study. Innately, I do not like moving on from one task to start another until the first has been completed, but this period of research has taught me I need to be fluid and flexible in order to have good time management, otherwise I would have lost five months without doing anything productive. I think this is akin to clinical practice and there are often situations, which due to factors outside of my control, I would have to put a task on hold and move on to another in the meantime.

Recruitment to the study was relatively straight forward and most suitable patients coming through the transplant assessment pathway were amenable to participating if suitable for the study, this is most likely due to the nature of the study. However, acquiring the velocity data with the Combo wire was not straight forward at all. In some cases there was a beautiful velocity trace from the beginning but this would then dampen most likely because of the wire coming into contact with the wall of the pulmonary artery. In other cases, it would take a fair bit of finessing and manipulation before an acceptable velocity trace was achieved. Another point to make here is that the results of the WIA heavily depended on the segment of the study which was extracted and analysed, therefore if the study were to be repeated, there would be significant inter-observer bias and I would question the reproducibility of this technique. The high variability of the results in the durable LVAD group was also disappointing and I am convinced that any future work on WIA and LVAD therapy must plan for a wider range of pump speed changes. It is also important to point out that it may be the case that acute changes in the pump speeds may have no effect on WIA in the pulmonary circulation and a longer period

of observation may be required to detect an effect on wave propagation and or reflection. This is obviously not possible as it would be unethical to leave patients on a suboptimal pump speed for any significant period of time. Furthermore, with the Phillips Combo wire now out of commercial production, WIA may never be translated into any meaningful clinical tool and fall into abeyance indefinitely.

Prior to this period of research, I had limited experience with submitting papers to peer-reviewed journals. The process of submitting and re-writing the four (five anticipated) publications arising from this thesis was valuable experience to have gained. The example that comes to mind is submitting the systematic review in chapter 2, there was an extra-ordinary number of re-writes and re-formatting requests from the reviewers and editorial team which was out of keeping with the norm. It reached the point where I had to discuss with the my co-authors the options of persevering with continued re-writes and re-submitting to the same journal or retracting and submitting to a new journal. In the end, perseverance paid off and the paper got over the line to publication. My level of tenacity and patience have both matured over the past three to four years.

Another invaluable skill which I had to learn for this project is doing my own statistical analysis. Prior to my period of doctoral research, I had not had to perform any meaningful statistical analysis myself in any meaningful form and learning how to use SPSS from scratch was most informative. It has helped me understand the pitfalls and how to store and work with data in the most efficient way. After meeting other researchers and other clinicians who routinely do their own statistical analysis, perhaps SPSS is not the most flexible statistical software and in the future I would certainly consider exploring ‘R’ or ‘Graph Pad’.

8.3. Future Work

Given the difficulty in acquiring a clean velocity signal for WIA in some of the cases and the fact that the Combo wire is no longer in production, it would be pragmatic if future work could be carried out without the need for velocity data. The 'reservoir-wave' approach may fill this gap and be the technique which should be explored in future studies. Below, I outline a study proposal entitled 'Arterial reservoir-wave model in the assessment of fluid responsiveness' which is the next study we plan to carry out in our department and a BHF Accelerator Kick-Starter award has been granted for this study.

8.3.1. Introduction

Assessment of fluid responsiveness, ie. increase in stroke volume following administration of intravenous fluid, could guide fluid therapy and prevent unnecessary morbidity related to excessive fluid administration; this is not an uncommon problem in clinical practice. Respiratory variation in arterial blood pressure, or pulse pressure variation, is a dynamic parameter for assessment of fluid responsiveness, but it has limited clinical application as this method requires mechanical ventilation at high tidal volumes without respiratory effort by the patient. There is a clinical need for a measure of fluid responsiveness that is widely applicable and more sophisticated than the RAP.

The reservoir-wave model separates the pressure waveform into a reservoir pressure (Pr) related to aortic expansion and recoil, and a superimposed excess pressure (Px) related to input impedance and local arterial properties (Parker et al., 2012). Pr is charged in systole and discharges in diastole to generate blood flow at a given arterial resistance and compliance. Px

reflects the inefficient work that the heart is doing over and above the minimum work required to generate blood flow.

Therefore, we postulate that changes in Pr and Px could be used to assess response to fluid administration. For example, in a fluid responsive patient, with a fluid challenge, without inducing an acute change in input impedance and arterial resistance would charge the reservoir therefore increasing Pr, and that in turn will drive increase in blood flow. The increase in Pr would be of greater magnitude relative to Px, indicative of increased efficiency in the arterial system. On the other hand, in non-responders, there would be a small or no increase in Pr, with smaller increase in Pr relative to Px. It is also possible that changes in Pr and Px may have the potential to guide other therapeutic interventions such as inotropic and vasopressor use.

In this study, we hypothesise that fluid response is associated with an increase in Pr that is of greater magnitude relative to Px following fluid challenge. The secondary objective of this study is to evaluate the relationship between Pr and Px with pulse pressure variation during positive pressure ventilation.

8.3.2. Methods and Study Protocol

This study will aim to recruit ten patients undergoing elective cardiac surgery at the Queen Elizabeth Hospital Birmingham. All study participants will undergo routine work-up for cardiac surgery. Exclusion criteria will include patients with an ejection fraction below 40%; persistent atrial fibrillation and patients on mechanical circulatory support.

All study participants will undergo routine general anaesthesia for surgery. A PAC will be inserted for cardiac output measurement by thermodilution. A 4Fr arterial line will be inserted into either the right or left femoral artery for monitoring. A Millar Mikro-Cath high fidelity pressure catheter will be inserted into the arterial cannula for continuous blood pressure data acquisition and exported for analysis offline.

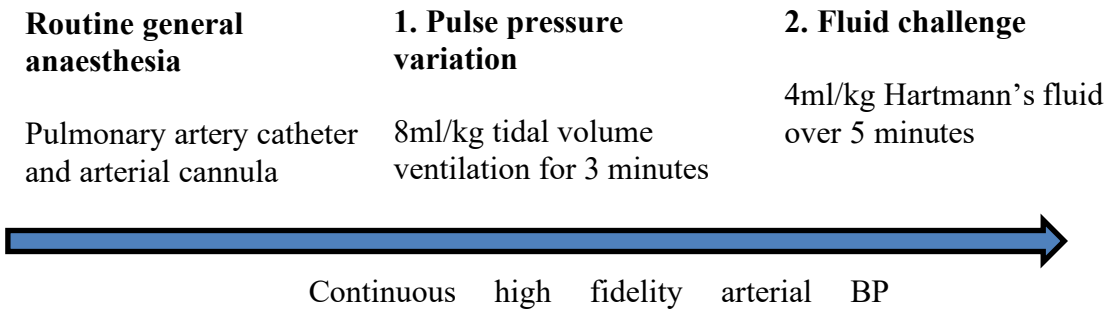

Figure 21. Flow diagram depicting the two parts of the proposed study.

Figure 21 displays the two parts of the study following routine induction of general anaesthesia. The patients will serve as their own control pre and post ventilation and fluid challenge. In the first phase of the study, the patients will be ventilated at tidal volumes of 8ml/kg for three minutes to assess the pulse pressure variation. The relationship between pulse pressure variation and changes to Pr and Px will be assessed off line. In the second phase of the study, the patients will be given a fluid challenge consisting of a bolus of Hartmann's solution 4ml/kg over 5 minutes, based on a study by Aya et al having shown the effects of different doses of fluid for fluid challenge (Aya et al., 2017). Baseline, immediately before fluid challenge, and post-challenge, immediately at the end of the five minute fluid administration period, stroke volume

will be derived from cardioac output measurements by thermodilution. Fluid responsiveness is defined as stroke volume increase of more than 15%.

8.3.3. Potential Application of Results

Should the results support our hypothesis that Pr is significantly increased in fluid responsive patients relative to Px, there may be potential to develop a script for real-time reservoir-wave analysis and in turn allow this concept to translated into a clinical tool in the intensive care setting.

8.3.4. Future Work with the Combo Wire

As the Combo wire is currently no longer in production, this section is written assuming that another company will produce a pressure/doppler velocity wire in the future or indeed if the Combo wire makes a return to the commercial markets. The major issue that needs to be resolved is the stability of the wire and the ease at which a clean velocity signal can be acquired. The reason why this is currently difficult is because the wire is exquisitely sensitive to movements and contact with the arterial walls. This also furthers limit the use of the wire beyond the main branch pulmonary arteries.

A stabilisation sheath could potentially solve this issue as it may prevent contact of the wire with the arterial sidewall however, the design of such a stabilisation device may be difficult to engineer. Firstly and most importantly, this device would need to allow blood flow into the sheath and therefore come into contact with the Combo wire, whilst not changing the flow characteristics and importantly the velocity of the blood. Secondly, this stabilisation device would have to be incorporated into the tip of the Swan Ganz catheter, perhaps an additional

plastic hollow tip with multiple holes on it allowing blood to flow through the device. Thus allowing the Comobowire to be inserted in the same fashion as it was in this study but giving it protection from hitting the arterial wall.

It would be interesting to perform WIA in the right atrium and in the right ventricle itself. There has been some previous work investigating WIA in the left ventricle. WIA has been performed in the left ventricle to assess ventricular filling and also function (MacRae et al., 1997a; Flewitt et al., 2007b). Using the same principles, WIA can be performed in the right atrium and right ventricle to assess filling and function, there are no published reports of this data. In the right atrium, it would be interesting to assess wave propagation with a range of different right atrial pressures. I would hypothesise that there would be a higher intensity forward waves with less wave reflection in a well-functioning right ventricle and a higher right atrial pressure would produce higher intensity forward compression waves.

The phenomenon of ventricular suction during diastole caused by the simultaneous contraction of the basal segments and the relaxation and extension of the apical segments of the ventricle (Tanaka et al., 2011) may also be investigated with wave intensity, there is some data from the left ventricle but not so much so in the right ventricle. Wang et al, in a canine model, utilising WIA has shown that in the left ventricle, during early diastole, there is an expansion wave that decelerates blood flow through the aorta and accelerates blood through the mitral valve (Wang et al., 2005b).

Despite the difficulties I faced during this study with the Combo wire, it is a shame that it is no longer in production and should it ever become available again, there are still important and interesting questions which can be investigated using this technology.

8.4. Conclusions

In this thesis I have laid out the results of my work on i.) WIA in the pulmonary circulation in patients with advanced heart failure, ii.) WIA in patients with durable LVAD devices, iii.) haemodynamic parameters which may be able to predict MCS use following heart transplantation and iv.) a novel stroke volume calculator derived from pulmonary haemodynamics.

In its current form, WIA is not ready to be developed into a clinical tool given the practical challenges associated with acquiring the velocity data. However, the reservoir-wave approach may hold promise as it does not require velocity data.

Finally, I have learnt a great deal through this whole journey in carrying out this work and writing this thesis. This has helped me develop some transferrable academic and practical skills which will has enabled me to become a more well-rounded Surgeon and Clinician.

References

Abdel-Aty, H., Simonetti, O. and Friedrich, M.G. (2007) T2-weighted cardiovascular magnetic resonance imaging. *Journal of Magnetic Resonance Imaging*. 26 (3) pp. 452–459. doi:10.1002/jmri.21028.

Addetia, K., Uriel, N., Maffessanti, F., et al. (2018) 3D Morphological Changes in LV and RV During LVAD Ramp Studies. *JACC. Cardiovascular imaging*, 11 (2 Pt 1): 159–169. doi:10.1016/j.jcmg.2016.12.019.

Aguado-Sierra, J., Alastruey, J., Wang, J.-J., et al. (2008) Separation of the reservoir and wave pressure and velocity from measurements at an arbitrary location in arteries. *Proceedings of the Institution of Mechanical Engineers. Part H, Journal of engineering in medicine*, 222 (4): 403–16. doi:10.1243/09544119JEIM315.

Aguiar Rosa, S., Timóteo, A.T., Ferreira, L., et al. (2018) Complete atrioventricular block in acute coronary syndrome: prevalence, characterisation and implication on outcome. *European heart journal. Acute cardiovascular care*, 7 (3): 218–223. doi:10.1177/2048872617716387.

Akimoto, T., Yamazaki, K., Litwak, P., et al. (1999) Rotary blood pump flow spontaneously increases during exercise under constant pump speed: Results of a chronic study. *Artificial Organs*, 23 (8): 797–801. doi:10.1046/j.1525-1594.1999.06426.x.

Alfirevic, A., Makarova, N., Kelava, M., et al. (2020) Predicting Right Ventricular Failure After LVAD Implantation: Role of Tricuspid Valve Annulus Displacement. *Journal of cardiothoracic and vascular anesthesia*, 34 (5): 1204–1210. doi:10.1053/j.jvca.2019.08.045.

Almutairi, H.M., Boubertakh, R., Miquel, M.E., et al. (2017) Myocardial deformation assessment using cardiovascular magnetic resonance-feature tracking technique. *British Journal of Radiology*. 90 (1080). doi:10.1259/bjr.20170072.

Aloia, E., Cameli, M., D'Ascenzi, F., et al. (2016) TAPSE: An old but useful tool in different

diseases. *International Journal of Cardiology*. 225 pp. 177–183. doi:10.1016/j.ijcard.2016.10.009.

Ambrosy, A.P., Fonarow, G.C., Butler, J., et al. (2014) The global health and economic burden of hospitalizations for heart failure: Lessons learned from hospitalized heart failure registries. *Journal of the American College of Cardiology*. 63 (12) pp. 1123–1133. doi:10.1016/j.jacc.2013.11.053.

Amsallem, M., Mercier, O., Kobayashi, Y., et al. (2018) Forgotten No More. *JACC: Heart Failure*, 6 (11): 891–903. doi:10.1016/j.jchf.2018.05.022.

Andersen, M.J., Olson, T.P., Melenovsky, V., et al. (2015) Differential hemodynamic effects of exercise and volume expansion in people with and without heart failure. *Circulation. Heart failure*, 8 (1): 41–8. doi:10.1161/CIRCHEARTFAILURE.114.001731.

Anderson, R.H. and Brown, N.A. (1996) The anatomy of the heart revisited. *Anatomical Record*. 246 (1) pp. 1–7. doi:10.1002/(SICI)1097-0185(199609)246:1<1::AID-AR1>3.0.CO;2-Y.

Anker, S.D., Butler, J., Filippatos, G., et al. (2021) Empagliflozin in Heart Failure with a Preserved Ejection Fraction. *New England Journal of Medicine*, 385 (16): 1451–1461. doi:10.1056/NEJMoa2107038.

Antoine, S., Vaidya, G., Imam, H., et al. (2017) Pathophysiologic Mechanisms in Heart Failure: Role of the Sympathetic Nervous System. *American Journal of the Medical Sciences*, 353 (1): 27–30. doi:10.1016/j.amjms.2016.06.016.

Antonini-Canterin, F., Pavan, D., Bello, V., et al. (2013) The ventricular-arterial coupling: From basic pathophysiology to clinical application in the echocardiography laboratory. *Journal of Cardiovascular Echography*, 23 (4): 91. doi:10.4103/2211-4122.127408.

Argiriou, M., Kolokotron, S.-M., Sakellaridis, T., et al. (2014) Right heart failure post left

ventricular assist device implantation. *Journal of thoracic disease*, 6 Suppl 1: S52-9. doi:10.3978/j.issn.2072-1439.2013.10.26.

Argueta, E.E. and Paniagua, D. (2019) Thermodilution Cardiac Output: A Concept over 250 Years in the Making. *Cardiology in Review*. 27 (3) pp. 138–144. doi:10.1097/CRD.0000000000000223.

Armstrong, H.F., Schulze, P.C., Kato, T.S., et al. (2013) Right ventricular stroke work index as a negative predictor of mortality and initial hospital stay after lung transplantation. *The Journal of heart and lung transplantation : the official publication of the International Society for Heart Transplantation*, 32 (6): 603–8. doi:10.1016/j.healun.2013.03.004.

Aslam, M.I., Jani, V., Lin, B.L., et al. (2021) Pulmonary artery pulsatility index predicts right ventricular myofilament dysfunction in advanced human heart failure. *European journal of heart failure*, 23 (2): 339–341. doi:10.1002/ejhf.2084.

Aukrust, P., Gullestad, L., Ueland, T., et al. (2005) Inflammatory and anti-inflammatory cytokines in chronic heart failure: Potential therapeutic implications. *Annals of Medicine*. 37 (2) pp. 74–85. doi:10.1080/07853890510007232.

Aukrust, P., Ueland, T., Lien, E., et al. (1999) Cytokine network in congestive heart failure secondary to ischemic or idiopathic dilated cardiomyopathy. *American Journal of Cardiology*, 83 (3): 376–382. doi:10.1016/S0002-9149(98)00872-8.

Aya, H.D., Rhodes, A., Chis Ster, I., et al. (2017) Hemodynamic Effect of Different Doses of Fluids for a Fluid Challenge: A Quasi-Randomized Controlled Study. *Critical care medicine*, 45 (2): e161–e168. doi:10.1097/CCM.0000000000002067.

BAAN, J., JONG, T.T.A., KERKHOF, P.L.M., et al. (1981) Continuous stroke volume and cardiac output from intra-ventricular dimensions obtained with impedance catheter. *Cardiovascular Research*, 15 (6): 328–334. doi:10.1093/cvr/15.6.328.

Bayram, Z., Dogan, C., Efe, S.C., et al. (2022) Prognostic Importance of Pulmonary Artery Pulsatility Index and Right Ventricular Stroke Work Index in End-Stage Heart Failure Patients. *Cardiology*, 147 (2): 143–153. doi:10.1159/000521205.

Bellavia, D., Iacovoni, A., Scardulla, C., et al. (2017) Prediction of right ventricular failure after ventricular assist device implant: systematic review and meta-analysis of observational studies. *European Journal of Heart Failure*, 19 (7): 926–946. doi:10.1002/ejhf.733.

Benjamin, M.M., Sundararajan, S., Sulaiman, S., et al. (2020) Association of preoperative duration of inotropy on prevalence of right ventricular failure following LVAD implantation. *ESC heart failure*, 7 (4): 1949–1955. doi:10.1002/ehf2.12791.

Bers, D.M. (2002) Cardiac excitation-contraction coupling. *Nature*. 415 (6868) pp. 198–205. doi:10.1038/415198a.

Bishop, A., White, P., Oldershaw, P., et al. (1997) Clinical application of the conductance catheter technique in the adult human right ventricle. *International Journal of Cardiology*, 58 (3): 211–221. doi:10.1016/S0167-5273(96)02880-X.

Bixler, T.J., Gott, V.L. and Gardner, T.J. (1981) Reversal of experimental pulmonary hypertension with sodium nitroprusside. *The Journal of Thoracic and Cardiovascular Surgery*, 81 (4): 537–545. doi:10.1016/S0022-5223(19)39484-X.

Bootsma, I.T., Boerma, E.C., Scheeren, T.W.L., et al. (2022) The contemporary pulmonary artery catheter. Part 2: measurements, limitations, and clinical applications. *Journal of clinical monitoring and computing*, 36 (1): 17–31. doi:10.1007/s10877-021-00673-5.

Bouwmeester, J.C., Belenkie, I., Shrive, N.G., et al. (2013) Partitioning pulmonary vascular resistance using the reservoir-wave model. *Journal of applied physiology (Bethesda, Md. : 1985)*, 115 (12): 1838–45. doi:10.1152/japplphysiol.00750.2013.

Bouwmeester, J.C., Belenkie, I., Shrive, N.G., et al. (2014) Wave reflections in the pulmonary

arteries analysed with the reservoir-wave model. *The Journal of physiology*, 592 (14): 3053–62. doi:10.1113/jphysiol.2014.273094.

Braunwald, E. (2013) Heart failure. *JACC: Heart Failure*. 1 (1) pp. 1–20. doi:10.1016/j.jchf.2012.10.002.

Brener, M.I., Burkhoff, D. and Sunagawa, K. (2020) Effective Arterial Elastance in the Pulmonary Arterial Circulation. *Circulation: Heart Failure*, 13 (3). doi:10.1161/CIRCHEARTFAILURE.119.006591.

Broyd, C.J., Davies, J.E., Escaned, J.E., et al. (2017) Wave intensity analysis and its application to the coronary circulation. *Global cardiology science & practice*, 2017 (1): e201705. doi:10.21542/gcsp.2017.5.

Burnett, H., Earley, A., Voors, A.A., et al. (2017) Thirty Years of Evidence on the Efficacy of Drug Treatments for Chronic Heart Failure with Reduced Ejection Fraction: A Network Meta-Analysis. *Circulation: Heart Failure*, 10 (1). doi:10.1161/CIRCHEARTFAILURE.116.003529.

Cacioli, G., Polizzi, V., Ciabatti, M., et al. (2022) Prediction of right ventricular failure after left ventricular assist device implantation: role of vasodilator challenge. *European heart journal. Acute cardiovascular care*, 11 (8): 629–639. doi:10.1093/ehjacc/zuac085.

Callan, P. and Clark, A.L. (2016) Right heart catheterisation: Indications and interpretation. *Heart*, 102 (2): 147–157. doi:10.1136/heartjnl-2015-307786.

Campbell, R.T., Jhund, P.S., Castagno, D., et al. (2012) What have we learned about patients with heart failure and preserved ejection fraction from DIG-PEF, CHARM-preserved, and I-PRESERVE? *Journal of the American College of Cardiology*. 60 (23) pp. 2349–2356. doi:10.1016/j.jacc.2012.04.064.

Cesini, S., Bhagra, S. and Pettit, S.J. (2020) Low Pulmonary Artery Pulsatility Index Is

Associated With Adverse Outcomes in Ambulatory Patients With Advanced Heart Failure. *Journal of cardiac failure*, 26 (4): 352–359. doi:10.1016/j.cardfail.2020.01.014.

Chemla, D., Castelain, V., Zhu, K., et al. (2013) Estimating right ventricular stroke work and the pulsatile work fraction in pulmonary hypertension. *Chest*, 143 (5): 1343–1350. doi:10.1378/chest.12-1880.

Chemla, D., Lau, E.M.T., Papelier, Y., et al. (2015) Pulmonary vascular resistance and compliance relationship in pulmonary hypertension. *The European respiratory journal*, 46 (4): 1178–89. doi:10.1183/13993003.00741-2015.

Cohn, J.N. and Tognoni, G. (2001) A Randomized Trial of the Angiotensin-Receptor Blocker Valsartan in Chronic Heart Failure. *New England Journal of Medicine*, 345 (23): 1667–1675. doi:10.1056/NEJMoa010713.

Cosío Carmena, M.D.G., Gómez Bueno, M., Almenar, L., et al. (2013) Primary graft failure after heart transplantation: characteristics in a contemporary cohort and performance of the RADIAL risk score. *The Journal of heart and lung transplantation : the official publication of the International Society for Heart Transplantation*, 32 (12): 1187–95. doi:10.1016/j.healun.2013.08.004.

Cournand, A. (1975) Cardiac catheterization. Development of the technique, its contribution to experimental medicine, and its initial applications in man. *Acta Medica Scandinavica*, 198 (Sup 579).

Cournand, A., Lauson, H.D., Bloomfield, R.A., et al. (1944) Recording of Right Heart Pressures in Man. *Experimental Biology and Medicine*, 55 (1): 34–36. doi:10.3181/00379727-55-14446P.

Cowie, M.R. (2017) The heart failure epidemic: a UK perspective. *Echo research and practice*, 4 (1): R15–R20. doi:10.1530/ERP-16-0043.

Critchley, L.A. and Critchley, J.A. (1999) A meta-analysis of studies using bias and precision

statistics to compare cardiac output measurement techniques. *Journal of clinical monitoring and computing*, 15 (2): 85–91. doi:10.1023/a:1009982611386.

Curtis, S.L., Zambanini, A., Mayet, J., et al. (2007) Reduced systolic wave generation and increased peripheral wave reflection in chronic heart failure. *American Journal of Physiology-Heart and Circulatory Physiology*, 293 (1): H557–H562. doi:10.1152/ajpheart.01095.2006.

Czepluch, F.S., Wollnik, B. and Hasenfuß, G. (2018) Genetic determinants of heart failure: facts and numbers. *ESC heart failure*, 5 (3): 211–217. doi:10.1002/ehf2.12267.

Danton, M.H.D., Greil, G.F., Byrne, J.G., et al. (2003) Right ventricular volume measurement by conductance catheter. *American Journal of Physiology-Heart and Circulatory Physiology*, 285 (4): H1774–H1785. doi:10.1152/ajpheart.00048.2003.

Davies, J.E., Aguado-Sierra, J., Francis, D.P., et al. (2007) 09.04 a Unifying Explanation of the Aortic Pulse Waveform in Humans. *Artery Research*, 1 (S1): S26. doi:10.1016/s1872-9312(07)70018-2.

Davies, J.E., Alastruey, J., Francis, D.P., et al. (2012) Attenuation of wave reflection by wave entrapment creates a “horizon effect” in the human aorta. *Hypertension (Dallas, Tex. : 1979)*, 60 (3): 778–85. doi:10.1161/HYPERTENSIONAHA.111.180604.

Davies, J.E., Lacy, P., Tillin, T., et al. (2014) Excess pressure integral predicts cardiovascular events independent of other risk factors in the conduit artery functional evaluation substudy of Anglo-Scandinavian Cardiac Outcomes Trial. *Hypertension (Dallas, Tex. : 1979)*, 64 (1): 60–8. doi:10.1161/HYPERTENSIONAHA.113.02838.

Davies, J.E., Sen, S., Dehbi, H.-M., et al. (2017) Use of the Instantaneous Wave-free Ratio or Fractional Flow Reserve in PCI. *The New England journal of medicine*, 376 (19): 1824–1834. doi:10.1056/NEJMoa1700445.

Davies, J.E., Whinnett, Z.I., Francis, D.P., et al. (2006a) Evidence of a dominant backward-

propagating “suction” wave responsible for diastolic coronary filling in humans, attenuated in left ventricular hypertrophy. *Circulation*, 113 (14): 1768–78. doi:10.1161/CIRCULATIONAHA.105.603050.

Davies, J.E., Whinnett, Z.I., Francis, D.P., et al. (2006b) Use of simultaneous pressure and velocity measurements to estimate arterial wave speed at a single site in humans. *American journal of physiology. Heart and circulatory physiology*, 290 (2): H878-85. doi:10.1152/ajpheart.00751.2005.

DELL’ITALIA, L.J. and WALSH, R.A. (1988) Application of a time varying elastance model to right ventricular performance in man. *Cardiovascular Research*, 22 (12): 864–874. doi:10.1093/cvr/22.12.864.

Doucette, J.W., Corl, P.D., Payne, H.M., et al. (1992) Validation of a Doppler guide wire for intravascular measurement of coronary artery flow velocity. *Circulation*, 85 (5): 1899–1911. doi:10.1161/01.CIR.85.5.1899.

Dupont, M., Mullens, W., Skouri, H.N., et al. (2012) Prognostic Role of Pulmonary Arterial Capacitance in Advanced Heart Failure. *Circulation: Heart Failure*, 5 (6): 778–785. doi:10.1161/CIRCHEARTFAILURE.112.968511.

Dutta, T. and Aronow, W.S. (2017) Echocardiographic evaluation of the right ventricle: Clinical implications. *Clinical Cardiology*. 40 (8) pp. 542–548. doi:10.1002/clc.22694.

Edwards (2005) *INVASIVE HEMODYNAMIC MONITORING: PHYSIOLOGICAL PRINCIPLES AND CLINICAL APPLICATIONS (Swan Ganz)*. Edwards LifeSciences. Available at: /Users/EWN/Documents/Arkiv_artikler/5700_5799/5746.pdf.

Elliott, P., Andersson, B., Arbustini, E., et al. (2008) Classification of the cardiomyopathies: A position statement from the european society of cardiology working group on myocardial and pericardial diseases. *European Heart Journal*, 29 (2): 270–276. doi:10.1093/eurheartj/ehm342.

Essandoh, M., Kumar, N., Hussain, N., et al. (2022) Pulmonary artery pulsatility index as a predictor of right ventricular failure in left ventricular assist device recipients: A systematic review. *The Journal of heart and lung transplantation : the official publication of the International Society for Heart Transplantation*, 41 (8): 1114–1123. doi:10.1016/j.healun.2022.04.007.

Everaars, H., de Waard, G.A., Driessen, R.S., et al. (2018) Doppler Flow Velocity and Thermodilution to Assess Coronary Flow Reserve. *JACC: Cardiovascular Interventions*, 11 (20): 2044–2054. doi:10.1016/j.jcin.2018.07.011.

Fang, J.C., Demarco, T., Givertz, M.M., et al. (2012) World Health Organization Pulmonary Hypertension Group 2: Pulmonary hypertension due to left heart disease in the adult - A summary statement from the Pulmonary Hypertension Council of the International Society for Heart and Lung Transplantation. *Journal of Heart and Lung Transplantation*, 31 (9): 913–933. doi:10.1016/j.healun.2012.06.002.

Flewitt, J.A., Hobson, T.N., Wang, J., et al. (2007a) Wave intensity analysis of left ventricular filling: application of windkessel theory. *American journal of physiology. Heart and circulatory physiology*, 292 (6): H2817-23. doi:10.1152/ajpheart.00936.2006.

Flewitt, J.A., Hobson, T.N., Wang, J., et al. (2007b) Wave intensity analysis of left ventricular filling: application of windkessel theory. *American Journal of Physiology-Heart and Circulatory Physiology*, 292 (6): H2817–H2823. doi:10.1152/ajpheart.00936.2006.

Forrester, J.S., Ganz, W., Diamond, G., et al. (1972) Thermodilution cardiac output determination with a single flow-directed catheter. *American Heart Journal*, 83 (3): 306–311. doi:10.1016/0002-8703(72)90429-2.

Fujimoto, N., Borlaug, B.A., Lewis, G.D., et al. (2013) Hemodynamic responses to rapid saline loading: the impact of age, sex, and heart failure. *Circulation*, 127 (1): 55–62.

doi:10.1161/CIRCULATIONAHA.112.111302.

Fukuta, H., Goto, T., Wakami, K., et al. (2017) The effect of beta-blockers on mortality in heart failure with preserved ejection fraction: A meta-analysis of observational cohort and randomized controlled studies. *International Journal of Cardiology*, 228: 4–10. doi:10.1016/j.ijcard.2016.11.239.

Fürst, D.O., Osborn, M., Nave, R., et al. (1988) The organization of titin filaments in the half-sarcomere revealed by monoclonal antibodies in immunoelectron microscopy: a map of ten nonrepetitive epitopes starting at the Z line extends close to the M line. *The Journal of cell biology*, 106 (5): 1563–72. doi:10.1083/jcb.106.5.1563.

Garg, R. and Yusuf, S. (1995) Overview of Randomized Trials of Angiotensin-Converting Enzyme Inhibitors on Mortality and Morbidity in Patients With Heart Failure. *JAMA: The Journal of the American Medical Association*, 273 (18): 1450–1456. doi:10.1001/jama.1995.03520420066040.

Ghimire, A., Andersen, M.J., Burrowes, L.M., et al. (2016) The reservoir-wave approach to characterize pulmonary vascular-right ventricular interactions in humans. *Journal of applied physiology (Bethesda, Md. : 1985)*, 121 (6): 1348–1353. doi:10.1152/japplphysiol.00697.2016.

Ghio, S., Gavazzi, A., Campana, C., et al. (2001) Independent and additive prognostic value of right ventricular systolic function and pulmonary artery pressure in patients with chronic heart failure. *Journal of the American College of Cardiology*, 37 (1): 183–188. doi:10.1016/S0735-1097(00)01102-5.

Gladden, J.D., Linke, W.A. and Redfield, M.M. (2014) Heart failure with preserved ejection fraction. *Pflugers Archiv European Journal of Physiology*. 466 (6) pp. 1037–1053. doi:10.1007/s00424-014-1480-8.

Glass, A., McCall, P., Arthur, A., et al. (2023) Pulmonary artery wave reflection and right

ventricular function after lung resection. *British journal of anaesthesia*, 130 (1): e128–e136. doi:10.1016/j.bja.2022.07.052.

Goldstein, D.J., Meyns, B., Xie, R., et al. (2019) Third Annual Report From the ISHLT Mechanically Assisted Circulatory Support Registry: A comparison of centrifugal and axial continuous-flow left ventricular assist devices. *The Journal of heart and lung transplantation : the official publication of the International Society for Heart Transplantation*, 38 (4): 352–363. doi:10.1016/j.healun.2019.02.004.

Gonzalez, M.H., Wang, Q., Yaranov, D.M., et al. (2021) Dynamic Assessment of Pulmonary Artery Pulsatility Index Provides Incremental Risk Assessment for Early Right Ventricular Failure After Left Ventricular Assist Device. *Journal of cardiac failure*, 27 (7): 777–785. doi:10.1016/j.cardfail.2021.02.012.

Goonasekera, S., Hammer, K., Auger-Messier, M., et al. (2012) Decreased cardiac L-type Ca2+ channel activity induces hypertrophy and heart failure in mice. *Journal of Clinical Investigation*, 122 (1): 280–290. doi:10.1172/JCI58227DS1.

Götberg, M., Christiansen, E.H., Gudmundsdottir, I.J., et al. (2017) Instantaneous Wave-free Ratio versus Fractional Flow Reserve to Guide PCI. *The New England journal of medicine*, 376 (19): 1813–1823. doi:10.1056/NEJMoa1616540.

Grandin, E.W., Zamani, P., Mazurek, J.A., et al. (2017) Right ventricular response to pulsatile load is associated with early right heart failure and mortality after left ventricular assist device. *The Journal of heart and lung transplantation : the official publication of the International Society for Heart Transplantation*, 36 (1): 97–105. doi:10.1016/j.healun.2016.06.015.

Grapsa, J., Pereira Nunes, M.C., Tan, T.C., et al. (2015) Echocardiographic and Hemodynamic Predictors of Survival in Precapillary Pulmonary Hypertension. *Circulation: Cardiovascular Imaging*, 8 (6). doi:10.1161/CIRCIMAGING.114.002107.

Grignola, J.C., Ginés, F., Bia, D., et al. (2007) Improved right ventricular-vascular coupling during active pulmonary hypertension. *International Journal of Cardiology*, 115 (2): 171–182. doi:10.1016/j.ijcard.2006.03.007.

Gudejko, M.D., Gebhardt, B.R., Zahedi, F., et al. (2019) Intraoperative Hemodynamic and Echocardiographic Measurements Associated With Severe Right Ventricular Failure After Left Ventricular Assist Device Implantation. *Anesthesia and analgesia*, 128 (1): 25–32. doi:10.1213/ANE.0000000000003538.

Guglin, M. and Omar, H.R. (2021) Right Atrial Pressure Predicts Mortality Among LVAD Recipients: Analysis of the INTERMACS Database. *Heart, lung & circulation*, 30 (4): 592–599. doi:10.1016/j.hlc.2020.10.018.

Guihaire, J., Haddad, F., Boulate, D., et al. (2013) Non-invasive indices of right ventricular function are markers of ventricular-arterial coupling rather than ventricular contractility: insights from a porcine model of chronic pressure overload. *European heart journal cardiovascular Imaging*, 14 (12): 1140–1149. doi:10.1093/ehjci/jet092.

Gulati, A., Japp, A.G., Raza, S., et al. (2018) Absence of Myocardial Fibrosis Predicts Favorable Long-Term Survival in New-Onset Heart Failure. *Circulation. Cardiovascular imaging*, 11 (9): e007722. doi:10.1161/CIRCIMAGING.118.007722.

Guven, G., Brankovic, M., Constantinescu, A.A., et al. (2018) Preoperative right heart hemodynamics predict postoperative acute kidney injury after heart transplantation. *Intensive care medicine*, 44 (5): 588–597. doi:10.1007/s00134-018-5159-z.

Hadian, M., Kim, H.K., Severyn, D.A., et al. (2010) Cross-comparison of cardiac output trending accuracy of LiDCO, PiCCO, FloTrac and pulmonary artery catheters. *Critical care (London, England)*, 14 (6): R212. doi:10.1186/cc9335.

Hadjiloizou, N., Davies, J.E., Malik, I.S., et al. (2008) Differences in cardiac microcirculatory

wave patterns between the proximal left mainstem and proximal right coronary artery. *American journal of physiology. Heart and circulatory physiology*, 295 (3): H1198–H1205. doi:10.1152/ajpheart.00510.2008.

Haft, J., Armstrong, W., Dyke, D.B., et al. (2007) Hemodynamic and exercise performance with pulsatile and continuous-flow left ventricular assist devices. *Circulation*, 116 (11 Suppl): I8-15. doi:10.1161/CIRCULATIONAHA.106.677898.

Hametner, B., Wassertheurer, S., Hughes, A.D., et al. (2014) Reservoir and excess pressures predict cardiovascular events in high-risk patients. *International journal of cardiology*, 171 (1): 31–6. doi:10.1016/j.ijcard.2013.11.039.

HAMILTON, W.F. and RILEY, R.L. (1948) Comparison of the Fick and dye injection methods of measuring the cardiac output in man. *Federation proceedings*, 7 (1): 49. doi:10.1016/0002-8703(49)91357-5.

Higgins, V. (2006) Human physiology: the basis of medicine. *British Journal of Sports Medicine*, 40 (10): 880–880. doi:10.1136/bjsm.2006.026120.

Hochman, J.S., Sleeper, L.A., Godfrey, E., et al. (1999) SHould we emergently revascularize Occluded Coronaries for cardiogenic shocK: an international randomized trial of emergency PTCA/CABG-trial design. The SHOCK Trial Study Group. *American heart journal*, 137 (2): 313–21. doi:10.1053/hj.1999.v137.95352.

Hoeper, M.M., Bogaard, H.J., Condliffe, R., et al. (2013) Definitions and Diagnosis of Pulmonary Hypertension. *Journal of the American College of Cardiology*, 62 (25): D42–D50. doi:10.1016/j.jacc.2013.10.032.

Hollander, E.H., Wang, J.-J., Dobson, G.M., et al. (2001) Negative wave reflections in pulmonary arteries. *American Journal of Physiology-Heart and Circulatory Physiology*, 281 (2): H895–H902. doi:10.1152/ajpheart.2001.281.2.H895.

Homma, S., Messé, S.R., Rundek, T., et al. (2016) Patent foramen ovale. *Nature Reviews Disease Primers*, 2: 1–15. doi:10.1038/nrdp.2015.86.

Huez, S., Brimioulle, S., Naeije, R., et al. (2004) Feasibility of routine pulmonary arterial impedance measurements in pulmonary hypertension. *Chest*, 125 (6): 2121–8. doi:10.1378/chest.125.6.2121.

Hughes, A.D., Davies, J.E. and Parker, K.H. (2013) The importance of wave reflection: A comparison of wave intensity analysis and separation of pressure into forward and backward components. *Proceedings of the Annual International Conference of the IEEE Engineering in Medicine and Biology Society, EMBS*, 2013: 229–232. doi:10.1109/EMBC.2013.6609479.

Hughes, A.D., Parker, K.H. and Davies, J.E. (2008) Waves in arteries: A review of wave intensity analysis in the systemic and coronary circulations. *Artery Research*, 2 (2): 51. doi:10.1016/j.artres.2008.02.002.

Humbert, M., Kovacs, G., Hoeper, M.M., et al. (2022) 2022 ESC/ERS Guidelines for the diagnosis and treatment of pulmonary hypertension. *European Heart Journal*, 43 (38): 3618–3731. doi:10.1093/eurheartj/ehac237.

Ibe, T., Wada, H., Sakakura, K., et al. (2021) Combined pre- and post-capillary pulmonary hypertension: The clinical implications for patients with heart failure. *PloS one*, 16 (3): e0247987. doi:10.1371/journal.pone.0247987.

Ishizu, T., Seo, Y., Atsumi, A., et al. (2017) Global and Regional Right Ventricular Function Assessed by Novel Three-Dimensional Speckle-Tracking Echocardiography. *Journal of the American Society of Echocardiography*, 30 (12): 1203–1213. doi:10.1016/j.echo.2017.08.007.

Jones, C.J.H., Sugawara, M., Kondoh, Y., et al. (2002) Compression and expansion wavefront travel in canine ascending aortic flow: wave intensity analysis. *Heart and vessels*, 16 (3): 91–8. doi:10.1007/s003800200002.

Jones, N., Burns, A.T. and Prior, D.L. (2019) Echocardiographic Assessment of the Right Ventricle–State of the Art. *Heart Lung and Circulation*. 28 (9) pp. 1339–1350. doi:10.1016/j.hlc.2019.04.016.

Jurcut, R., Giusca, S., La Gerche, A., et al. (2010) The echocardiographic assessment of the right ventricle: What to do in 2010? *European Journal of Echocardiography*. 11 (2) pp. 81–96. doi:10.1093/ejechocard/jep234.

Kang, G., Ha, R. and Banerjee, D. (2016) Pulmonary artery pulsatility index predicts right ventricular failure after left ventricular assist device implantation. *The Journal of heart and lung transplantation : the official publication of the International Society for Heart Transplantation*, 35 (1): 67–73. doi:10.1016/j.healun.2015.06.009.

Kapur, N.K., Esposito, M.L., Bader, Y., et al. (2017) Mechanical Circulatory Support Devices for Acute Right Ventricular Failure. *Circulation*, 136 (3): 314–326. doi:10.1161/CIRCULATIONAHA.116.025290.

Karamitsos, T.D., Francis, J.M., Myerson, S., et al. (2009) The Role of Cardiovascular Magnetic Resonance Imaging in Heart Failure. *Journal of the American College of Cardiology*. 54 (15) pp. 1407–1424. doi:10.1016/j.jacc.2009.04.094.

Kass, D.A., Maughan, W.L., Guo, Z.M., et al. (1987) Comparative influence of load versus inotropic states on indexes of ventricular contractility: experimental and theoretical analysis based on pressure-volume relationships. *Circulation*, 76 (6): 1422–1436. doi:10.1161/01.CIR.76.6.1422.

Kaul, S., Tei, C., Hopkins, J.M., et al. (1984) Assessment of right ventricular function using two-dimensional echocardiography. *American Heart Journal*, 107 (3): 526–531. doi:10.1016/0002-8703(84)90095-4.

Khalid, M.U. and Deswal, A. (2017a) Heart failure with preserved ejection fraction. *Cardiology*

Secrets, 69 (1): 209–215. doi:10.1016/B978-0-323-47870-0.00023-4.

Khalid, M.U. and Deswal, A. (2017b) Heart failure with preserved ejection fraction. *Cardiology Secrets*. pp. 209–215. doi:10.1016/B978-0-323-47870-0.00023-4.

Kiernan, M.S., Grandin, E.W., Brinkley, M., et al. (2017) Early Right Ventricular Assist Device Use in Patients Undergoing Continuous-Flow Left Ventricular Assist Device Implantation. *Circulation: Heart Failure*, 10 (10). doi:10.1161/CIRCHEARTFAILURE.117.003863.

Kim, R.J., Fieno, D.S., Parrish, T.B., et al. (1999) Relationship of MRI delayed contrast enhancement to irreversible injury, infarct age, and contractile function. *Circulation*, 100 (19): 1992–2002. doi:10.1161/01.CIR.100.19.1992.

Kim, R.J., Wu, E., Rafael, A., et al. (2000) The Use of Contrast-Enhanced Magnetic Resonance Imaging to Identify Reversible Myocardial Dysfunction. *New England Journal of Medicine*, 343 (20): 1445–1453. doi:10.1056/nejm200011163432003.

Kimura, M., Nishimura, T., Kinoshita, O., et al. (2012) Hemodynamic influence of tilting disc valve type on pump performance with the NIPRO-ventricular assist device. *Journal of artificial organs : the official journal of the Japanese Society for Artificial Organs*, 15 (2): 134–9. doi:10.1007/s10047-011-0616-2.

Kirklin, J.K., Naftel, D.C., Kormos, R.L., et al. (2013) Fifth INTERMACS annual report: Risk factor analysis from more than 6,000 mechanical circulatory support patients. *Journal of Heart and Lung Transplantation*, 32 (2): 141–156. doi:10.1016/j.healun.2012.12.004.

Kobashigawa, J., Zuckermann, A., Macdonald, P., et al. (2014) Report from a consensus conference on primary graft dysfunction after cardiac transplantation. *The Journal of Heart and Lung Transplantation*, 33 (4): 327–340. doi:10.1016/j.healun.2014.02.027.

Kochav, S.M., Flores, R.J., Truby, L.K., et al. (2018) Prognostic Impact of Pulmonary Artery Pulsatility Index (PAPi) in Patients With Advanced Heart Failure: Insights From the ESCAPE

Trial. *Journal of cardiac failure*, 24 (7): 453–459. doi:10.1016/j.cardfail.2018.03.008.

Koenraadt, W.M.C., Tokmaji, G., DeRuiter, M.C., et al. (2016) Coronary anatomy as related to bicuspid aortic valve morphology. *Heart*, 102 (12): 943–949. doi:10.1136/heartjnl-2015-308629.

Koh, T.W., Pepper, J.R., DeSouza, A.C., et al. (1998) Analysis of wave reflections in the arterial system using wave intensity: a novel method for predicting the timing and amplitude of reflected waves. *Heart and vessels*, 13 (3): 103–13. doi:10.1007/BF01747827.

Korabathina, R., Heffernan, K.S., Paruchuri, V., et al. (2012) The pulmonary artery pulsatility index identifies severe right ventricular dysfunction in acute inferior myocardial infarction. *Catheterization and cardiovascular interventions : official journal of the Society for Cardiac Angiography & Interventions*, 80 (4): 593–600. doi:10.1002/ccd.23309.

Kovacs, G., Berghold, A., Scheidl, S., et al. (2009) Pulmonary arterial pressure during rest and exercise in healthy subjects: a systematic review. *The European respiratory journal*, 34 (4): 888–94. doi:10.1183/09031936.00145608.

Krishnan, A., Markham, R., Savage, M., et al. (2019) Right Heart Catheterisation: How To Do It. *Heart Lung and Circulation*, 28 (4): e71–e78. doi:10.1016/j.hlc.2018.08.005.

Kubo, S.H., Burchenal, J.E. and Cody, R.J. (1987) Comparison of direct Fick and thermodilution cardiac output techniques at high flow rates. *The American journal of cardiology*, 59 (4): 384–6. doi:10.1016/0002-9149(87)90829-0.

Kukucka, M., Potapov, E., Stepanenko, A., et al. (2011) Acute impact of left ventricular unloading by left ventricular assist device on the right ventricle geometry and function: Effect of nitric oxide inhalation. *Journal of Thoracic and Cardiovascular Surgery*, 141 (4): 1009–1014. doi:10.1016/j.jtcvs.2010.08.010.

Kussmaul, W.G., Altschuler, J.A., Herrmann, H.C., et al. (1992) Effects of pacing tachycardia

and balloon valvuloplasty on pulmonary artery impedance and hydraulic power in mitral stenosis. *Circulation*, 86 (6): 1770–9. doi:10.1161/01.cir.86.6.1770.

Lamia, B., Kim, H.K., Severyn, D.A., et al. (2018) Cross-comparisons of trending accuracies of continuous cardiac-output measurements: pulse contour analysis, bioreactance, and pulmonary-artery catheter. *Journal of clinical monitoring and computing*, 32 (1): 33–43. doi:10.1007/s10877-017-9983-4.

Lankhaar, J.-W., Westerhof, N., Faes, T.J.C., et al. (2006) Quantification of right ventricular afterload in patients with and without pulmonary hypertension. *American journal of physiology. Heart and circulatory physiology*, 291 (4): H1731-7. doi:10.1152/ajpheart.00336.2006.

Lankhaar, J.-W., Westerhof, N., Faes, T.J.C., et al. (2008) Pulmonary vascular resistance and compliance stay inversely related during treatment of pulmonary hypertension. *European heart journal*, 29 (13): 1688–95. doi:10.1093/eurheartj/ehn103.

Laskey, W.K., Ferrari, V.A., Palevsky, H.I., et al. (1993) Pulmonary artery hemodynamics in primary pulmonary hypertension. *Journal of the American College of Cardiology*, 21 (2): 406–12. doi:10.1016/0735-1097(93)90682-q.

Lee, E.-J., Peng, J., Radke, M., et al. (2010) Calcium sensitivity and the Frank-Starling mechanism of the heart are increased in titin N2B region-deficient mice. *Journal of molecular and cellular cardiology*, 49 (3): 449–58. doi:10.1016/j.yjmcc.2010.05.006.

Lee, J.Z., Low, S.W., Pasha, A.K., et al. (2018) Comparison of tricuspid annular plane systolic excursion with fractional area change for the evaluation of right ventricular systolic function: A metaanalysis. *Open Heart*, 5 (1). doi:10.1136/openhrt-2017-000667.

Lefkowitz, R.J., Rockman, H.A. and Koch, W.J. (2000) Catecholamines, cardiac β-adrenergic receptors, and heart failure. *Circulation*. 101 (14) pp. 1634–1637. doi:10.1161/01.CIR.101.14.1634.

Leibundgut, G., Rohner, A., Grize, L., et al. (2010) Dynamic Assessment of Right Ventricular Volumes and Function by Real-Time Three-Dimensional Echocardiography: A Comparison Study With Magnetic Resonance Imaging in 100 Adult Patients. *Journal of the American Society of Echocardiography*, 23 (2): 116–126. doi:10.1016/j.echo.2009.11.016.

Liberati, A., Altman, D.G., Tetzlaff, J., et al. (2009) The PRISMA statement for reporting systematic reviews and meta-analyses of studies that evaluate healthcare interventions: explanation and elaboration. *BMJ (Clinical research ed.)*, 339: b2700. doi:10.1136/bmj.b2700.

Lim, H.S. and Gustafsson, F. (2020) Pulmonary artery pulsatility index: physiological basis and clinical application. *European journal of heart failure*, 22 (1): 32–38. doi:10.1002/ejhf.1679.

Lim, H.S., Howell, N. and Ranasinghe, A. (2017) The Physiology of Continuous-Flow Left Ventricular Assist Devices. *Journal of Cardiac Failure*, 23 (2): 169–180. doi:10.1016/j.cardfail.2016.10.015.

Lim, H.S. and Zaphiriou, A. (2016) Sodium Nitroprusside in Patients With Mixed Pulmonary Hypertension and Left Heart Disease: Hemodynamic Predictors of Response and Prognostic Implications. *Journal of Cardiac Failure*, 22 (2): 117–124. doi:10.1016/j.cardfail.2015.10.018.

Lim, Y., Low, T.-T., Chan, S.P., et al. (2021) Does pulmonary artery pulsatility index predict mortality in pulmonary arterial hypertension? *ESC heart failure*, 8 (5): 3835–3844. doi:10.1002/ehf2.13450.

Loforte, A., Montalto, A., Musumeci, F., et al. (n.d.) Calculation of the ALMA Risk of Right Ventricular Failure After Left Ventricular Assist Device Implantation. *ASAIO journal (American Society for Artificial Internal Organs : 1992)*, 64 (6): e140–e147. doi:10.1097/MAT.0000000000000800.

Longobardo, L., Suma, V., Jain, R., et al. (2017) Role of Two-Dimensional Speckle-Tracking Echocardiography Strain in the Assessment of Right Ventricular Systolic Function and

Comparison with Conventional Parameters. *Journal of the American Society of Echocardiography*. 30 (10) pp. 937-946.e6. doi:10.1016/j.echo.2017.06.016.

Loukas, M., Bilinsky, S., Bilinsky, E., et al. (2009) Cardiac veins: A review of the literature. *Clinical Anatomy*. 22 (1) pp. 129–145. doi:10.1002/ca.20745.

Loukas, M., Youssef, P., Gielecki, J., et al. (2016) History of cardiac anatomy: A comprehensive review from the egyptians to today. *Clinical Anatomy*, 29 (3): 270–284. doi:10.1002/ca.22705.

MacRae, J.M., Sun, Y.-H., Isaac, D.L., et al. (1997a) Wave-intensity analysis: a new approach to left ventricular filling dynamics. *Heart and Vessels*, 12 (2): 53–59. doi:10.1007/BF02820867.

MacRae, J.M., Sun, Y.H., Isaac, D.L., et al. (1997b) Wave-intensity analysis: a new approach to left ventricular filling dynamics. *Heart and vessels*, 12 (2): 53–9. doi:10.1007/BF02820867.

Madigan, J.D., Barbone, A., Choudhri, A.F., et al. (2001) Time course of reverse remodeling of the left ventricle during support with a left ventricular assist device. *Journal of Thoracic and Cardiovascular Surgery*, 121 (5): 902–908. doi:10.1067/mtc.2001.112632.

Mahapatra, S., Nishimura, R.A., Oh, J.K., et al. (2006a) The Prognostic Value of Pulmonary Vascular Capacitance Determined by Doppler Echocardiography in Patients with Pulmonary Arterial Hypertension. *Journal of the American Society of Echocardiography*, 19 (8): 1045–1050. doi:10.1016/j.echo.2006.03.008.

Mahapatra, S., Nishimura, R.A., Sorajja, P., et al. (2006b) Relationship of Pulmonary Arterial Capacitance and Mortality in Idiopathic Pulmonary Arterial Hypertension. *Journal of the American College of Cardiology*, 47 (4): 799–803. doi:10.1016/j.jacc.2005.09.054.

Masri, S.C., Tedford, R.J., Colvin, M.M., et al. (2017) Pulmonary Arterial Compliance Improves Rapidly After Left Ventricular Assist Device Implantation. *ASAIO journal (American*

Society for Artificial Internal Organs : 1992), 63 (2): 139–143. doi:10.1097/MAT.0000000000000467.

Mathews, L. and Singh, R.K.K. (2008) Cardiac output monitoring. *Annals of cardiac anaesthesia*. 11 (1) pp. 56–68. doi:10.4103/0971-9784.38455.

McCarthy, P.M., Nakatani, S., Vargo, R., et al. (1995) Structural and left ventricular histologic changes after implantable LVAD insertion. *The Annals of Thoracic Surgery*, 59 (3): 609–613. doi:10.1016/0003-4975(94)00953-8.

McCrohon, J.A., Moon, J.C.C., Prasad, S.K., et al. (2003) Differentiation of heart failure related to dilated cardiomyopathy and coronary artery disease using gadolinium-enhanced cardiovascular magnetic resonance. *Circulation*, 108 (1): 54–59. doi:10.1161/01.CIR.0000078641.19365.4C.

McDonagh, T.A., Metra, M., Adamo, M., et al. (2023) 2023 Focused Update of the 2021 ESC Guidelines for the diagnosis and treatment of acute and chronic heart failure. *European Heart Journal*, 44 (37): 3627–3639. doi:10.1093/eurheartj/ehad195.

McEwan, P.E., Gray, G.A., Sherry, L., et al. (1998) Differential effects of angiotensin II on cardiac cell proliferation and intramyocardial perivascular fibrosis in vivo. *Circulation*, 98 (24): 2765–2773. doi:10.1161/01.CIR.98.24.2765.

McMurray, J.J.V., Packer, M., Desai, A.S., et al. (2013) Dual angiotensin receptor and neprilysin inhibition as an alternative to angiotensin-converting enzyme inhibition in patients with chronic systolic heart failure: Rationale for and design of the Prospective comparison of ARNI with ACEI to Determine Impact. *European Journal of Heart Failure*, 15 (9): 1062–1073. doi:10.1093/eurjhf/hft052.

McMurray, J.J.V., Solomon, S.D., Inzucchi, S.E., et al. (2019) Dapagliflozin in Patients with Heart Failure and Reduced Ejection Fraction. *New England Journal of Medicine*, 381 (21):

1995–2008. doi:10.1056/NEJMoa1911303.

McNally, E.M., Barefield, D.Y. and Puckelwartz, M.J. (2015) The genetic landscape of cardiomyopathy and its role in heart failure. *Cell metabolism*, 21 (2): 174–182. doi:10.1016/j.cmet.2015.01.013.

Mehra, M.R., Naka, Y., Uriel, N., et al. (2017) A Fully Magnetically Levitated Circulatory Pump for Advanced Heart Failure. *New England Journal of Medicine*, 376 (5): 440–450. doi:10.1056/nejmoa1610426.

Mehra, M.R., Uriel, N., Naka, Y., et al. (2019) A Fully Magnetically Levitated Left Ventricular Assist Device — Final Report. *New England Journal of Medicine*, 380 (17): 1618–1627. doi:10.1056/NEJMoa1900486.

Metra, M. and Teerlink, J.R. (2017) Heart failure. *The Lancet*, 390 (10106): 1981–1995. doi:10.1016/S0140-6736(17)31071-1.

Meyer, J.A. (1990) Werner Forssmann and catheterization of the heart, 1929. *The Annals of Thoracic Surgery*, 49 (3): 497–499. doi:10.1016/0003-4975(90)90272-8.

Mihaljevic, T., von Segesser, L.K., Tonz, M., et al. (1995) Continuous versus bolus thermodilution cardiac output measurements--A comparative study. *Critical Care Medicine*, 23 (5): 944–949. doi:10.1097/00003246-199505000-00025.

Miller, W.L., Grill, D.E. and Borlaug, B.A. (2013) Clinical features, hemodynamics, and outcomes of pulmonary hypertension due to chronic heart failure with reduced ejection fraction: Pulmonary hypertension and heart failure. *JACC: Heart Failure*, 1 (4): 290–299. doi:10.1016/j.jchf.2013.05.001.

Milnor, W.R. (1982) *Hemodynamics*. Williams & WIlkins.

Milnor, W.R., Bergel, D.H. and Bargainer, J.D. (1966) Hydraulic power associated with pulmonary blood flow and its relation to heart rate. *Circulation research*, 19 (3): 467–480.

doi:10.1161/01.RES.19.3.467.

Mora, B., Ince, I., Birkenberg, B., et al. (2011) Validation of cardiac output measurement with the LiDCO^{TM} pulse contour system in patients with impaired left ventricular function after cardiac surgery. *Anaesthesia*, 66 (8): 675–81. doi:10.1111/j.1365-2044.2011.06754.x.

Morine, K.J., Kiernan, M.S., Pham, D.T., et al. (2016) Pulmonary Artery Pulsatility Index Is Associated With Right Ventricular Failure After Left Ventricular Assist Device Surgery. *Journal of cardiac failure*, 22 (2): 110–6. doi:10.1016/j.cardfail.2015.10.019.

Muresian, H. (2016) The clinical anatomy of the right ventricle. *Clinical Anatomy*, 29 (3): 380–398. doi:10.1002/ca.22484.

Muslem, R., Ong, C.S., Tomashitis, B., et al. (2019) Pulmonary Arterial Elastance and INTERMACS-Defined Right Heart Failure Following Left Ventricular Assist Device. *Circulation. Heart failure*, 12 (8): e005923. doi:10.1161/CIRCHEARTFAILURE.119.005923.

Naeije, R. and D'Alto, M. (n.d.) The Diagnostic Challenge of Group 2 Pulmonary Hypertension. *Progress in cardiovascular diseases*, 59 (1): 22–9. doi:10.1016/j.pcad.2016.05.003.

Najjar, E., Thorvaldsen, T., Dalén, M., et al. (2020) Validation of non-invasive ramp testing for HeartMate 3. *ESC heart failure*, 7 (2): 663–672. doi:10.1002/ehf2.12638.

Nassif, M.E., Windsor, S.L., Borlaug, B.A., et al. (2021) The SGLT2 inhibitor dapagliflozin in heart failure with preserved ejection fraction: a multicenter randomized trial. *Nature Medicine*, 27 (11): 1954–1960. doi:10.1038/s41591-021-01536-x.

Niki, K., Sugawara, M., Chang, D., et al. (2002) A new noninvasive measurement system for wave intensity: evaluation of carotid arterial wave intensity and reproducibility. *Heart and vessels*, 17 (1): 12–21. doi:10.1007/s003800200037.

Niki, K., Sugawara, M., Uchida, K., et al. (1999) A noninvasive method of measuring wave

intensity, a new hemodynamic index: application to the carotid artery in patients with mitral regurgitation before and after surgery. *Heart and vessels*, 14 (6): 263–71. doi:10.1007/BF03257237.

Nitta, D., Kinugawa, K., Imamura, T., et al. (2018) A Useful Scoring System For Predicting Right Ventricular Assist Device Requirement Among Patients with a Paracorporeal Left Ventricular Assist Device. *International heart journal*, 59 (5): 983–990. doi:10.1536/ihj.17-487.

Noble, M.I.M. (1978) The Frank Starling curve. *Clinical Science and Molecular Medicine*. 54 (1) pp. 1–7. doi:10.1042/cs0540001.

Nossaman, B.D., Scruggs, B.A., Nossaman, V.E., et al. (2010) History of Right Heart Catheterization. *Cardiology in Review*, 18 (2): 94–101. doi:10.1097/CRD.0b013e3181ceff67.

Ohte, N., Narita, H., Sugawara, M., et al. (2003) Clinical usefulness of carotid arterial wave intensity in assessing left ventricular systolic and early diastolic performance. *Heart and vessels*, 18 (3): 107–11. doi:10.1007/s00380-003-0700-5.

Ojo, A., Tariq, S., Harikrishnan, P., et al. (2017) Cardiac Resynchronization Therapy for Heart Failure. *Interventional Cardiology Clinics*. 6 (3) pp. 417–426. doi:10.1016/j.iccl.2017.03.010.

Ozenc, E., Yildiz, O., Baydar, O., et al. (2020) Impact of right ventricular stroke work index on predicting hospital readmission and functional status of patients with advanced heart failure. *Revista Portuguesa de Cardiologia*, 39 (10): 565–572. doi:10.1016/j.repc.2020.06.014.

Packer, M., Anker, S.D., Butler, J., et al. (2020) Cardiovascular and Renal Outcomes with Empagliflozin in Heart Failure. *New England Journal of Medicine*, 383 (15): 1413–1424. doi:10.1056/NEJMoa2022190.

Pagani, F.D., Mehra, M.R., Cowger, J.A., et al. (2021) Clinical outcomes and healthcare expenditures in the real world with left ventricular assist devices – The CLEAR-LVAD study.

The Journal of Heart and Lung Transplantation, 40 (5): 323–333. doi:10.1016/j.healun.2021.02.010.

Parameshwar, J., Hogg, R., Rushton, S., et al. (2019) Patient survival and therapeutic outcome in the UK bridge to transplant left ventricular assist device population. *Heart*, 105 (4): 291–296. doi:10.1136/heartjnl-2018-313355.

Parker, K.H. (2009) An introduction to wave intensity analysis. *Medical and Biological Engineering and Computing*, 47 (2): 175–188. doi:10.1007/s11517-009-0439-y.

Parker, K.H., Alastruey, J. and Stan, G.-B. (2012) Arterial reservoir-excess pressure and ventricular work. *Medical & biological engineering & computing*, 50 (4): 419–24. doi:10.1007/s11517-012-0872-1.

Parker, K.H. and Jones, C.J.H. (1990a) Forward and backward running waves in the arteries: Analysis using the method of characteristics. *Journal of Biomechanical Engineering*, 112 (3): 322–326. doi:10.1115/1.2891191.

Parker, K.H. and Jones, C.J.H. (1990b) Forward and backward running waves in the arteries: Analysis using the method of characteristics. *Journal of Biomechanical Engineering*. doi:10.1115/1.2891191.

Paulus, W.J. and Tschöpe, C. (2013) A novel paradigm for heart failure with preserved ejection fraction: Comorbidities drive myocardial dysfunction and remodeling through coronary microvascular endothelial inflammation. *Journal of the American College of Cardiology*. 62 (4) pp. 263–271. doi:10.1016/j.jacc.2013.02.092.

Pejković, B., Krajnc, I., Anderhube, F., et al. (2008) Anatomical aspects of the arterial blood supply to the sinoatrial and atrioventricular nodes of the human heart. *Journal of International Medical Research*, 36 (4): 691–698. doi:10.1177/147323000803600410.

Peterzan, M.A., Rider, O.J. and Anderson, L.J. (2016) The Role of Cardiovascular Magnetic

Resonance Imaging in Heart Failure. *Cardiac Failure Review*, p. 115. doi:10.15420/cfr.2016.2.2.115.

Pfeffer, M.A., Shah, A.M. and Borlaug, B.A. (2019) Heart Failure with Preserved Ejection Fraction in Perspective. *Circulation Research*. 124 (11) pp. 1598–1617. doi:10.1161/CIRCRESAHA.119.313572.

Pitt, B., Zannad, F., Remme, W.J., et al. (1999) The Effect of Spironolactone on Morbidity and Mortality in Patients with Severe Heart Failure. *New England Journal of Medicine*, 341 (10): 709–717. doi:10.1056/nejm199909023411001.

Porenta, G., Schima, H., Pentaris, A., et al. (1999) Assessment of coronary stenoses by Doppler wires: a validation study using in vitro modeling and computer simulations. *Ultrasound in Medicine & Biology*, 25 (5): 793–801. doi:10.1016/S0301-5629(99)00033-2.

Prabhu, S.D. (2007) Altered left ventricular-arterial coupling precedes pump dysfunction in early heart failure. *Heart and Vessels*, 22 (3): 170–177. doi:10.1007/s00380-006-0954-9.

Prijic, S. and Buchhorn, R. (2014) Mechanisms of Beta-Blockers Action in Patients with Heart Failure. *Reviews on Recent Clinical Trials*, 9 (2): 58–60. doi:10.2174/1574887109666140908125402.

Punetha, J. and Hoffman, E.P. (2013) Short read (next-generation) sequencing: a tutorial with cardiomyopathy diagnostics as an exemplar. *Circulation. Cardiovascular genetics*, 6 (4): 427–34. doi:10.1161/CIRCGENETICS.113.000085.

Raymer, D.S., Moreno, J.D., Sintek, M.A., et al. (n.d.) The Combination of Tricuspid Annular Plane Systolic Excursion and HeartMate Risk Score Predicts Right Ventricular Failure After Left Ventricular Assist Device Implantation. *ASAIO journal (American Society for Artificial Internal Organs : 1992)*, 65 (3): 247–251. doi:10.1097/MAT.0000000000000808.

Rehwald, W.G., Fieno, D.S., Chen, E.L., et al. (2002) Myocardial magnetic resonance imaging

contrast agent concentrations after reversible and irreversible ischemic injury. *Circulation*, 105 (2): 224–229. doi:10.1161/hc0202.102016.

Renner, L.E., Morton, M.J. and Sakuma, G.Y. (1993) Indicator amount, temperature, and intrinsic cardiac output affect thermodilution cardiac output accuracy and reproducibility. *Critical care medicine*, 21 (4): 586–97. doi:10.1097/00003246-199304000-00021.

Reuben, S.R. (1971) Compliance of the human pulmonary arterial system in disease. *Circulation research*, 29 (1): 40–50. doi:10.1161/01.res.29.1.40.

Rong, L.Q., Rahouma, M., Neuburger, P.J., et al. (2020) Use of Pulmonary Artery Pulsatility Index in Cardiac Surgery. *Journal of Cardiothoracic and Vascular Anesthesia*, 34 (5): 1220–1225. doi:10.1053/j.jvca.2019.09.023.

Rosenkranz, S., Gibbs, J.S.R., Wachter, R., et al. (2016) Left ventricular heart failure and pulmonary hypertension. *European Heart Journal*, 37 (12): 942–954. doi:10.1093/eurheartj/ehv512.

Rudski, L.G., Lai, W.W., Afilalo, J., et al. (2010) Guidelines for the Echocardiographic Assessment of the Right Heart in Adults: A Report from the American Society of Echocardiography. Endorsed by the European Association of Echocardiography, a registered branch of the European Society of Cardiology, and . *Journal of the American Society of Echocardiography*. 23 (7) pp. 685–713. doi:10.1016/j.echo.2010.05.010.

Ruiz-Cano, M.J., Morshuis, M., Koster, A., et al. (2020) Risk factors of early right ventricular failure in patients undergoing LVAD implantation with intermediate Intermacs profile for advanced heart failure. *Journal of cardiac surgery*, 35 (8): 1832–1839. doi:10.1111/jocs.14696.

Ryan, M., De Silva, K., Morgan, H., et al. (2022) Coronary Wave Intensity Analysis as an Invasive and Vessel-Specific Index of Myocardial Viability. *Circulation. Cardiovascular interventions*, 15 (12): e012394. doi:10.1161/CIRCINTERVENTIONS.122.012394.

Saba, M.M., Ventura, H.O., Saleh, M., et al. (2006) Ancient Egyptian Medicine and the Concept of Heart Failure. *Journal of Cardiac Failure*, 12 (6): 416–421. doi:10.1016/j.cardfail.2006.03.001.

Sabbah, H.N., Sharov, V.G., Lesch, M., et al. (1995) Progression of heart failure: A role for interstitial fibrosis. *Molecular and Cellular Biochemistry*, 147 (1–2): 29–34. doi:10.1007/BF00944780.

Sagawa, K., Lie, R.K. and Schaefer, J. (1990) Translation of Otto frank's paper "Die Grundform des arteriellen Pulses" zeitschrift für biologie 37: 483-526 (1899). *Journal of Molecular and Cellular Cardiology*, 22 (3): 253–254. doi:10.1016/0022-2828(90)91459-K.

Saidi, A., Selzman, C.H., Ahmadjee, A., et al. (2018) Favorable Effects on Pulmonary Vascular Hemodynamics with Continuous-Flow Left Ventricular Assist Devices Are Sustained 5 Years After Heart Transplantation. *ASAIO journal (American Society for Artificial Internal Organs : 1992)*, 64 (1): 38–42. doi:10.1097/MAT.0000000000000614.

Saouti, N., Westerhof, N., Helderman, F., et al. (2010) Right ventricular oscillatory power is a constant fraction of total power irrespective of pulmonary artery pressure. *American Journal of Respiratory and Critical Care Medicine*, 182 (10): 1315–1320. doi:10.1164/rccm.200910-1643OC.

Schaefer, S., Malloy, C.R., Katz, J., et al. (1988) Gadolinium-DTPA-enhanced nuclear magnetic resonance imaging of reperfused myocardium: Identification of the myocardial bed at risk. *Journal of the American College of Cardiology*, 12 (4): 1064–1072. doi:10.1016/0735-1097(88)90477-9.

Segovia, J., Cosío, M.D.G., Barceló, J.M., et al. (2011) RADIAL: A novel primary graft failure risk score in heart transplantation. *The Journal of Heart and Lung Transplantation*, 30 (6): 644–651. doi:10.1016/j.healun.2011.01.721.

Sen, S., Escaned, J., Malik, I.S., et al. (2012) Development and validation of a new adenosine-independent index of stenosis severity from coronary wave-intensity analysis: results of the ADVISE (ADenosine Vasodilator Independent Stenosis Evaluation) study. *Journal of the American College of Cardiology*, 59 (15): 1392–402. doi:10.1016/j.jacc.2011.11.003.

Sert, D.E., Karahan, M., Aygun, E., et al. (2020) Prediction of right ventricular failure after continuous flow left ventricular assist device implantation. *Journal of cardiac surgery*, 35 (11): 2965–2973. doi:10.1111/jocs.14952.

Shah, K.S., Xu, H., Matsouaka, R.A., et al. (2017) Heart Failure With Preserved, Borderline, and Reduced Ejection Fraction: 5-Year Outcomes. *Journal of the American College of Cardiology*, 70 (20): 2476–2486. doi:10.1016/j.jacc.2017.08.074.

Simonneau, G., Montani, D., Celermajer, D.S., et al. (2019a) Haemodynamic definitions and updated clinical classification of pulmonary hypertension. *The European respiratory journal*, 53 (1). doi:10.1183/13993003.01913-2018.

Simonneau, G., Montani, D., Celermajer, D.S., et al. (2019b) Haemodynamic definitions and updated clinical classification of pulmonary hypertension. *European Respiratory Journal*, 53 (1): 1801913. doi:10.1183/13993003.01913-2018.

Simonneau, G., Robbins, I.M., Beghetti, M., et al. (2009) Updated Clinical Classification of Pulmonary Hypertension. *Journal of the American College of Cardiology*, 54 (1): S43–S54. doi:10.1016/j.jacc.2009.04.012.

Slaughter, M.S., Pagani, F.D., Rogers, J.G., et al. (2010) Clinical management of continuous-flow left ventricular assist devices in advanced heart failure. *The Journal of heart and lung transplantation : the official publication of the International Society for Heart Transplantation*, 29 (4 Suppl): S1-39. doi:10.1016/j.healun.2010.01.011.

Slaughter, M.S., Rogers, J.G., Milano, C.A., et al. (2009) Advanced Heart Failure Treated with

Continuous-Flow Left Ventricular Assist Device. *New England Journal of Medicine*, 361 (23): 2241–2251. doi:10.1056/NEJMoa0909938.

Smith, K.R., Hsu, C.C., Berei, T.J., et al. (2018) PARADIGM-HF Trial: Secondary Analyses Address Unanswered Questions. *Pharmacotherapy*. 38 (2) pp. 284–298. doi:10.1002/phar.2075.

Smith, N.F., Salehi Omran, S., Genuardi, M. V, et al. (2022) Primary Graft Dysfunction in Heart Transplant Recipients-Risk Factors and Longitudinal Outcomes. *ASAIO journal (American Society for Artificial Internal Organs : 1992)*, 68 (3): 394–401. doi:10.1097/MAT.0000000000001469.

Spencer, J.H., Anderson, S.E. and Iaizzo, P.A. (2013) Human coronary venous anatomy: Implications for interventions. *Journal of Cardiovascular Translational Research*, 6 (2): 208–217. doi:10.1007/s12265-012-9443-y.

Starr, I., Jeffers, W.A. and Meade, R.H. (1943) The absence of conspicuous increments of venous pressure after severe damage to the right ventricle of the dog, with a discussion of the relation between clinical congestive failure and heart disease. *American Heart Journal*, 26 (3): 291–301. doi:10.1016/S0002-8703(43)90325-4.

STEENDIJK, P. (2004) Pressure?volume measurements by conductance catheter during cardiac resynchronization therapy. *European Heart Journal Supplements*, 6: D35–D42. doi:10.1016/j.ehjsup.2004.05.012.

Stewart, G.C., Kittleson, M.M., Patel, P.C., et al. (2016) INTERMACS (Interagency Registry for Mechanically Assisted Circulatory Support) Profiling Identifies Ambulatory Patients at High Risk on Medical Therapy After Hospitalizations for Heart Failure. *Circulation. Heart failure*, 9 (11). doi:10.1161/CIRCHEARTFAILURE.116.003032.

Stricagnoli, M., Sciaccaluga, C., Mandoli, G.E., et al. (2022) Clinical, echocardiographic and

hemodynamic predictors of right heart failure after LVAD placement. *The international journal of cardiovascular imaging*, 38 (3): 561–570. doi:10.1007/s10554-021-02433-7.

Su, J., Hilberg, O., Howard, L., et al. (2016) A review of wave mechanics in the pulmonary artery with an emphasis on wave intensity analysis. *Acta physiologica (Oxford, England)*, 218 (4): 239–249. doi:10.1111/apha.12803.

Su, J., Hughes, A.D., Simonsen, U., et al. (2019) Impact of pulmonary endarterectomy on pulmonary arterial wave propagation and reservoir function. *American journal of physiology. Heart and circulatory physiology*, 317 (3): H505–H516. doi:10.1152/ajpheart.00181.2019.

Su, J., Manisty, C., Parker, K.H., et al. (2017a) Wave Intensity Analysis Provides Novel Insights Into Pulmonary Arterial Hypertension and Chronic Thromboembolic Pulmonary Hypertension. *Journal of the American Heart Association*, 6 (11). doi:10.1161/JAHA.117.006679.

Su, J., Manisty, C., Simonsen, U., et al. (2017b) Pulmonary artery wave propagation and reservoir function in conscious man: impact of pulmonary vascular disease, respiration and dynamic stress tests. *The Journal of physiology*, 595 (20): 6463–6476. doi:10.1113/JP274385.

Su, J., Simonsen, U., Mellemkjaer, S., et al. (2021) Limited value of pulse wave analysis in assessing arterial wave reflection and stiffness in the pulmonary artery. *Physiological reports*, 9 (18): e15024. doi:10.14814/phy2.15024.

Sun, Q., Rogiers, P., Pauwels, D., et al. (2002) Comparison of continuous thermodilution and bolus cardiac output measurements in septic shock. *Intensive care medicine*, 28 (9): 1276–80. doi:10.1007/s00134-002-1415-2.

Sun, Y., Belenkie, I., Wang, J.-J., et al. (2006) Assessment of right ventricular diastolic suction in dogs with the use of wave intensity analysis. *American journal of physiology. Heart and circulatory physiology*, 291 (6): H3114-21. doi:10.1152/ajpheart.00853.2005.

Sun, Y.H., Anderson, T.J., Parker, K.H., et al. (2000) Wave-intensity analysis: a new approach to coronary hemodynamics. *Journal of applied physiology (Bethesda, Md. : 1985)*, 89 (4): 1636–44. doi:10.1152/jappl.2000.89.4.1636.

Swan, H.J.C., Ganz, W., Forrester, J., et al. (1970) Catheterization of the Heart in Man with Use of a Flow-Directed Balloon-Tipped Catheter. *New England Journal of Medicine*, 283 (9): 447–451. doi:10.1056/nejm197008272830902.

Sztechman, D., Czarzasta, K., Cudnoch-Jedrzejewska, A., et al. (2018) Aldosterone and mineralocorticoid receptors in regulation of the cardiovascular system and pathological remodelling of the heart and arteries. *Journal of Physiology and Pharmacology*. 69 (6) pp. 829–845. doi:10.26402/jpp.2018.6.01.

Takeda, K., Takayama, H., Colombo, P.C., et al. (2015) Incidence and clinical significance of late right heart failure during continuous-flow left ventricular assist device support. *Journal of Heart and Lung Transplantation*, 34 (8): 1024–1032. doi:10.1016/j.healun.2015.03.011.

Tanai, E. and Frantz, S. (2016) Pathophysiology of heart failure. *Comprehensive Physiology*, 6 (1): 187–214. doi:10.1002/cphy.c140055.

Tanaka, M., Sakamoto, T., Sugawara, S., et al. (2011) Physiological basis and clinical significance of left ventricular suction studied using echo-dynamography. *Journal of Cardiology*, 58 (3): 232–244. doi:10.1016/j.jjcc.2011.06.011.

Tedford, R.J., Hassoun, P.M., Mathai, S.C., et al. (2012) Pulmonary capillary wedge pressure augments right ventricular pulsatile loading. *Circulation*, 125 (2): 289–97. doi:10.1161/CIRCULATIONAHA.111.051540.

Trip, P., Kind, T., Van De Veerdonk, M.C., et al. (2013) Accurate assessment of load-independent right ventricular systolic function in patients with pulmonary hypertension. *Journal of Heart and Lung Transplantation*, 32 (1): 50–55. doi:10.1016/j.healun.2012.09.022.

Tubbs, R.S. (2016) The heart is simply a muscle. *Clinical Anatomy*. 29 (3) pp. 267–268. doi:10.1002/ca.22704.

Tyberg, J. V., Bouwmeester, J.C., Parker, K.H., et al. (2014) The case for the reservoir-wave approach. *International Journal of Cardiology*, 172 (2): 299–306. doi:10.1016/j.ijcard.2013.12.178.

Tyberg, J. V., Davies, J.E., Wang, Z., et al. (2009) Wave intensity analysis and the development of the reservoir-wave approach. *Medical and Biological Engineering and Computing*, 47 (2): 221–232. doi:10.1007/s11517-008-0430-z.

Uriel, N., Adatya, S., Malý, J., et al. (2017) Clinical hemodynamic evaluation of patients implanted with a fully magnetically levitated left ventricular assist device (HeartMate 3). *The Journal of Heart and Lung Transplantation*, 36 (1): 28–35. doi:10.1016/j.healun.2016.07.008.

Uriel, N., Medvedofsky, D., Imamura, T., et al. (2019) Echocardiographic Changes in Patients Implanted With a Fully Magnetically Levitated Left Ventricular Assist Device (Heartmate 3). *Journal of cardiac failure*, 25 (1): 36–43. doi:10.1016/j.cardfail.2018.11.015.

Uriel, N., Morrison, K.A., Garan, A.R., et al. (2012) Development of a novel echocardiography ramp test for speed optimization and diagnosis of device thrombosis in continuous-flow left ventricular assist devices: the Columbia ramp study. *Journal of the American College of Cardiology*, 60 (18): 1764–75. doi:10.1016/j.jacc.2012.07.052.

Uriel, N., Sayer, G., Addetia, K., et al. (2016) Hemodynamic Ramp Tests in Patients With Left Ventricular Assist Devices. *JACC: Heart Failure*, 4 (3): 208–217. doi:10.1016/j.jchf.2015.10.001.

Vonk-Noordegraaf, A. and Westerhof, N. (2013) Describing right ventricular function. *European Respiratory Journal*, 41 (6): 1419–1423. doi:10.1183/09031936.00160712.

Vonk Noordegraaf, A., Westerhof, B.E. and Westerhof, N. (2017) The Relationship Between

the Right Ventricle and its Load in Pulmonary Hypertension. *Journal of the American College of Cardiology*. 69 (2) pp. 236–243. doi:10.1016/j.jacc.2016.10.047.

Wagner, A., Mahrholdt, H., Holly, T.A., et al. (2003) Contrast-enhanced MRI and routine single photon emission computed tomography (SPECT) perfusion imaging for detection of subendocardial myocardial infarcts: An imaging study. *Lancet*, 361 (9355): 374–379. doi:10.1016/S0140-6736(03)12389-6.

Wagner, T., Magnussen, C., Bernhardt, A., et al. (2022) Impact of diastolic pulmonary gradient and pulmonary artery pulse index on outcomes in heart transplant patients-Results from the Eurotransplant database. *Frontiers in cardiovascular medicine*, 9: 1036547. doi:10.3389/fcvm.2022.1036547.

Walsh, R., Rutland, C., Thomas, R., et al. (2010) Cardiomyopathy: a systematic review of disease-causing mutations in myosin heavy chain 7 and their phenotypic manifestations. *Cardiology*, 115 (1): 49–60. doi:10.1159/000252808.

Wang, J.J., O'Brien, A.B., Shrive, N.G., et al. (2003) Time-domain representation of ventricular-arterial coupling as a windkessel and wave system. *American Journal of Physiology - Heart and Circulatory Physiology*, 284 (4 53-4): H1358-68. doi:10.1152/ajpheart.00175.2002.

Wang, J.J., Shrive, N.G., Parker, K.H., et al. (2011) Wave propagation and reflection in the canine aorta: Analysis using a reservoir-wave approach. *Canadian Journal of Cardiology*, 27 (3): 389.e1-389.e10. doi:10.1016/j.cjca.2010.12.072.

Wang, Z., Jalali, F., Sun, Y.-H., et al. (2005a) Assessment of left ventricular diastolic suction in dogs using wave-intensity analysis. *American journal of physiology. Heart and circulatory physiology*, 288 (4): H1641-51. doi:10.1152/ajpheart.00181.2004.

Wang, Z., Jalali, F., Sun, Y.-H., et al. (2005b) Assessment of left ventricular diastolic suction

in dogs using wave-intensity analysis. *American Journal of Physiology-Heart and Circulatory Physiology*, 288 (4): H1641–H1651. doi:10.1152/ajpheart.00181.2004.

Welch, G.R. (1991) Thermodynamics and Living Systems: Problems and Paradigms. *The Journal of Nutrition*, 121 (11): 1902–1906. doi:10.1093/jn/121.11.1902.

Wells, G., Shea, B., O'Connell, D., et al. (n.d.) *The Newcastle-Ottawa Scale (NOS) for assessing the quality of nonrandomised studies in meta-analyses*. Available at: http://www.ohri.ca/programs/clinical_epidemiology/oxford.asp (Accessed: 9 January 2022).

White, P. and Myers, M. (1921) The Classification of Cardiac Diagnosis. *Journal of the American Medical Association*, 77 (18): 1414–1415.

Wu, K.C., Weiss, R.G., Thiemann, D.R., et al. (2008) Late Gadolinium Enhancement by Cardiovascular Magnetic Resonance Heralds an Adverse Prognosis in Nonischemic Cardiomyopathy. *Journal of the American College of Cardiology*, 51 (25): 2414–2421. doi:10.1016/j.jacc.2008.03.018.

Yancy, C.W., Jessup, M., Bozkurt, B., et al. (2013) 2013 ACCF/AHA Guideline for the Management of Heart Failure. *Circulation*, 128 (16). doi:10.1161/CIR.0b013e31829e8776.

Yelderman, M.L., Ramsay, M.A., Quinn, M.D., et al. (1992) Continuous thermodilution cardiac output measurement in intensive care unit patients. *Journal of cardiothoracic and vascular anesthesia*, 6 (3): 270–4. doi:10.1016/1053-0770(92)90137-v.

Yim, I.H.W., Khan-Kheil, A.M., Drury, N.E., et al. (2023) A Systematic Review and Physiology of Pulmonary Artery Pulsatility Index in Left Ventricular Assist Device Therapy. *Interdisciplinary cardiovascular and thoracic surgery*, 36 (5). doi:10.1093/icvts/ivad068.

Yoshida, T., Mandour, A.S., Matsuura, K., et al. (2021) Changes in the Pulmonary Artery Wave Reflection in Dogs with Experimentally-Induced Acute Pulmonary Embolism and the Effect of Vasodilator. *Animals : an open access journal from MDPI*, 11 (7). doi:10.3390/ani11071977.

Zambanini, A., Cunningham, S.L., Parker, K.H., et al. (2005) Wave-energy patterns in carotid, brachial, and radial arteries: a noninvasive approach using wave-intensity analysis. *American journal of physiology. Heart and circulatory physiology*, 289 (1): H270-6. doi:10.1152/ajpheart.00636.2003.

Zhang, Z., Tendulkar, A., Sun, K., et al. (2011) Comparison of the young-laplace law and finite element based calculation of ventricular wall stress: Implications for postinfarct and surgical ventricular remodeling. *Annals of Thoracic Surgery*, 91 (1): 150–156. doi:10.1016/j.athoracsur.2010.06.132.

Zile, M.R., Baicu, C.F., Ikonomidis, J.S., et al. (2015) Myocardial stiffness in patients with heart failure and a preserved ejection fraction contributions of collagen and titin. *Circulation*, 131 (14): 1247–1259. doi:10.1161/CIRCULATIONAHA.114.013215.

Zimpfer, D., Zrunek, P., Roethy, W., et al. (2007) Left ventricular assist devices decrease fixed pulmonary hypertension in cardiac transplant candidates. *Journal of Thoracic and Cardiovascular Surgery*, 133 (3): 689–695. doi:10.1016/j.jtcvs.2006.08.104.

Appendices

Appendix 1. WIA Patient Information Leaflet

CLINICAL APPLICATION OF WAVE INTENSITY ANALYSIS IN ADVANCED HEART FAILURE

Invitation and brief summary

We would like to invite you to take part in our research study. Joining the study is entirely up to you, before you decide we would like you to understand why the research is being done and what it would involve for you. One of our team will go through this information sheet with you, to help you decide whether or not you would like to take part and answer any questions you may have. We would suggest this should take 5-10 minutes. Please feel free to talk to others about the study if you wish.

The first half of this document explains the purpose of this study and what will happen to you if you choose to take part. The second half gives you more detailed information about the conduct of the study. If something doesn`t make sense or is not clear, please ask us questions and tell us if you would like more information.

In summary, this study will investigate the underlying mechanism of right heart failure. This will help us to develop treatment for pulmonary hypertension in patients with heart failure, as well as guide us in developing a haemodynamic measure of the right heart function in the clinical setting. Patients with heart failure who are invited to attend routine right heart examination will be recruited. Recruited patients will undergo their routine right heart examination; with an additional test with a combined dual-tipped pressure and Doppler wire (ComboWire) to obtain extra haemodynamic measurements. Further details are outlined as below.

What's involved?

Background Information

Although the main problem of chronic heart failure (HF) is usually caused by failure of the left ventricle (the bottom left heart chamber that pumps blood to all the organs in the body except the lungs), this is frequently complicated by right ventricular problems (the right ventricle is responsible for pumping blood from the major veins to the lungs for oxygenation). As the left ventricle fails, the pressure required to fill the chamber increases causing back flow pressure in the blood vessels in the lungs. This leads to high pressure in the blood vessels in the lungs, termed pulmonary hypertension due to left heart disease. The high pressure in the pulmonary artery puts more stress on the right ventricle. As a result, the pumping function of the right ventricle fails over time.

Left ventricular assist devices (LVAD) are heart pumps that support the left ventricle. The LVAD pump speed is adjusted for the individual patient. If the pump speed is set too low, the LVAD would not provide enough support for the patient. However, if the pump speed is set too high, the LVAD can worsen the right ventricular function. It is usual practice to perform a 'ramp test' to identify the optimal pump speed for each patient.

Study purpose

1. The first objective of this study is to investigate the pressure waves in the artery of the lungs, and how the reflected waves affect the right heart function using a technique known as wave intensity analysis (WIA).

2. The second objective is to investigate the effects of LVAD treatment on the pressure waves in the artery of the lungs using WIA in patients with LVAD.

Study participation

Up to 40 patients (20 with and 20 without LVAD) will be recruited through the advance heart failure service at the Queen Elizabeth Hospital Birmingham. You have been invited to take part in this study because: (i) you are undergoing a right heart catheter study as part of the assessment for heart transplantation or LVAD treatment; or (ii) you are undergoing a right heart catheter study as part of the assessment following your LVAD surgery.

What would taking part involve?

If you decide to participate you will be recruited to the study and asked to sign the consent form.

You will undergo right heart catheter examination, blood tests and an ultrasound scan of the heart (echocardiogram) as part of the routine assessment for heart transplantation or LVAD, or after your LVAD implant. There is no need to change or stop any of your medications.

The only additional test from this study will involve collecting additional data during your right heart catheter examination using a combined dual-tipped pressure and Doppler wire. This dual-tipped pressure and Doppler wire is already in normal clinical use (ie: it is not an experimental equipment). This wire is inserted into the catheter that is used for the right heart catheter examination. No additional needle punctures, scans or blood tests will be needed for this study.

The routine right heart examination procedural steps are described below:

1. The right heart catheter examination will be performed in the standard way under local anaesthetic from the vein in the neck.
2. A standard pulmonary artery catheter will be inserted and positioned in the pulmonary artery (blood vessel in the lung) to obtain the measurements of pressures in the lung circulation.
3. In patients with high pressure in the lung circulation, it is routine to perform a vasodilator challenge with a medication called sodium nitroprusside (SNP) to see if the pressures can be reduced. The pressure and flow measurements will continue to be collected during the administration of SNP.
4. In patients with LVAD, the pump speed will be altered as part of the 'ramp test' to identify the optimal pump speed at this point. For the 'ramp test', the LVAD pump speed is briefly reduced and then increased while continuously measuring the pressures in the lungs to identify the ideal pump speed setting.
5. The catheter and the wire will be removed at the end of the procedure. A chest X-ray will be arranged, which is routine practice. Outpatient attendees will go home on the same day.
6. There are no further follow-up procedures or clinic visits required for this study.

Additional procedural steps of this study:

After measurements of the lung circulation pressures are taken (step 2), the dual-tipped pressure and Doppler wire will be inserted into the catheter. Therefore, no additional needle puncture is needed. Pressure and flow measurements will then be acquired simultaneously

using this wire. This step will also be repeated after the SNP challenge (step 3). The dual-tipped pressure and Doppler wire will also collect data during the 'ramp test' (step 4).

What are the possible disadvantages and risks of taking part?

The wire is inserted into the catheter and does not cause any discomfort or add any risk to the procedure. However, it does add about 10-15 minutes to your procedure for us to collect additional data. You do not need to participate in this study. Your treatment will not change if you choose not to participate. You will undergo your routine assessments.

If you take part in this study you will have a wire inserted into the catheter. This step will be extra to those that you would have if you did not take part. We use ionising radiation (X-ray) to confirm the position of the wire. Ionising radiation can cause cell damage that may, after many years or decades, turn cancerous. In patients with your current clinical condition, the chance of this happening to you is extremely small.

What are the possible benefits of taking part?

It is possible that the high definition pressure measurements from the pressure-flow wire will provide clearer measurements of the pressure in the lung circulation and improve assessment for transplantation or LVAD. The information gained from this study may help management of patients with heart failure.

Data protection & Confidentiality

Only the doctor copying the data from your health records will know your name. We will replace your name with a code number and also make sure that any other information that could show who you are is removed. For example, instead of using your date of birth, we will use your age. As there is no information that could show who you are, this is called anonymous data.

All research reports about the study will be written in a way that no-one can work out that you took part in the study.

Once we have finished the study, we will keep the research data for several years, in case we need to check it. Your details such as your name or NHS number will be removed, and other researchers will not be able to contact you to ask you about future research.

Any information that could show who you are will be held safely with strict limits on who can access it. Please also see University Hospitals Birmingham's privacy statement for research participants at https://www.uhb.nhs.uk/privacy-notice/.

Who is organising and funding this study?

This study is designed and organised by the investigator (Dr Sern Lim, Consultant Cardiologist, Queen Elizabeth Hospital Birmingham, University Hospitals Birmingham NHS Foundation Trust). This study has been reviewed and funded by Heart Research UK.

Financial costs and payments to participants

There are no costs involved in your participation in this study. If your health suffers you will receive immediate and appropriate hospital treatment. Your study doctor will advise you on possible medical treatments should complications occur. You will not receive money for participating in this clinical study.

Participation is voluntary

Your signature on the patient consent form attached towards the end of this document acknowledges your voluntary participation in the study and you cannot take part in this study unless you sign this form. This does not release the investigators, institutions, or sponsorsfrom their professional and ethical responsibility to you.

You are free to withdraw from the study at any time for any reason. If you do withdraw from the study after it is started, this will have no impact on your medical care or other services to which you are otherwise entitled. Your study doctor may withdraw you with or without your consent if he/she believes it is in your best interest.

Further information, complaints, or any problems

If you are not happy with the general care and treatment you receive during the study, please speak first to your study doctor or nurse, who will try to resolve the problem. He/she should also tell you about the clinic standard complaints procedure in case you wish to take the matter further.

You may contact your local Patient Advice and Liaison Services (PALS) or equivalent service for further advice if you have concerns or problems or to get independent help if you decide to make a complaint or for any other study or health related enquiry. The number for your local PALs is Tel: 0121 371 3280.

Approval by the NHS Research Ethics Committee

All relevant study documents, the patient information together with the consent form been approved by the Welsh Research and Ethics Committee

Appendix 2. WIA Patient Consent Form v.2.0

PATIENT CONSENT FORM

CLINICAL APPLICATION OF WAVE INTENSITY ANALYSIS IN ADVANCED HEART FAILURE

Please initial each box that you agree and will abide to:

☐ I confirm that I have read (or have had read to me) and understand the information contained in the Patient Information Sheet version number 1.0 dated 17 June 2019 for participation in the "Clinical application of wave intensity analysis in advanced heart failure" study.

☐ I understand that participation in this clinical study is voluntary and that I may decline to participate at any time. If I elect not to participate, my future medical treatment will not be influenced by my decision.

☐ I have been given the opportunity to ask questions and I am satisfied with the answers that I have received.

☐ I understand that I have the right to ask for additional information at any time during the study and that this information will be provided. I also understand that when there are new findings or information about the study that may influence my participation, I have the right to decide to discontinue my participation in this study and that this decision will not affect my future medical treatment.

☐ I understand and agree that the sponsor will collect personal data about me relating my health and stored at the hospital where this research is taking place in paper form and on electronic data storage media within the scope of this clinical study.

☐ I understand that relevant sections of my medical notes and data collected during the study, may be looked at by individuals from the sponsor, regulatory authorities or from the NHS Trust, where it is relevant to my taking part in this research. I give permission for these individuals to have access to my records.

☐ I agree to my data being kept for 10 year after completion of the study. After that, my personal data will be deleted unless this conflicts with legal, statutory or contractual retention periods.

☐ I understand that the information collected about me will be used to support other research in the future, and may be shared anonymously with other researchers.

☐ I agree to take part in the above study.

Declaration by investigator*:

I have given a verbal explanation of the clinical study, its procedures and risks and I believe that the person named bellow as the participant has understood that explanation.

Investigator`s Name and Signature

Name (printed)…….. Date……Signature ……..

*A senior member of the research team must provide the explanation and provision of information concerning the research project

Full name of participant	Date	Signature of participant

Please Note:
All parties signing the consent form must write their own name and date their own signature
When completed, 1 for patient; 1 for researcher site file; 1 (original) to be kept in patient's medical notes.

Appendix 3. WIA Matlab Full Script

```
%% PA_wia_resp.m  -- analyse PA data including respiration
% KHP (11/09/18)
% adapted from PA_wia_resp_v3.m

flagr=0;                  % rawdata=0  resp corr data=1



%% load data

% NOTE: import data as numerical array ??

% choose file - setting the path here allows a standard directory to be
% used for all analyses which speeds the process up
% [file,path] = uigetfile('*.mat');
% if isstr(file)
%    wirefilename =[path,file];
% end

%read combowire data
SR=200;             % sample frequency of Combomap


% delimiterIn=' '; %'\t';
% HeaderlinesIn=3;

% A = importdata(wirefilename,'',HeaderlinesIn);
%,delimiterIn,headerlinesIn);
%
% A=load(wirefilename);
% Data=A.Data;
% Events=A.Events;
% Notes=A.Notes;
% % Data=cell2mat(struct2cell(A));
% realtime=(Data(:, 1));
% Pdata=(Data(:, 3));
% Edata=(Data(:, 4));      % scaledecg=(E-min(E))/(max(E)-min(E)); %
repeated below
% Udata=(Data(:, 5));
% rwave=(Data(:, 7));         % seems to be NaN in the e.c.g. I have - is
it redundant

% Events=[2.36,5.30,6.48,8.00,10.00,11.50,13.30];     % Patient specific
% Notes=['Right PA';'Main PA ';'Dob05   ';'Right PA';'Dob10   ';'Dob15
';'Dob20   '];

% [Nstart,Nend]=SelectEpoch(Pdata,Udata,Edata,SR,Events,Notes);
P=Pdata(Nstart:Nend);
U=Udata(Nstart:Nend);
E=Edata(Nstart:Nend);

%% check the polarity of the ECG
% uses a 1s window to determine maxima and identifies outlier artifacts
% that can give incorrect ECG polarity if just using maxima
```

```
% (use line w1=1 to plot (E=-E) for most cases.
% (use line Emean =mean(E) to end) if the above fails, e.g. in PAH1 PA)

% w1=1;
% for i=1:floor(length(E)/SR)
%     maxE(:,i)=max(E(w1:w1+SR));
%     minE(:,i)=min(E(w1:w1+SR));
%     w1=w1+SR;
% end
% if median(abs(minE-median(E)))>median(abs(maxE-median(E)))
%     disp('inverted ECG corrected')
%     E=-E;
% end
% plot(E)

Emean=mean(E);
Emax=max(E-Emean);
Emin=min(E-Emean);
if (abs(Emin)>abs(Emax))
    E=-E;                    % necessary if ECG is upside down
end
% E=-E;                       % fix for spike in pt 7 & 8 PA

% look at raw data

N=length(P);
n=(1:N);
t=n/SR/60;
figure(5); clf;
Umean=mean(U);
Usd=std(U);
Pmean=mean(P);
Psd=std(P);
Poff=Umean+2*Usd;
plot(n,P+Poff,'k',n,U,'b',n,E,'r'),grid on
ylim([-round(Usd) round(Pmean+3*Psd+Poff)]);
zoom xon;

%% look at normalised data
%
pp=(P-min(P))/(max(P)-min(P));              %distal pressure
pp=P/max(P);
uu=U/max(U);
ee=(E-min(E))/(max(E)-min(E));
N=length(P);
n=(1:N);
t=(0:N-1)/SR;
figure(10); clf;       % remove comments if you want to see the raw data
grid on, hold on;
plot(n,pp+2,'k',n,uu,'b',n,ee-1,'r');  % NOTE: if E is inverted let E=-E;
axis tight;
ylabel '        E                                   U
P';
xlabel 't (s)'
title 'Normalised P, U and E'
legend('P','U','E');
% zoom xon;
```

```
%% shift U using max of cross correlation for time dely

N=length(P);
fU=fft(U-mean(U));
fP=fft(P-mean(P));
cor=real(ifft(fU.*conj(fP)));
[cmax,ncp]=max(cor);
% figure(111);
% plot(cor,'.-'),grid on,zoom xon, hold on;
% [cmax ncmax]=max(cor);
% plot(ncmax,cmax,'r.');
% title 'correlation of U and P';
nshift=(1:N);
if (ncp<round(N/2))
    DTU=ncp;
%     nshift=[ncp:N N*ones(1,ncp-1)];
else
    DTU=ncp-N;
    nshift=[ones(1,N-ncp) 1:ncp];
end
U=U(nshift);

%% shift U to give straight line during early systole
% % NOTE: this routine shifts the original data, to recover use U=data(:,5)

% UU=U;
% L=length(UU);
% dtu=0;
% figure(21);
% Nprelim=400;       % number of points for preliminary Ushift
% plot(UU(1:Nprelim),P(1:Nprelim),'b.-');grid on
% h=gcf; set(h,'DefaultTextColor','blue')
% ip=[2:L,L];
% im=[1,1:L-1];
% flag=1;                   % initial Ushift
% % flag=0;                   % no initial Ushift
% while (flag)
%   clf;   plot(UU(1:Nprelim),P(1:Nprelim),'b.-'),grid on,hold on;
%   plot(UU(1),P(1),'r*');
%   string=['ushift = ' num2str(dtu)];
%   title(string);
%   [X,Y,B]=ginput(1);
%   if (isempty(B))
%      flag=0;
%   elseif (B==1)
%      dtu=dtu-1;
%      UU=UU(im);
%   elseif (B==3)
%      dtu=dtu+1;
%      UU=UU(ip);
%   end
% end
% DTU=dtu;                 % remember original Ushift
% U=UU;

%% power spectrum

N=length(P);
fp=fft(P-mean(P));
```

```
fu=fft(U-mean(U));
f=(0:N-1)*SR/N;
% figure(11); clf; grid on, hold on;   % remove comments to view spectrum
% plot(f(1:round(N/2)),abs(fp(1:round(N/2))),'b.-
',f(1:round(N/2)),abs(fu(1:round(N/2))),'r.-');
% zoom xon;
% xlabel 'f (Hz)';ylabel 'power';
% legend('Pressure','Velocity');
% title 'Power spectra of P and U';

[fpmax npmax] = max(abs(fp(1:round(N/2))));          %max peak of spectrum
corresponds to beat freq
[fumax numax] = max(abs(fu(1:round(N/2))));
T=1;         % IDU!!
index = find(abs(fp(1:round(N/2)))== T); %find its index
c_freq = f(numax);                          %frequency of cardiac beat
% c_freq = f(npmax);                          %frequency of cardiac beat
c_time = 1/c_freq;
% c_time = 0.83;  % For patient 1 during valsalva
% c_time = 0.7;  % For patient 4 RPA
% c_time = 0.9;  % For patient 4 PA
% c_time = 0.61; % For patient 6
% c_time = 0.625; % For patient 7 during handgrip and valsalva
% c_time = 0.67; % For patient 9 and PAH1
%% separate respiration and cardiac signals
%skip this section
p=P;
fpp=fp;
nblank=round(npmax/1.5);
fpp(2:2+nblank-1)=zeros(nblank,1);
fpp(end-nblank+1:end)=zeros(nblank,1);
pp=mean(p)+real(ifft(fpp));
fpr=fp-fpp;
pr=real(ifft(fpr));
% figure(115); clf;
% plot(p),grid on,hold on;
% plot(pp,'r');
% plot(pr,'k');
% ylabel 'Pr                    P   Pp  (mmHg)';
% xlabel 't  (ms)';

%% savitsky-golay differences

Npoly=2;                  % Order of polynomial fit
F=11;                     % Window length
[b,g]=sgolay(Npoly,F);    % Calculate S-G coefficients
HalfWin=((F+1)/2) -1;

u=U;
p=P;
flagr=0;
if flagr
    p=pp;                % use raw data
end;
dp=zeros(N,1); du=dp; ps=dp; us=dp;
for n=(F+1)/2:N-(F+1)/2
  % Zero-th derivative (smoothing only)
  ps(n)=dot(g(:,1),p(n-HalfWin:n+HalfWin));
  us(n)=dot(g(:,1),u(n-HalfWin:n+HalfWin));
```

```
  % 1st differential
  dp(n)=dot(g(:,2),p(n-HalfWin:n+HalfWin));
  du(n)=dot(g(:,2),u(n-HalfWin:n+HalfWin));
end

ps(1:5,1) = ps(6,1);          %correct for halfwin
ps(end-5:end,1) = ps(end-6,1);
dp(1:5,1) = dp(6,1);          %correct for halfwin
dp(end-5:end,1) = dp(end-6,1);
du(1:5,1) = du(6,1);          %correct for halfwin
du(end-5:end,1) = du(end-6,1);

di=dp.*du;
rhocss=sqrt(sum(dp.^2)/sum(du.^2));

% figure(119);
% if flagr
%     plot(us,'r'),grid on, hold on;
% else
%     plot(us,'b'),grid on, hold on;
% end

%% Rwave function

e=E;
% ns=200;                              %sampling freq of cath lab
% nd=80;                               %delay time (trial & error)
% use c_time to define nominal ns and nd
ns = round(1.1*c_time*SR);          % ns 20% longer than nominal beat
length
nd = round(ns/10);

[a,nmax]=max(e(1:ns));              %a:amplitude - nmax:index corresponfind
to max peak
j=1;
nb=[];
nb(j)=nmax;
nend=nb(j)+nd+ns;
while nb(j)+nd+ns<length(e);
     nstart=nb(j)+nd;
     nend=nstart+ns;
     [a,nmax]=max(e(nstart:nend));
     j=j+1;
     nb(j)=nmax+nstart-1;
end
n=1:length(e);
% figure(13);                      % ('Color','w');
% plot(n,e,nb,e(nb),'ro');
% grid on; zoom xon;

% %% ensemble average
% % manual beat selection
% reply=input('Do you want to select ensemble manually? y/n [n]: ', 's');
% flagmanual=0;
% if reply=='y'
%     flagmanual=1;
% end
% % flagmanual=1;          % inserted for program development
% if flagmanual
```

```
%     Nb=length(nb);              % the number of beats detected
%     figure(131); clf;
%     plot(p), grid on, hold on;
%     pmax=max(p);
%     umax=max(u);
%     plot(pmax*u/(3*umax),'r');
%     ylimits=ylim;
%     for n=1:Nb
%         plot([nb(n) nb(n)],[ylimits(1) ylimits(2)],'k');
%     end
%     display('Click on beats to be ensembled (l->r)');
%     a=ginput;
%     Nbe=length(a);
%     for n=1:Nbe
%         j=find(nb>a(n));
%         nbe(n)=nb(j(1));
%     end
%     nperiod=round(mean(diff(nb)));    % find the average cardiac period
%     nshortest=min(diff(nb));   % find the shortest beat
%     nint=round(1.2*nperiod);   % chose a beat interval slightly longer
than nperiod
%     uens=zeros(Nbe,nint);
%     pens=zeros(Nbe,nint);
%     for n=1:Nbe
%         uens(n,:)=us(nbe(n):nbe(n)+nint-1);
%         pens(n,:)=ps(nbe(n):nbe(n)+nint-1);
%     end
%     uensavg=mean(uens);
%     uenssd=std(uens);
%     pensavg=mean(pens);
%     penssd=std(pens);
% %     figure(241);
% %     plot(pens');
% %     figure(242);
% %     plot(uens');
% end

%% automatic ensemble average

flagmanual=0;
Nb=length(nb);              % the number of beats detected
nperiod=round(mean(diff(nb)));    % find the average cardiac period
nshortest=min(diff(nb));   % find the shortest beat
nint=round(1.2*nperiod);   % chose a beat interval slightly longer than
nperiod
tens=(0:nint-1)/SR;
Tperiod=nperiod/SR;
Tshortest=nshortest/SR;

if ~flagmanual
    %---- Velocity ----------%
    uens=zeros(Nb-1,nint);
    for n=1:Nb-1
        uens(n,:)=us(nb(n):nb(n)+nint-1);
    end
    uensavg=mean(uens);
    uenssd=std(uens);
end
%
figure(14); clf;
```

```
subplot(2,1,2)
plot(tens,uens'), grid on, hold on;
plot(tens,uensavg,'k',tens,uensavg+uenssd,'k:',tens,uensavg-
uenssd,'k:','LineWidth',2);
ylims=ylim;
plot([Tperiod Tperiod],[ylims(1) ylims(2)],'k--');   % mark average period
axis tight;
ylabel 'U';
xlabel 't (s)';
title 'Ensemble Average Velocity'

if ~flagmanual
    %---- Pressure ----------%
    pens=zeros(Nb-1,nint);
    for n=1:Nb-1
        pens(n,:)=ps(nb(n):nb(n)+nint-1);
    end
    pensavg=mean(pens);
    penssd=std(pens);
end

subplot(2,1,1)
pd=min(pensavg);
plot(tens,pens'-pd),grid on, hold on;
plot(tens,pensavg-pd,'k',tens,pensavg+penssd-pd,'k:',tens,pensavg-penssd-
pd,'k:','LineWidth',2),grid on;
ylims=ylim;
plot([Tperiod Tperiod],[ylims(1) ylims(2)],'k--');   % mark average period
axis tight;
ylabel 'P-Pd';
xlabel 't (s)'; hold off;
if flagmanual
    str=num2str(Nbe);
else
    str=num2str(Nb-1);
end
tstr=['Ensemble Average Pressure, N = ' str];
title(tstr); grid on; %axis tight;

% %% display means and st deviations
% figure, grid on, axis tight;
% subplot(1,2,1)              %pressure
% plot(tens,pensavg_a,'r',tens,pensavg_a+penssd_a,'r:',tens,pensavg_a-
penssd_a,'r:','LineWidth',2);
% hold on;
% plot(tens,pensavg_d,'b',tens,pensavg_d+penssd_d,'b:',tens,pensavg_d-
penssd_d,'b:','LineWidth',2);
% legend('Pa mean', 'Pa + 1 StDev','Pa  - 1 StDev','Pd mean','Pd + 1
StDev','Pd  - 1 StDev');
% hold off;
% subplot(1,2,2)              %velocity
% plot(tens,uensavg,'k',tens,uensavg+uenssd,'k:',tens,uensavg-
uenssd,'k:','LineWidth',2);
% legend('U mean', 'U + 1 StDev','U  - 1 StDev');

% %% iterative correction of ensemble average
% % work on uens - assume pens is ok (check)
% umed=median(uens);
% Ne=Nb-1;
```

```
% for n=1:Ne
%     udiffav(n)=mean(uens(n,:)-umed);
%     udiffsd(n)=std(uens(n,:)-umed);
% end
% figure;
% plot(udiffav,'.-'), grid on, hold on; plot(udiffsd,'r.-');

%% correct ensemble averages using standard errors - (15/4/14)
if ~flagmanual
% calculate corr coeffs, order beats by corr, calculate min se omitting
% lowest corr beats from ensenble, use that ensemble for U and P
c_v = zeros();
ue = uens;                          % save the original ensemble of
velocities
a_v=uensavg-mean(uensavg);
for n = 1:Nb-1                        % calculates the cross correlation
between ens and uensavg
    b_v=ue(n,:)-mean(ue(n,:));
    c_v(n)=(b_v*a_v')/sqrt((b_v*b_v')*(a_v*a_v'));
end
[c_v_sort k_sort]=sort(c_v);          % sort corr coeffs in ascending order
ue_sort=ue(k_sort,:);               % sort uens by corr coeff
for n=1:Nb-3
    u_se(n)=mean(std(ue_sort(n:end,:)))/sqrt(Nb-n);
end
[u_se_min k_min]=min(u_se);
ue_corr=ue_sort(k_min:end,:);
ua_corr=mean(ue_corr);
usd_corr=std(ue_corr);

% % diagnostic plot of usd_corr
% figure(123); clf;
% plot(u_se,'o-'),grid on;
% ylabel 'U_{se}';
% xlabel 'n-excluded';
% title 'standard error of U';

figure(15); clf;
subplot(2,1,2);
plot(tens,ua_corr,'k',tens,ua_corr+usd_corr,'k:',tens,ua_corr-
usd_corr,'k:','LineWidth',2),hold on;
plot(tens,ue_sort(k_min:end,:)');
ylims=ylim;
plot([Tperiod Tperiod],[ylims(1) ylims(2)],'k--');   % mark average period
axis tight;
ylabel 'U (cm/s)';
xlabel 't (s)';
title('Corrected Ensemble Average Velocity'); grid on; %axis tight;

% ensemble P for same beats
pe = pens;                          % save the original ensemble of
velocities
pe_sort=pe(k_sort,:);               % sort uens by corr coeff
pe_corr=pe_sort(k_min:end,:);
pa_corr=mean(pe_corr);
psd_corr=std(pe_corr);
figure(15);
subplot(2,1,1);
```

```
plot(tens,pa_corr-pd,'k',tens,pa_corr+psd_corr-pd,'k:',tens,pa_corr-
psd_corr-pd,'k:','LineWidth',2),hold on;
plot(tens,pe_sort(k_min:end,:)'-pd);
ylims=ylim;
plot([Tperiod Tperiod],[ylims(1) ylims(2)],'k--');   % mark average period
axis tight;
ylabel 'P -P_d (mmHg)';
tstr=['Corrected Ensemble Average Pressure, N = ' num2str(Nb-k_min)];
title(tstr); grid on; %axis tight;

% use corrected ensemble averages
pensavg=pa_corr;
uensavg=ua_corr;

% figure(119);
% nstart=N+200;
% nplot=(1:nint)+nstart;
% if flagr
%     plot(nplot,pensavg,'r'),grid on, hold on;
%     plot(nplot,pensavg+psd_corr,'r--');
%     plot(nplot,pensavg-psd_corr,'r--');
% else
%     plot(nplot,pensavg,'b'),grid on, hold on;
%     plot(nplot,pensavg+psd_corr,'b--');
%     plot(nplot,pensavg-psd_corr,'b--');
% end
end
%% determination of wave speed - PU loop method

% shift velocity to give best linear line
UU=uensavg;
P=pensavg;
L=length(UU);
dtu=0;
figure(21);
plot(UU,P,'b.-');grid on
title 'Ushift using R&L mouse buttons'
h=gcf; set(h,'DefaultTextColor','blue')
ip=[2:L,L];
im=[1,1:L-1];
flag=1;
while (flag)
  clf;
  plot(UU,P,'b.-'),grid on,hold on;
  plot(UU(1),P(1),'r*');
  string=['ushift = ' num2str(dtu)];
  title(string);
  [X,Y,B]=ginput(1);
  if (isempty(B))
     flag=0;
  elseif (B==1)
     dtu=dtu-1;
     UU=UU(im);
  elseif (B==3)
     dtu=dtu+1;
     UU=UU(ip);
  end
end
Ushift=DTU+dtu;
uensavg=UU;
```

```
figure(21); clf;
plot(uensavg(1:nperiod),pensavg(1:nperiod),'.-'),grid on, hold on;
plot(uensavg(1),pensavg(1),'ro');                % mark start of loop
title 'select linear portion of systole';
b=ginput(2);
string=['net ushift = ' num2str(Ushift)];
title(string);

rhoc=(b(2,2)-b(1,2))/(b(2,1)-b(1,1));
if rhoc<0
    rhoc=-rhoc;
end
rhocd=rhoc;
cms=133.3*rhoc/(.01*1040);          % c in m/s
cmss=133.3*rhocss/(.01*1040);       % css in m/s

disp(strcat('Wave speed (m/s): ', num2str(cms)));    % display value of
wave speed
close(21);

%% wave intensity of the ensemble averages

dped=zeros(nint,1); dued=dped;
for n=(F+1)/2:nint-(F+1)/2                                  % 1st
differential
  dped(n)=dot(g(:,2),pensavg(n-HalfWin:n+HalfWin));
  dued(n)=dot(g(:,2),uensavg(n-HalfWin:n+HalfWin));
end

dped(1:5,1) = dped(6,1);          %correct for halfwin
dped(end-5:end,1) = dped(end-6,1);
dued(1:5,1) = dued(6,1);          %correct for halfwin
dued(end-5:end,1) = dued(end-6,1);

died=dped.*dued;

% figure(16); clf; zoom xon;
% subplot(3,1,1);
% pd=min(pensavg);
% plot(tens,pensavg-pd,'k', 'LineWidth',2),hold on,grid on;
% ylims=ylim;
% plot([Tperiod Tperiod],[ylims(1) ylims(2)],'k--');   % mark average
period
% axis tight;
% ylabel 'Pe-Pd';
% title 'Net Wave Intensity'
% subplot(3,1,2);
% plot(tens,uensavg,'b','Linewidth',2),hold on,grid on; % axis tight;
% ylims=ylim;
% plot([Tperiod Tperiod],[ylims(1) ylims(2)],'k--');   % mark average
period
% axis tight;
% ylabel 'Ue';
% subplot(3,1,3);
% plot(tens,died,'k', 'LineWidth',2),hold on,grid on; % axis tight;
% ylims=ylim;
% plot([Tperiod Tperiod],[ylims(1) ylims(2)],'k--');   % mark average
period
```

```
% axis tight;
% ylabel 'dIe'; xlabel 't (s)';
% figureHandle = gcf;
% set(findall(figureHandle,'type','text'),'fontSize',14);

PeakDI = max(died);
disp(strcat('peak wave intensity: ', num2str(PeakDI)));    % display value
of peak wave intensity

% %% determination of wave speed - SUM of squares method
%
% ind = find(tens<(c_time+0.0025)&tens>(c_time-0.0025));   %find index in
tens corresponding to time of cardiac period
% % rhoc = sqrt(sum(dpe(1:ind).^2)/ sum(due(1:ind).^2));   %find wavespeed
over cardiac period using that index in time
% rhocd = sqrt(sum(dped(1:ind).^2)/ sum(dued(1:ind).^2));

%% separation of forward and backward waves (ensemble average)

ind = find(tens<(c_time+0.0025)&tens>(c_time-0.0025));   %find index in
tens corresponding to time of cardiac period

dpep_d=(dped + rhocd .* dued)/2;        % forward pressure difference
dpem_d=(dped - rhocd .* dued)/2;        % backward pressure difference
duep_d=dpep_d./rhocd;                   % forward velocity difference
duem_d=-dpem_d./rhocd;                  % backward velocity difference
diep_d=dpep_d.*duep_d;                   % forward wave intensity
diem_d=dpem_d.*duem_d;

pep_d=cumtrapz(dpep_d)+pensavg(1);               % forward pressure
waveform
uep_d=cumtrapz(duep_d)+uensavg(1);               % forward velocity
waveform
pem_d=cumtrapz(dpem_d)+pensavg(1);               % backward pressure
waveform
uem_d=cumtrapz(duem_d)+uensavg(1);


% Plot separated variables
f=figure(18); clf;
f.Position(2)=f.Position(2)-300;
f.Position(4)=f.Position(4)+300;
subplot(3,1,1);
plot(tens,pensavg,'k','LineWidth',2);
grid on, hold on;
plot(tens,pep_d,'b:','LineWidth',2);
plot(tens,pem_d,'r:','LineWidth',2);
ylabel 'Pe';
title(casenumber);
x = [tens(ind) tens(ind)];
ylims=ylim;
plot([Tperiod Tperiod],[ylims(1) ylims(2)],'k--','LineWidth', 1.5);   %
mark average period
axis tight;
legend('Total','Forward','Backward');

subplot(3,1,2);
plot(tens,uensavg,'k','LineWidth',2);hold on;
```

```
grid on, hold on;
plot(tens,uep_d,'b:','LineWidth',2);
plot(tens,uem_d,'r:','LineWidth',2);
ylabel 'Ue';
ylims=ylim;
title 'Forward and backward separation',
plot([Tperiod Tperiod],[ylims(1) ylims(2)],'k--','LineWidth', 1.5);   %
mark average period
axis tight;
% legend('Total','Forward','Backward');

subplot(3,1,3);
plot(tens,died,'k','LineWidth',2); hold on;
plot(tens,diep_d,'b:','LineWidth',2);
plot(tens,diem_d,'r:','LineWidth',2),grid on;
ylabel 'dIe';
xlabel 't (s)';
x = [tens(ind) tens(ind)];
ylims=ylim;
plot([Tperiod Tperiod],[ylims(1) ylims(2)],'k--','LineWidth', 1.5);   %
mark average period
axis tight;
% legend('Total','Forward','Backward');
cstr=['c (PU) = ' num2str(cms,3) ' (m/s)'];
xsc=xlim; xphi=xsc(1)+.5*(xsc(2)-xsc(1));
ysc=ylim; yphi=ysc(1)+.75*(ysc(2)-ysc(1));
text(xphi,yphi,cstr);
csstr=['c (SS) = ' num2str(cmss,3) ' (m/s)'];
yssc=ylim; yphi=ysc(1)+.65*(ysc(2)-ysc(1));
text(xphi,yphi,csstr);
%% calculate RV work
% truncate pensavg using minima
Nhalf=floor(length(pensavg)/2);
[Psystmin,Nsystmin]=min(pensavg(1:Nhalf));
[Pdiasmin,Ndiasmin]=min(pensavg(Nhalf:end));
if (Pdiasmin<pensavg(end))
    pensavgtrunc=pensavg(Nsystmin:Nhalf+Ndiasmin);
    uensavgtrunc=uensavg(Nsystmin:Nhalf+Ndiasmin);
else
    pensavgtrunc=pensavg(Nsystmin:end);
    uensavgtrunc=uensavg(Nsystmin:end);
end
Neatrunc=length(pensavgtrunc);

Tperiodtrunc=Neatrunc/SR;
% for Pr try using kreservoir (compare with Pr = f(U)
w=cumtrapz(pensavgtrunc.*uensavgtrunc);
[pres,A,B,Pinf,Tn,Pn]=kreservoir_v10(pensavgtrunc,Tperiod);
wr=cumtrapz(pres.*uensavgtrunc);

figure(301); clf;
tr=(0:length(pres)-1)/SR;
yyaxis left;
plot(tr,pensavgtrunc,'b',tr,pres,'r-','LineWidth',1.5),hold on;
ylabel 'Pr        P (mmHg)'
yyaxis right;
plot(tr,uensavgtrunc,'k:','LineWidth',1.5),grid on;
ylabel 'U  (cm/s)';
xlabel 't (s)';
title(casenumber);
```

```
legend('P','Pr','U');
% hydraulic efficiency
phi=wr(end)/w(end);          % note units are strange (mmHg.cm/s)
phistr=['Wr/W = ',num2str(phi,2)];
xsc=xlim; xphi=xsc(1)+.75*(xsc(2)-xsc(1));
ysc=ylim; yphi=ysc(1)+.75*(ysc(2)-ysc(1));
text(xphi,yphi,phistr);
```

Reservoir Pressure Script

```
%% kreservoir  -  calculate reservoir pressure from pressure waveform
%
%  Copyright 2008 Kim H Parker
%  This software is distributed under under the terms of the GNU General
Public License
%  This program is free software: you can redistribute it and/or modify
%  it under the terms of the GNU General Public License as published by
%  the Free Software Foundation, either version 3 of the License, or
%  (at your option) any later version.
%
%  This program is distributed in the hope that it will be useful,
%  but WITHOUT ANY WARRANTY; without even the implied warranty of
%  MERCHANTABILITY or FITNESS FOR A PARTICULAR PURPOSE.  See the
%  GNU General Public License for more details.
%
%  http://www.gnu.org/licenses/gpl.html
%
%  v.03 (06/03/08)
%  v.04 (27/03/08) eliminate anonymous functions for backward compatability
%  v.05 (11/04/08) separate pinf for systole and diastole
%  v.06 (26/04/08) clean up code for use on sphygmacor data sets
%  v.07 (30/07/08) optimise fit for the whole of diastole
%  v.07.1 (05/09/08) fit to model results during diastole rather than data
%  v.07.2 (01/10/08) fixed error in fitting routine
%  v.08 (02/11/09) use polynomial approximation for inverting R(B)
%  v.08 (03/11/09) if convergence fails set pr=min(p)
%  v.09 (18/11/09) use inflection point as marker of diastole
%  v.10 (21/01/10) redefine Pres using diastolic exponential decay
%  v.10 (10/02/10) use Simpson's rule to calculate integrals
%  v.10 (14/07/10) clean up code and provide more comments

function [Pr,A,B,Pinf,Tn,Pn]=kreservoir_v10(P,Tb,Tn)

%   inputs  P    - pressure starting at diastolic pressure
%           Tb   - duration of beat
%           Tn   - time of start of diastole (if missing it is calculated
%                  found by the function; if ==0 it is done interactively
%   outputs Pr   - reservoir pressure waveform
%           A    - rate constant relating Pw to U
%           B    - rate constant = 1/tau
%           Pinf - pressure asymptote
%           Tn   - detected time of the dichrotic notch
%           Pn   - pressure at dichrotic notch
% uses functions: fsg521, kexpint, kexpmomrat, dias_int, dias_fit, beat_int
% assumes data are smooth enough to find derivative using 7-pt SG filter

plot_flag=0;        % set to 1 to plot the results
%plot_flag=1;        % set to 1 to plot the results
```

```
sP=size(P);
if (sP(1)>sP(2));
    P=P';
end
p=P;
Nb=length(P);
dt=Tb/(Nb-1);
t=(0:dt:Tb);

% determine Tn
if (nargin == 3)
    if (Tn~=0)              % Tn given as input
        tn=Tn;
%        nn=find(t == tn);
        [Tmin,nn]=min(abs(t-tn));
    else
        figure;             % determine Tn interactively
        plot(P);
        disp('click on start of diastole');
        inp=ginput(1);
        nn=round(inp(1,1));
        tn=t(nn);
    end
else
% determine Tn automatically from the minimum dp
    dp=fsg721(p);
    [dpmin,nn]=min(dp);
    tn=t(nn);
end

% calculate moments of pressure during diastole using model d=a*exp(-bt)+c
pd=p(nn:end);
td=t(nn:end)-tn;
Td=Tb-tn;
dt=td(2)-td(1);
N=length(pd)-1;
% calculation of E2/E1 using Simpson's rule
E0=(pd(1)+4*sum(pd(2:2:N))+2*sum(pd(3:2:N))+pd(N+1))*dt/(3*Td);
if (mod(N,2))
    E0=E0+(pd(N)+pd(N+1))*dt/(6*Td);
end
pde1=(pd-E0).*exp(td/Td);
E1=(pde1(1)+4*sum(pde1(2:2:N))+2*sum(pde1(3:2:N))+pde1(N+1))*dt/3;
if (mod(N,2))
    E1=E1+(pde1(N)+pde1(N+1))*dt/6;
end
pde2=(pd-E0).*exp(2*td/Td);
E2=(pde2(1)+4*sum(pde2(2:2:N))+2*sum(pde2(3:2:N))+pde2(N+1))*dt/3;
if (mod(N,2))
    E2=E2+(pde2(N)+pde2(N+1))*dt/6;
end
r=E2/E1;

% invert R(BTd)=r
global Rexp_inline
    Rexp_inline=r;

%options=optimset('Display','iter','TolX',1e-16);
```

```
options=optimset('TolX',1e-16);
y=fzero(@ratio21,1,options);
BTd=y;

% given b calculate a from E1
e1=exp(1);
if (BTd==1)
    denom= (3-e1-1/e1);
else
    denom=(1-e1*exp(-BTd))/(BTd-1) - (e1-1)*(1-exp(-BTd))/BTd;
end
a=E1(end)/(Td*denom);

% Given b & a calculate c from E0
c = E0 - ((a./BTd) *(1 - exp(-BTd)));

% calculate b in s
b=BTd/Td;
pinf=c;
prd=a*exp(-b*td)+c;

% find a by fitting to the measured data
% alternative that workds with earlier versions of Matlab
global p_inline
  p_inline=p;
global t_inline
  t_inline=t;
global b_inline
  b_inline=b;
global pinf_inline
  pinf_inline=pinf;
global nn_inline
  nn_inline=nn;
global prd_inline
  prd_inline=prd;

  options=optimset('TolX',1e-6);
% following line can be used in versions that support explicit functions
%y=fminsearch(@dias_fit,[b],options);
[y,rhubarb,exitflag]=fminsearch(@dias_fit,b,options);
aa=y;
pr=beat_int(p,t,aa,b,pinf,nn);
if ~exitflag
    pr=min(p)*ones(1,length(p));
end

% plot fit
if (plot_flag)
    figure
    plot(t,p,'-'); hold on; grid on
    plot(t,pr,'r-');
    plot(t(nn:end),prd,'g-');
    xlabel('t (s)');
    ylabel('P (kPa)');
end
%find crossover point
Nd=length(pd);
np=[2:Nd Nd];
prend=pr(nn:end);
```

```
k=find((prend-prd).*(prend(np)-prd(np))<=0);
prr=pr;
prr(nn+k:end)=prd(k+1:end);

% return variables
Pr=prr;
A=aa;
B=b;
Pinf=pinf;
Tn=t(nn);
Pn=p(nn);
end

%% ratio21.m - calculate the ratio of exponential moments R(bTd)
% KHP (27/01/10)
% added y==0 condition (06/02/10)

function Rdiff=ratio21(y)
%   input   y - value of bTd
%   output  R - ratio of E2/E1

global Rexp_inline

if (y==1)
    R=((exp(1)-1)-(1-exp(-1))*(exp(2)-1)/2)/(1-(1-exp(-1))*(exp(1)-1));
elseif (y==2)
    R=(1-(1-exp(-2))*(exp(2)-1)/4)/(-(exp(-1)-1)-(1-exp(-2))*(exp(1)-1)/2);
elseif (y==0)
    R=1/(3-exp(1));
else
    R=((exp(2-y)-1)/(2-y)-(1-exp(-y))*(exp(2)-1)/(2*y))/((exp(1-y)-1)/(1-
y)-(1-exp(-y))*(exp(1)-1)/y);
end
Rdiff=R-Rexp_inline;
end


%% kexpint.m  -  calculate the exponential integral Z = I_0^t Y*exp(at)dt
%  KHP (27/02/08)
function Z=kexpint(Y,T,A)
%   inputs  Y(t) - row vector
%           T    - duration of Y
%           A    - exponential factor
%   Outputs Z    - row vector
N=length(Y)-1;
t=(0:N)*T/N;
dt=t(2)-t(1);
% calculate integral of y using trapezoidal rule
ye=Y.*exp(A*t);
Z=(cumtrapz(ye))*dt;

end

%% dias_int
%  khp (30/07/08)
% calculate the indefinite integral during diastole, returning Prd
% inputs    Ps   - row vector of pressure for whole beat
%           Ts   - row vector of times for whole beat
```

```
%           a    - fitting parameter
%           b    - reciprocal of the diastolic time constant tau
%           Pinf - asymptote of diastolic pressure
%           nn   - index of notch
% output    Prd  - Pr during diastole

function Prd = dias_int(Ps,Ts,a,b,Pinf,nn)

% calculate the integral using the trapezoidal rule
dt=Ts(2)-Ts(1);
pse=cumtrapz(Ps.*exp((a+b)*Ts))*dt;
prb = exp(-(a+b)*Ts).*(a*pse + Ps(1) - (b*Pinf/(a+b))) + b*Pinf/(a+b);
Prd=prb(nn:end);
end

%% beat_int
%  khp (30/07/08)
% calculate the indefinite integral during whole beat, returning Pr
% inputs    Ps   - row vector of pressure for whole beat
%           Ts   - row vector of times for whole beat
%           a    - fitting parameter
%           b    - reciprocal of the diastolic time constant tau
%           Pinf - asymptote of diastolic pressure
%           nn   - index of notch

function Pr = beat_int(Ps,Ts,a,b,Pinf,rhubarb)
% calculate the integral using the trapezoidal rule
dt=Ts(2)-Ts(1);
pse=cumtrapz(Ps.*exp((a+b)*Ts))*dt;
prb = exp(-(a+b)*Ts).*(a*pse + Ps(1) - (b*Pinf/(a+b))) + b*Pinf/(a+b);
Pr=prb;
end

%% dias_fit
function afind = dias_fit(y)

global p_inline
global t_inline
global b_inline
global pinf_inline
global nn_inline
global prd_inline

aa=y;
%afind = sum((p_inline(nn_inline:end) -
dias_int(p_inline,t_inline,aa,b_inline,pinf_inline,nn_inline)).^2);
afind = sum((prd_inline -
dias_int(p_inline,t_inline,aa,b_inline,pinf_inline,nn_inline)).^2);
end

%% Savitsky-Golay smoothing filter function
% dx=fsg720(x)
%   7 point SavGol filter, 2nd order polynomial, 0th derivative
%   input   x
%   output  dx
%   corrected for time shift
% modified for linear interpolation at ends of data KHP (27/04/08)
```

```
function dx=fsg720(x)

% 2nd order polynomial
C=[-0.095238,0.142857,0.285714];

B=zeros(1,7);
for i=1:3;
    B(i)=C(i);
end
B(4)=0.333333;
for i=5:7
    B(i)=C(8-i);
end
A=[1,0];

s=size(x,2);
dx=filter(B,A,x);
% linear interpolation at ends
Dstart=(dx(7)-x(1))/3; Dend=(x(end)-dx(s))/3.;
dx=[x(1),x(1)+Dstart,x(1)+2*Dstart,dx(7:s),x(end)-2*Dend,x(end)-
Dend,x(end)];

end

%% Savitsky-Golay first derivative filter function
% dx=fsg721(x)
%   7 point SavGol filter, 2nd order polynomial, 1st derivative
%   input   x
%   output  dx
%   corrected for time shift

function dx=fsg721(x)

% 2nd order polynomial
C=[0.107143,0.071429,0.035714];

B=zeros(1,7);
for i=1:3;
    B(i)=C(i);
end
B(4)=0.0;
for i=5:7
    B(i)=-C(8-i);
end
A=[1,0];

s=size(x,2);
dx=filter(B,A,x);
dx=[dx(7),dx(7),dx(7),dx(7:s),dx(s),dx(s),dx(s)];

end

%% Savitsky-Golay first derivative filter function
% dx=fsg521(x)
%   5 point SavGol filter, 2nd order polynomial, 1st derivative
%   input   x
%   output  dx
%   corrected for time shift
```

```
function dx=fsg521(x)

C=[0.2,0.1];

B=zeros(1,5);
for i=1:2;
    B(i)=C(i);
end
B(3)=0.0;
for i=4:5;
    B(i)=-C(6-i);
end
A=[1,0];

s=size(x,2);
dx=filter(B,A,x);
dx=[dx(5)*ones(1,2),dx(5:s),dx(s)*ones(1,2)];

end
```